

Quark-hadron matter & neutron star observations

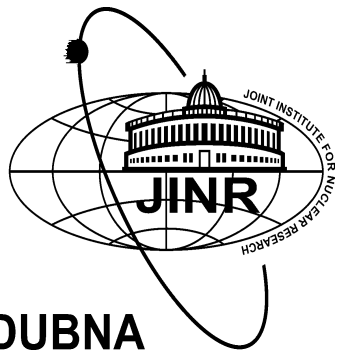
David Blaschke (University Wroclaw, JINR Dubna & MEPhI Moscow)

1. “Measuring” the cold Equation of States with Compact Stars
2. Microphysics of strong 1st order Phase Transitions
3. New Bayesian Analysis Scheme

The New is often the well-forgotten Old



“Modern Problems in Nuclear Physics II”, Lecture 2, 08.02.2017

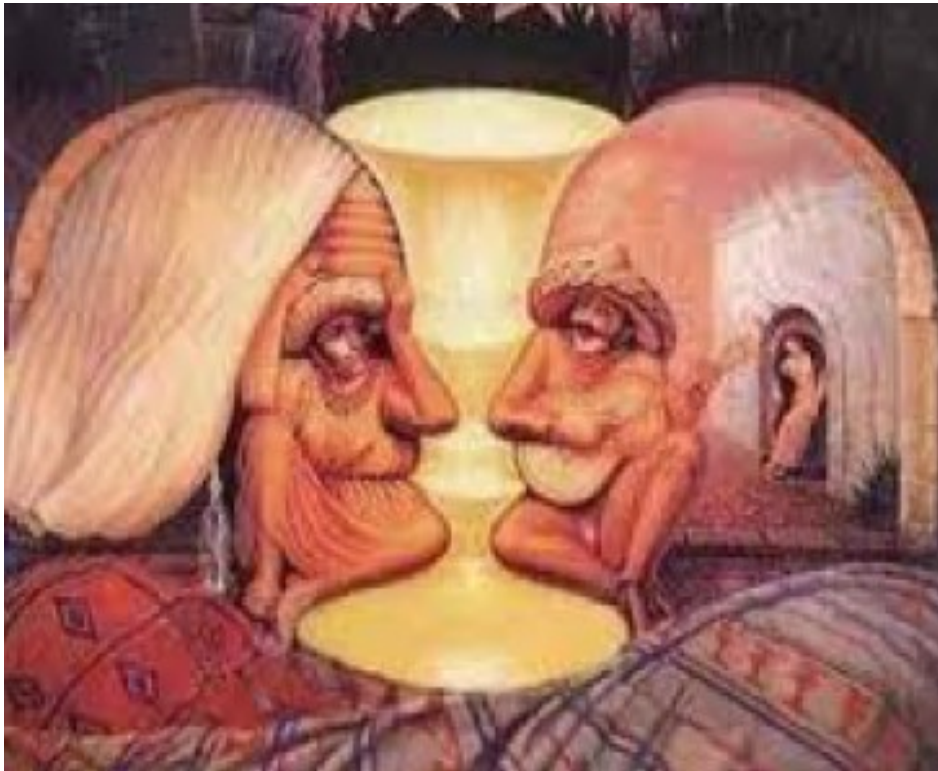


“The many faces of neutron stars” ...

phase transition = transition from a vase to a face



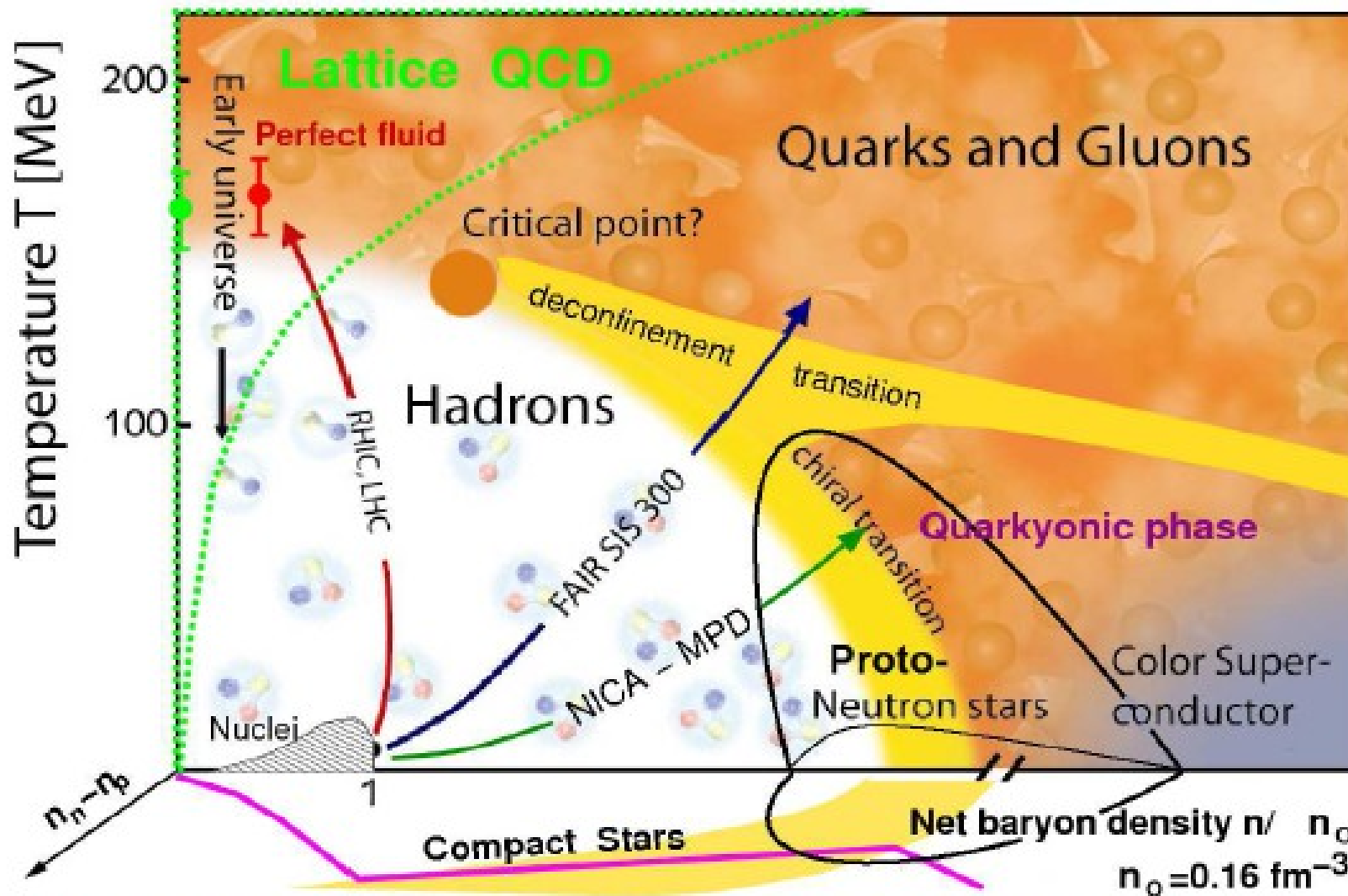
“holy grail”



face diagram



Support a CEP in QCD phase diagram with Astrophysics?



NICA White Paper, <http://theor.jinr.ru/twiki-cgi/view/NICA/WebHome>

Crossover at finite T (Lattice QCD) + First order at zero T (Astrophysics) = Critical endpoint exists!

Goal: Measure the cold EoS !

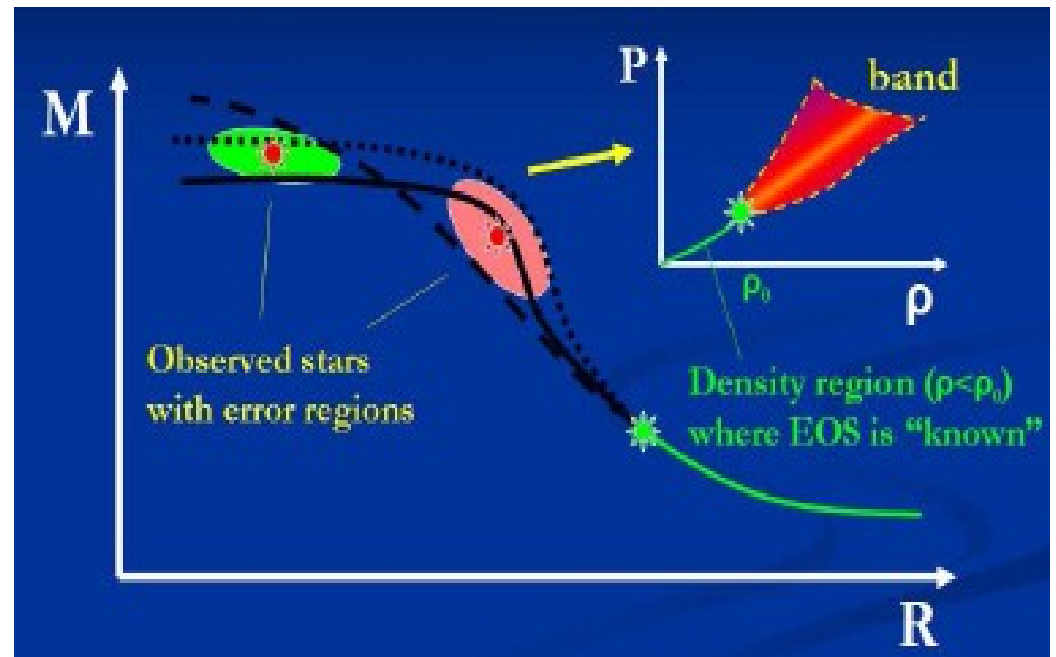
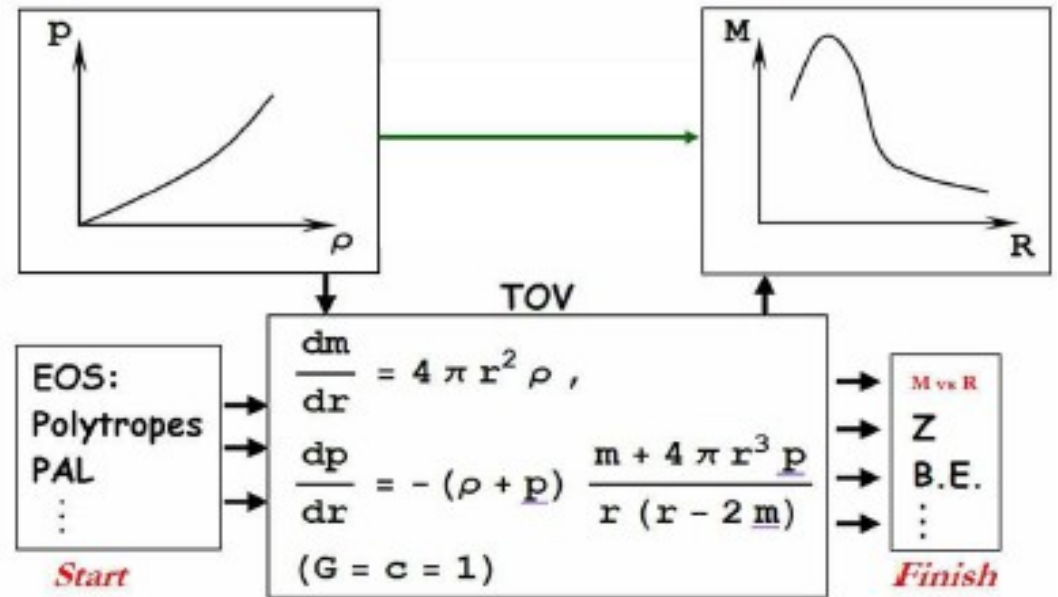
Direct approach:

EoS is given as $P(\rho)$
 \rightarrow solve the TOV Equation
 to find $M(R)$

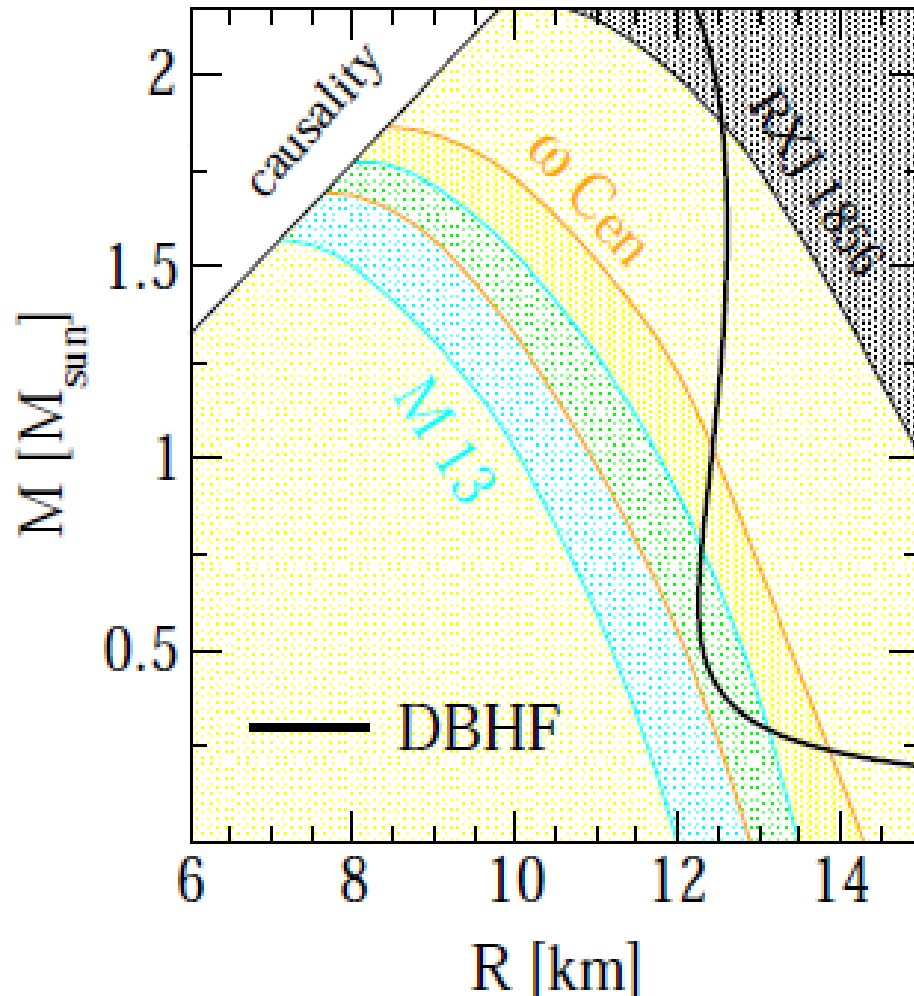
Idea: Invert the approach

Given $M(R) \rightarrow$ find the EoS

Bayesian analysis



Measure masses and radii of CS!



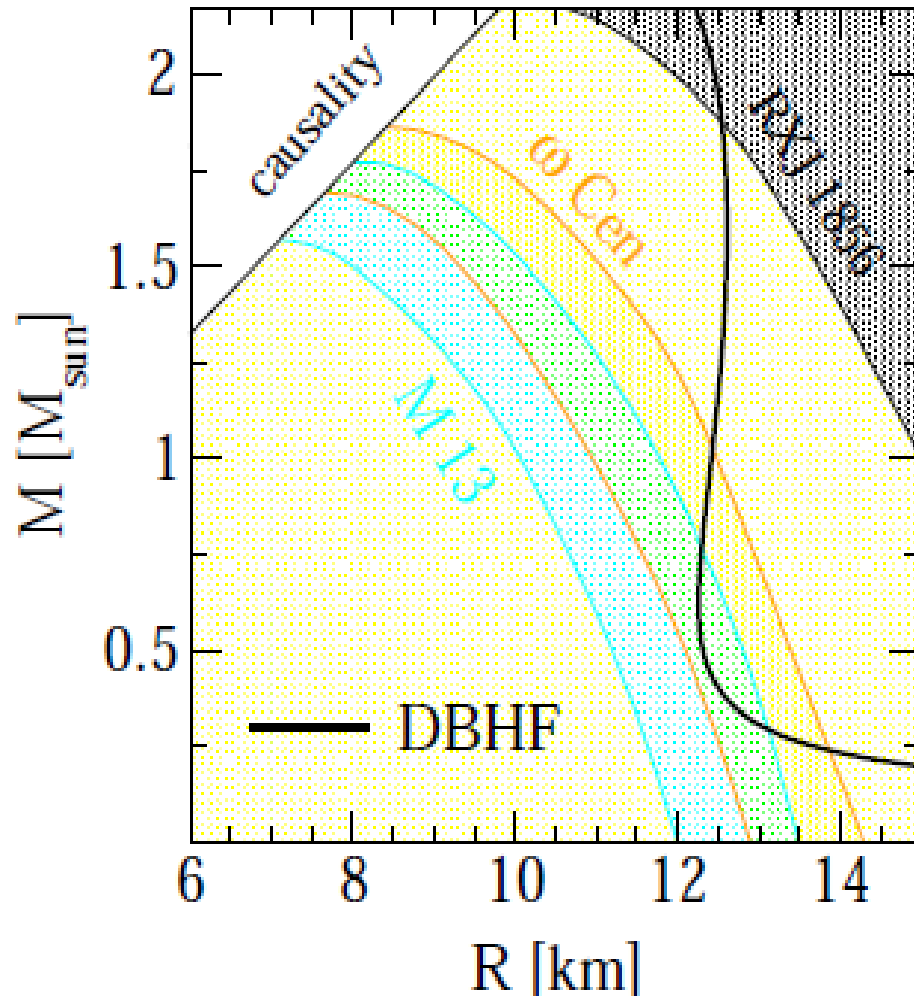
- Distance measured
 - Spectrum measured (ROSAT, XMM, Chandra)
 - Luminosity measured
- effective temperature T_{∞}
 → photospheric radius

$$R_{\infty} = \frac{R}{\sqrt{1 - R_s/R}}, \quad R_s = 2GM$$

Object	R_{∞} [km]	Reference
RXJ 1856	16.8	Trümper et al. (2004)
ω Cen	13.6 ± 0.3	Gendre et al. (2003)
M13	12.8 ± 0.4	Gendre et al. (2004)

Lower limit from RXJ 1856 incompatible with ω Cen and M13 ?

Measure masses and radii of CS!



- Distance measured
 - Spectrum measured (ROSAT, XMM, Chandra)
 - Luminosity measured
- effective temperature T_{∞}
 → photospheric radius

$$R_{\infty} = \frac{R}{\sqrt{1 - R_s/R}}, \quad R_s = 2GM$$

Object	R_{∞} [km]	Reference
RXJ 1856	16.8	Trümper et al. (2004)
ω Cen	13.6 ± 0.3	Gendre et al. (2003)
M13	12.8 ± 0.4	Gendre et al. (2004)

Lower limit from RXJ 1856 incompatible with ω Cen and M13 ?

... unless the latter sources emit X-rays from “hot spots” → lower limit on R

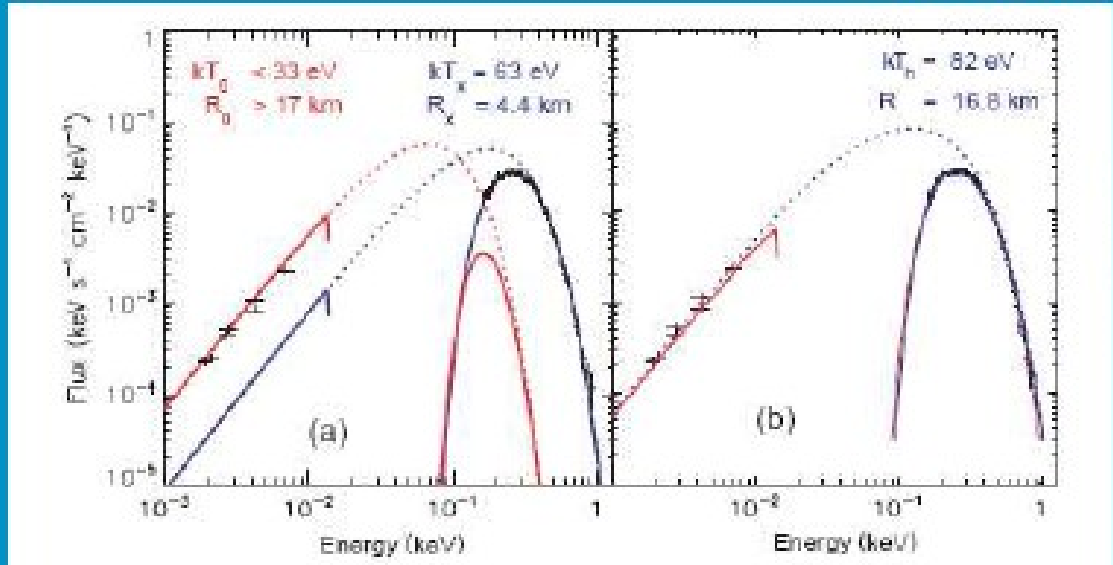
The lesson learned from RX J1856

blackbody fits to the optical and X-ray spectra of RX J1856.5-3754 (Trümper, 2004)

radius determination \Rightarrow EoS \Rightarrow state of matter at high densities

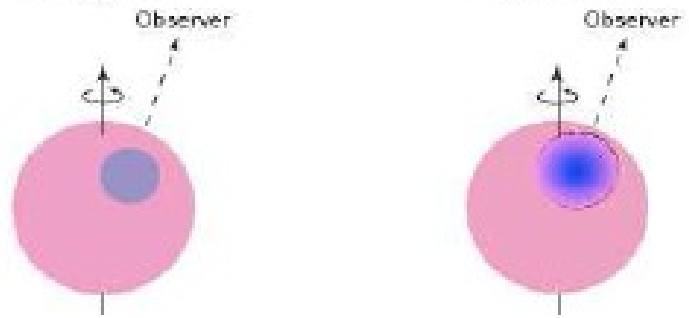
two-component model

model with continuous T-distribution



completely featureless X-ray spectrum:
condensed surface?
 \Rightarrow strong B?

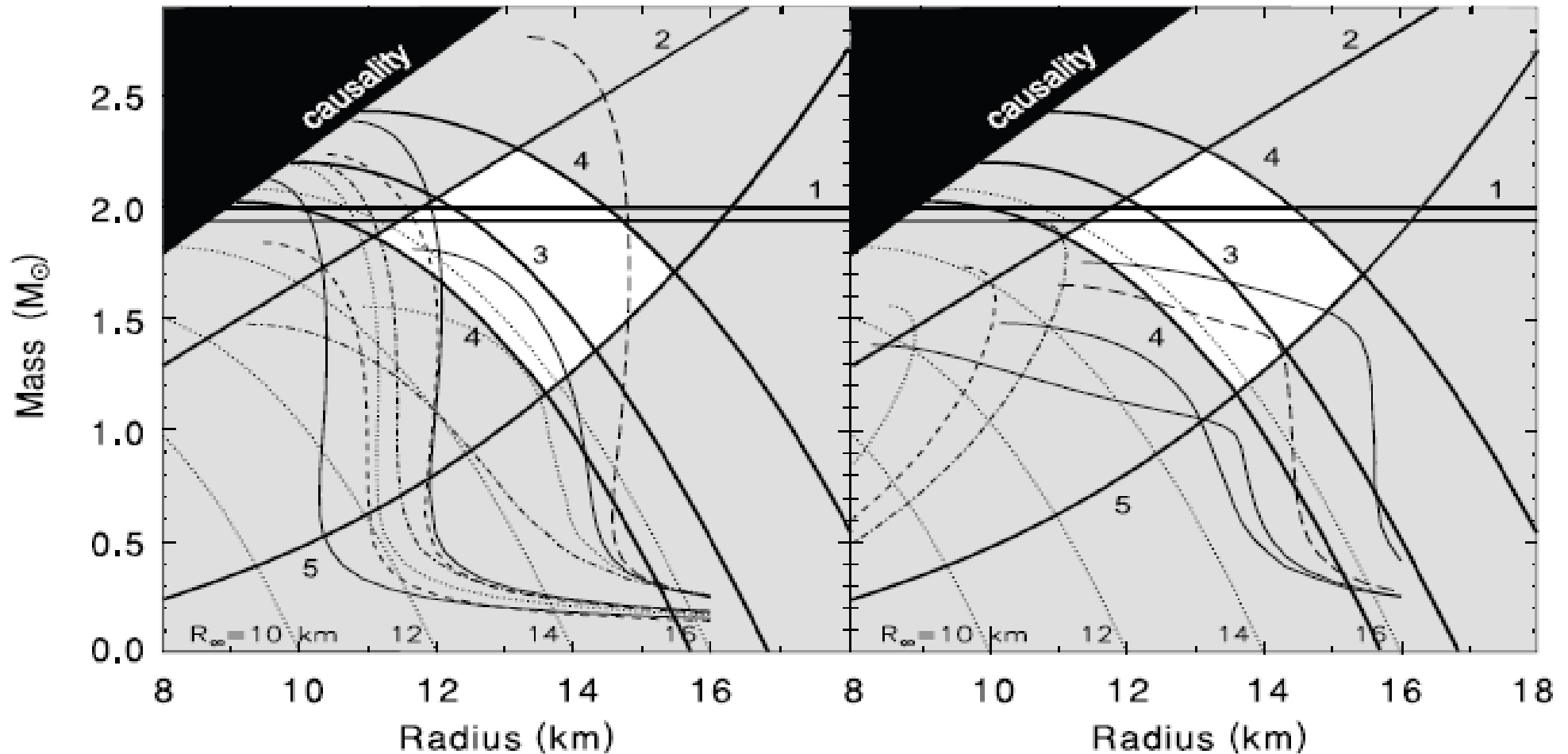
$L_x = 5.4 \times 10^{30} \text{ erg s}^{-1}$



pulsed fraction $< 1\% \Rightarrow$
line of sight \parallel rotation axis?

X-ray emitting region is a “hot spot”, J. Trümper et al., Nucl. Phys. Proc. Suppl. 132 (2004) 560

Which constraints can be trusted ?



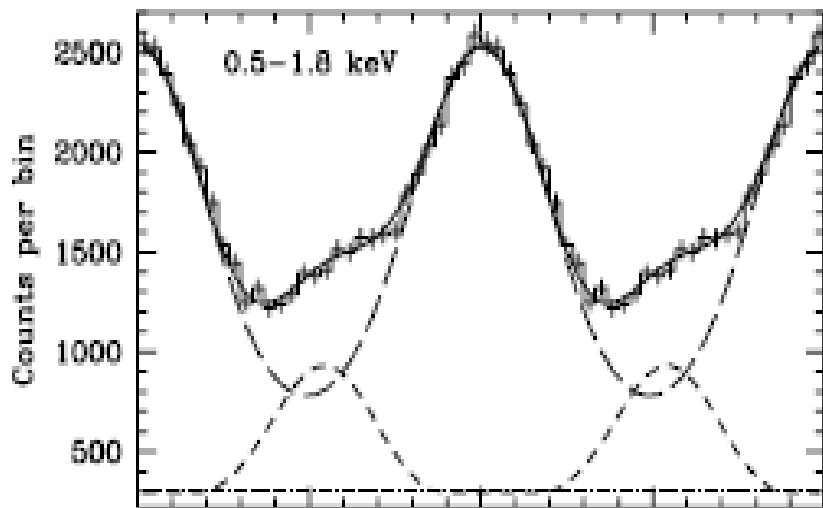
- 1 – Largest mass J1614 – 2230 (Demorest et al. 2010)
- 2 – Maximum gravity XTE 1814 – 338 (Bhattacharyya et al. (2005)
- 3 – Minimum radius RXJ 1856 – 3754 (Trumper et al. 2004)
- 4 – Radius, 90% confidence limits LMXB X7 in 47 Tuc (Heinke et al. 2006)
- 5 – Largest spin frequency J1748 – 2446 (Hessels et al. 2006)

Which constraints can be trusted ?

Nearest millisecond pulsar PSR J0437 – 4715 revisited by XMM Newton

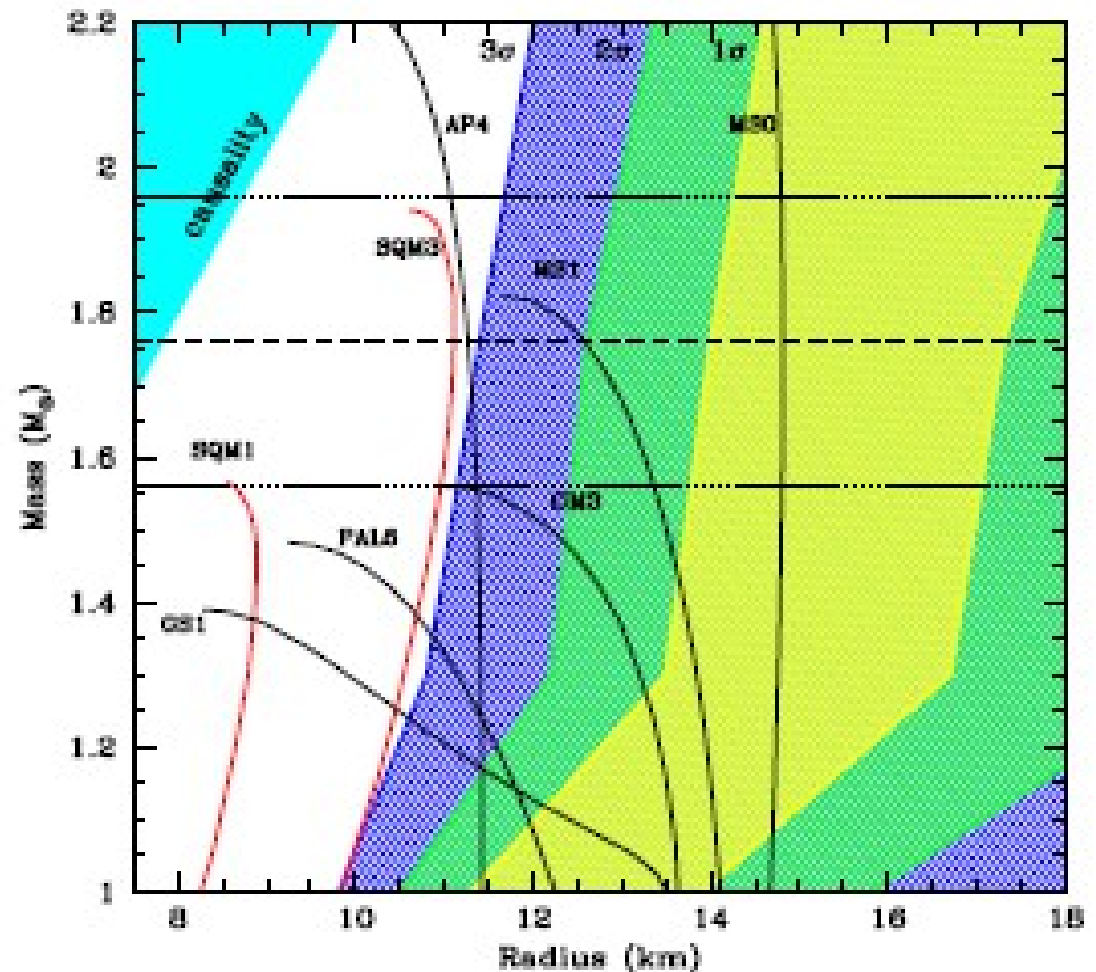
Distance: $d = 156.3 \pm 1.3$ pc

Period: $P = 5.76$ ms, $\dot{P} = 10^{-20}$ s/s, field strength $B = 3 \times 10^8$ G



Three thermal component fit
 $R > 11.1$ km (at 3 sigma level)
 $M = 1.76 M_{\text{sun}}$

S. Bogdanov, arxiv:1211.6113 (2012)



Nuclear Matter Equations of State (EoS)

Several approaches to describe dense nuclear matter

➔ Equations of State at $T = 0$

$$\varepsilon(n_n, n_p, n_e, n_\mu) \rightarrow \varepsilon_h(n_n, n_p) + \sum_{e,\mu} \varepsilon_i(n_i),$$

$$\mu_i = \frac{d\varepsilon}{dn_i}, P = \sum_{n,p,e,\mu} \mu_i n_i - \varepsilon_h - \varepsilon_l$$

➔ expanding binding energy per particle in terms of isospin asymmetry $\beta = \frac{n_n - n_p}{n_n + n_p} = 1 - 2x_p$, $n = n_n + n_p$

$$E(n, \beta) = E_0(n) + \beta^2 E_S(n)$$

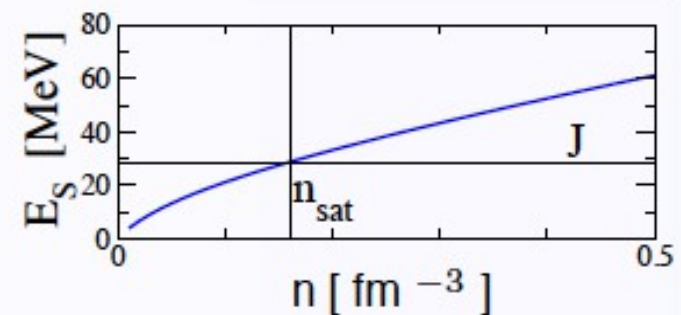
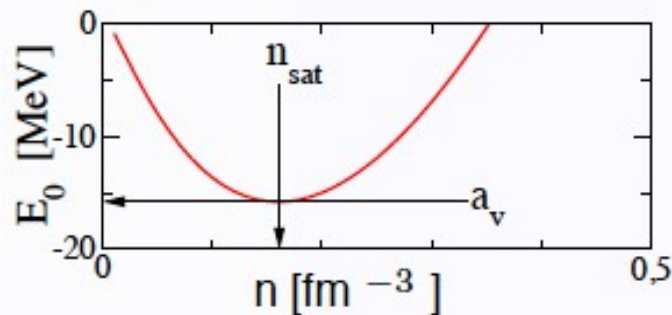
➔ Thermodynamical Identities hold in SNM and NSM

Nuclear Matter Equations of State (EoS)

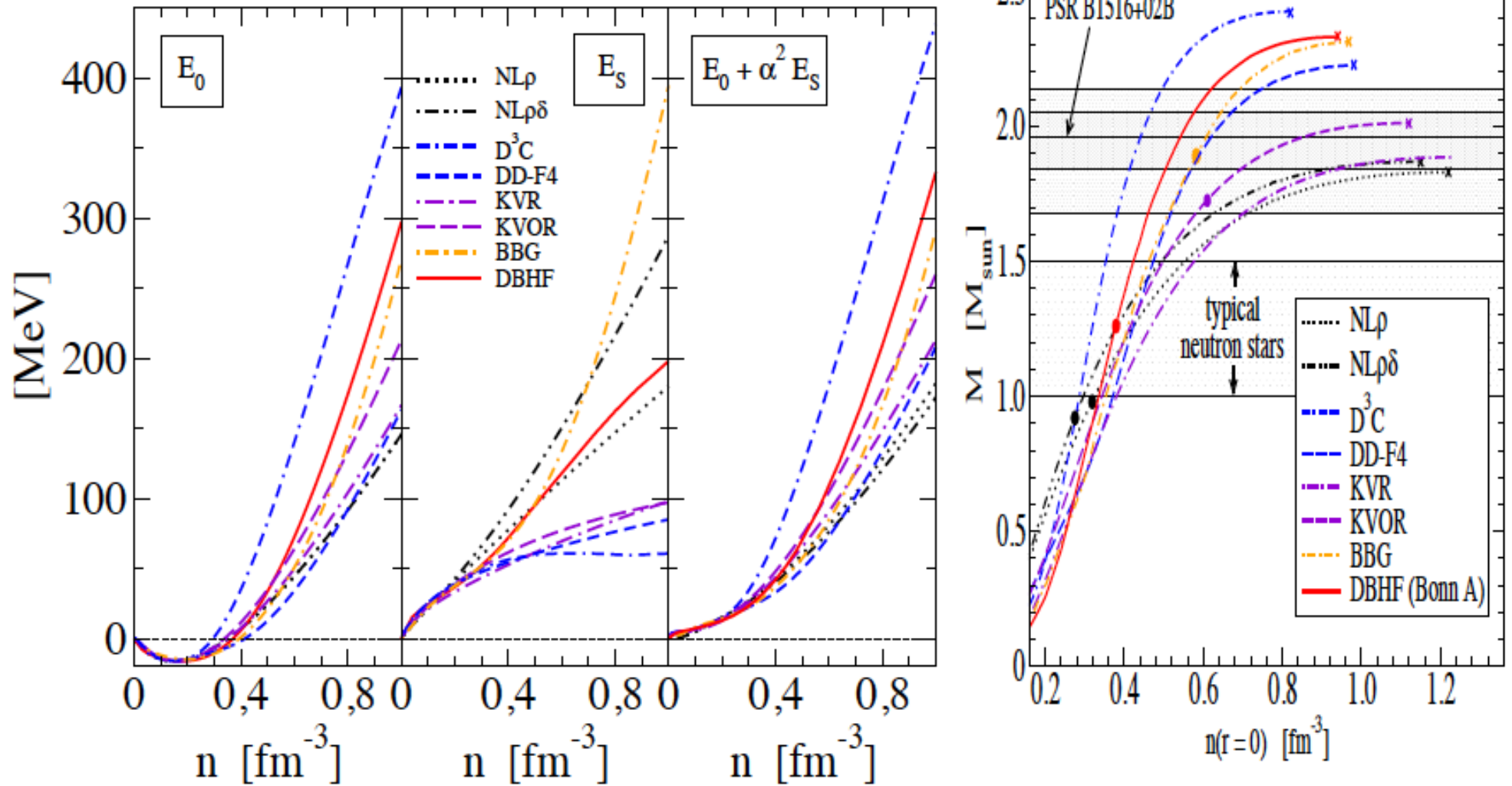
$$E(n, \beta) = E_0(n) + \beta^2 E_S(n) \approx a_V + \frac{K}{18} \epsilon^2 - \frac{K'}{162} \epsilon^3 + \dots + \beta^2 \left(J + \frac{L}{3} \epsilon + \dots \right) + \dots$$

$$\epsilon = (n - n_{\text{sat}})/n \quad \beta = (n_n - n_p)/(n_n + n_p)$$

Model	n_{sat}	a_V	K	K'	J	L	m_D/m
	[fm ⁻³]	[MeV]	[MeV]	[MeV]	[MeV]	[MeV]	
NL ρ	0.1459	-16.062	203.3	576.5	30.8	83.1	0.603
NL $\rho\delta$	0.1459	-16.062	203.3	576.5	31.0	92.3	0.603
DBHF	0.1779	-16.160	201.6	507.9	33.7	69.4	0.684
DD	0.1487	-16.021	240.0	-134.6	32.0	56.0	0.565
D ³ C	0.1510	-15.981	232.5	-716.8	31.9	59.3	0.541
KVR	0.1600	-15.800	250.0	528.8	28.8	55.8	0.800
KVOR	0.1600	-16.000	275.0	422.8	32.9	73.6	0.800
DD-F	0.1469	-16.024	223.1	757.8	31.6	56.0	0.556

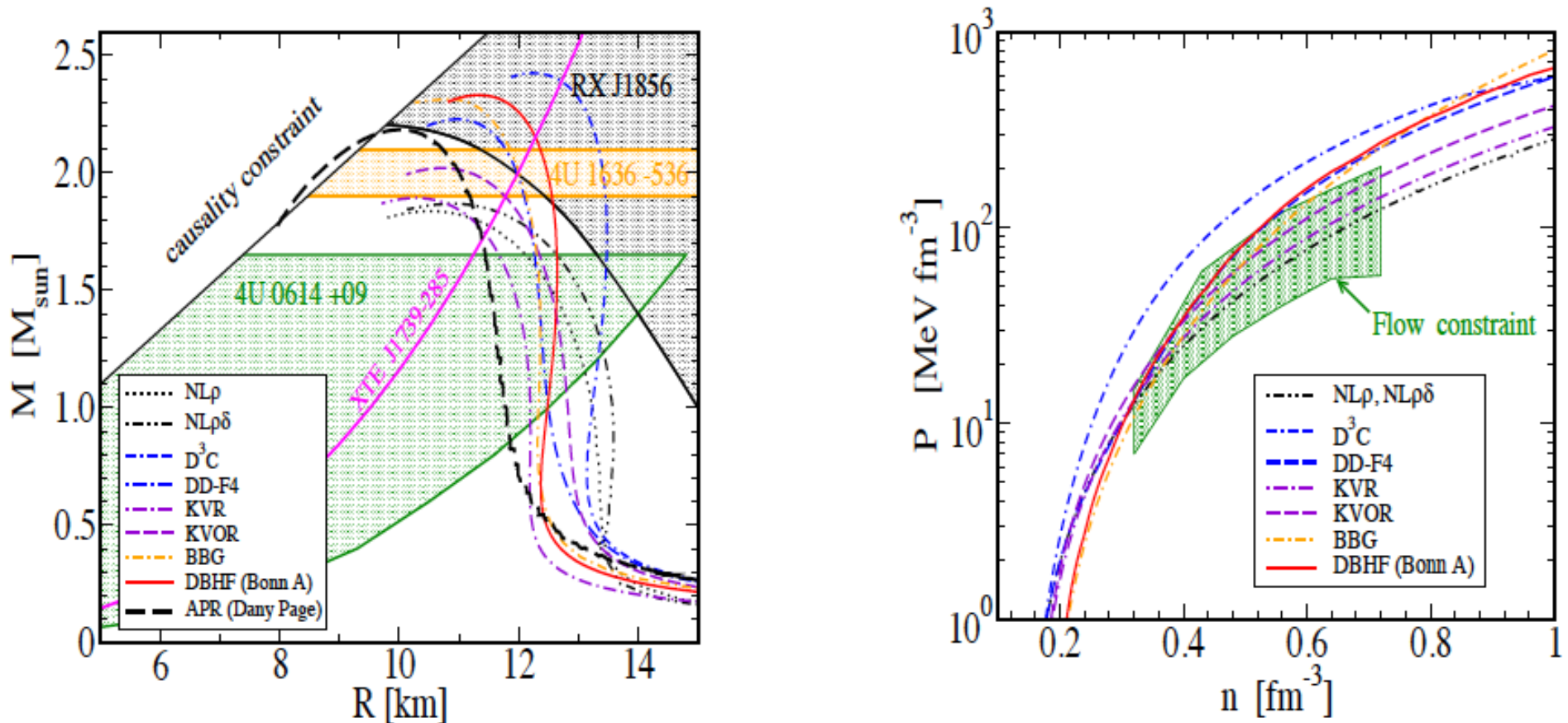


EoS and masses - DU constraint



DU threshold for most hadronic EoS active in neutron stars with typical masses !
 Klähn, et al., PRC 74, 035802 (2006); [nucl-th/0602038]

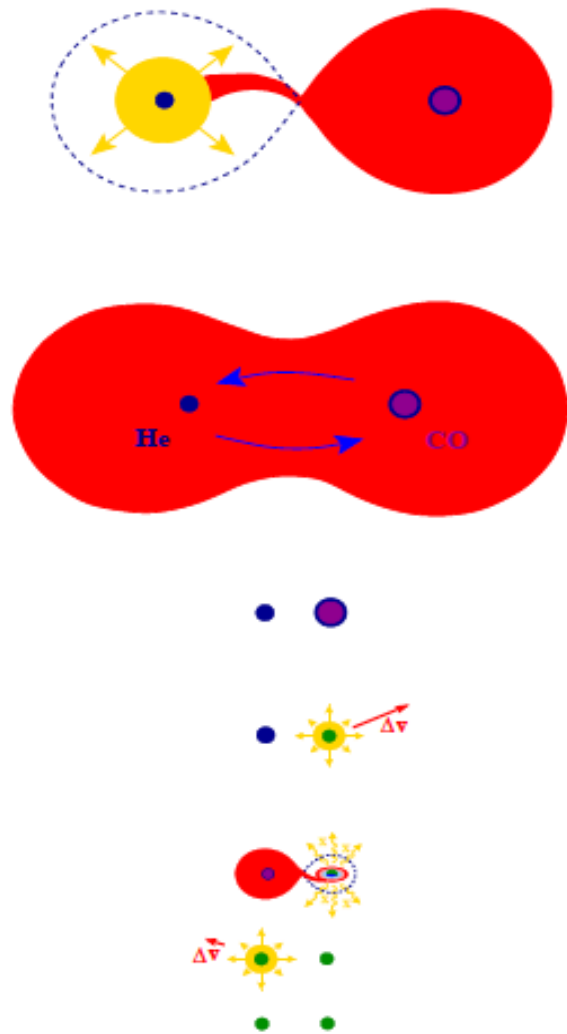
Mass-Radius constraint and Flow constraint



- Large Mass ($\sim 2 M_{\odot}$) and radius ($R \geq 12$ km) \Rightarrow stiff EoS;
- Flow in Heavy-Ion Collisions \Rightarrow not too stiff EoS !

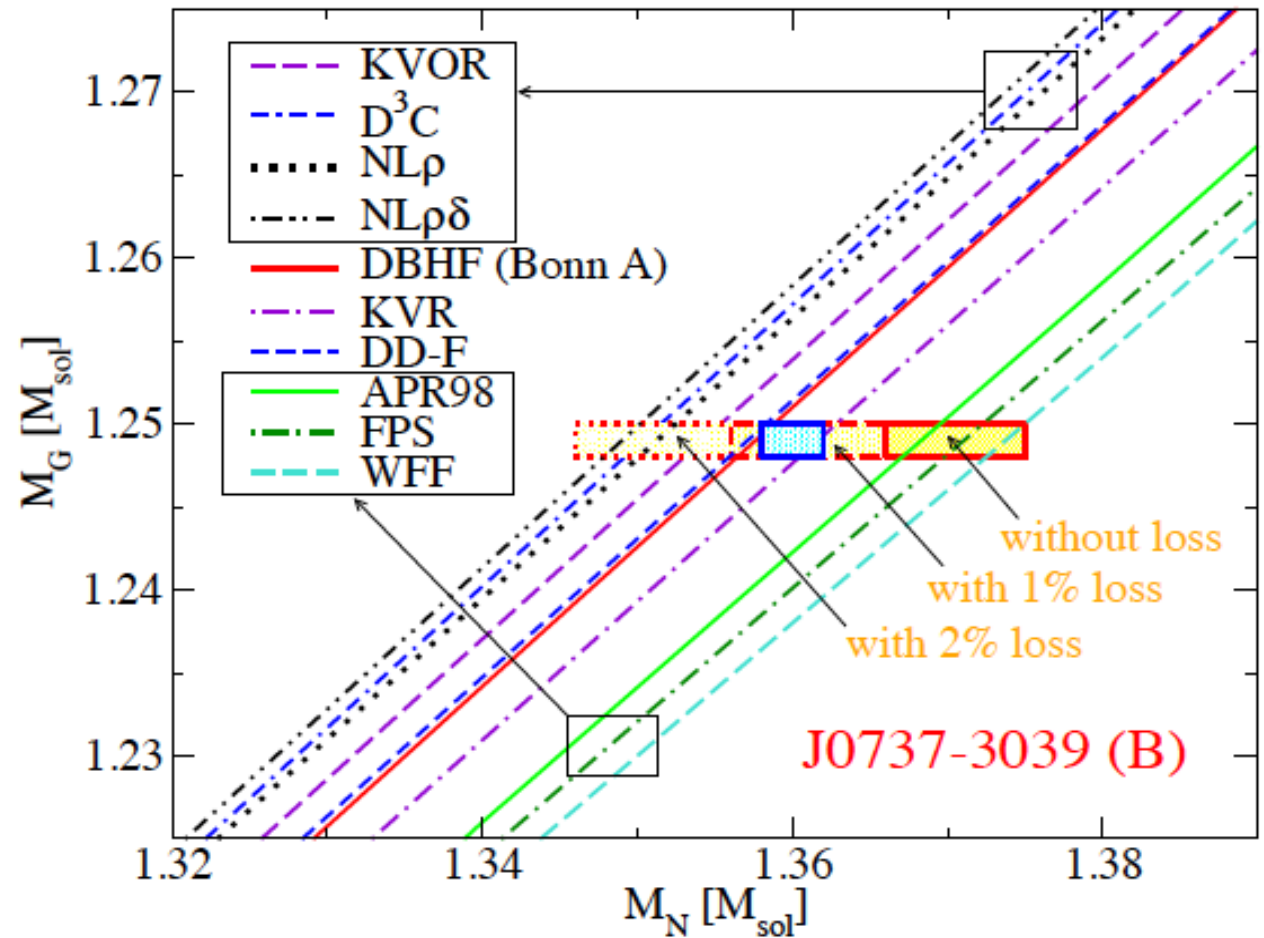
EoS constraint from double pulsar J0737-3039?

Double core scenario:



Dewi et al., MNRAS (2006)

Baryon mass vs. gravitational mass - constraint or consistency check?

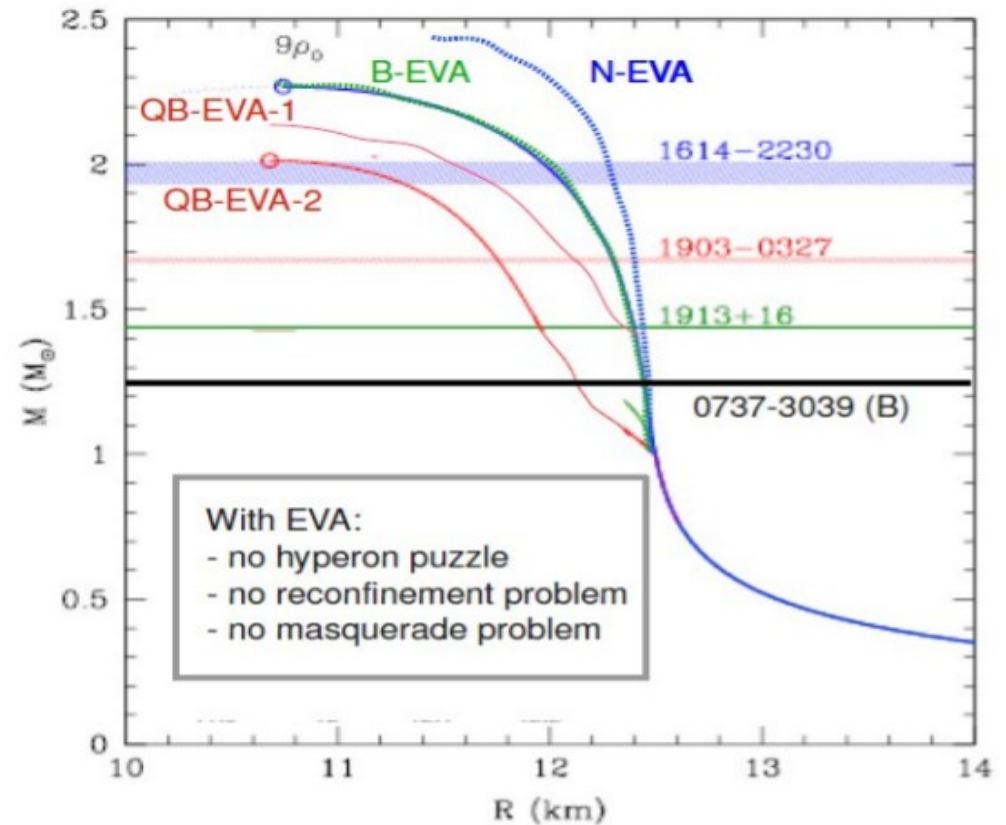
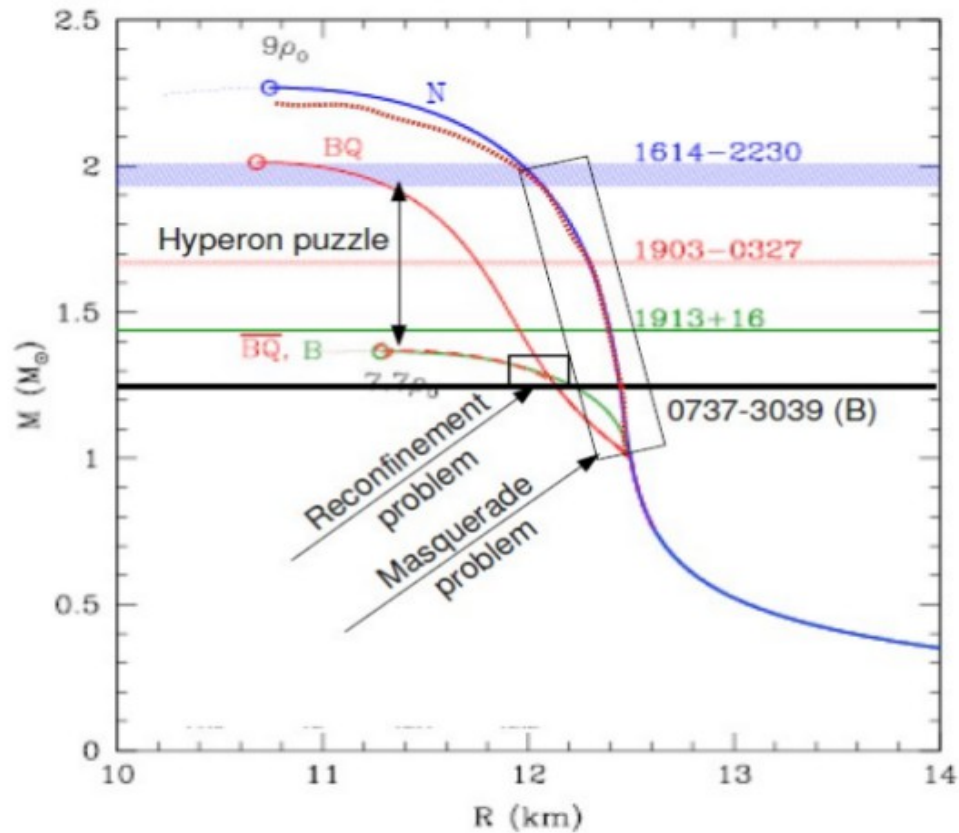


Podsiadlowski et al., MNRAS 361 (2005) 1243

Kitaura, Janka, Hillebrandt, A& A (2006); [astro-ph/0512065]

D.B., T. Klähn, F. Weber, CBM Physics Book (2008)

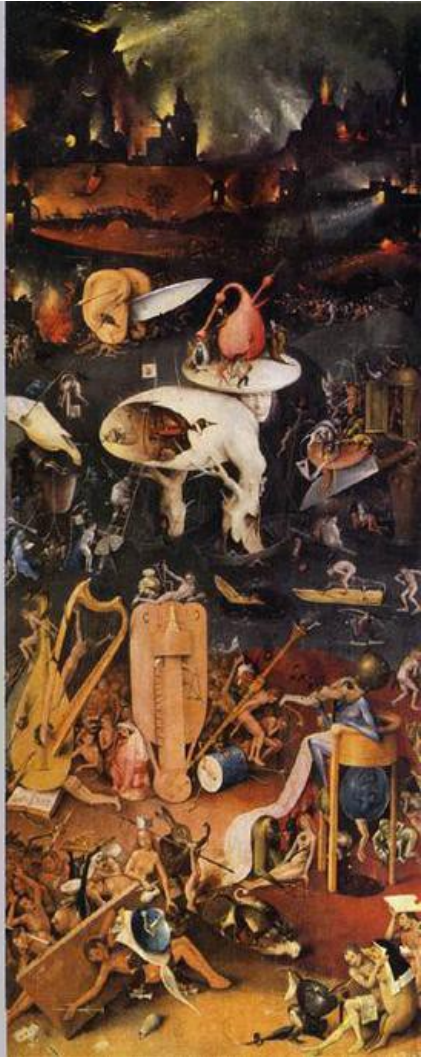
Hyperon puzzle & quark matter



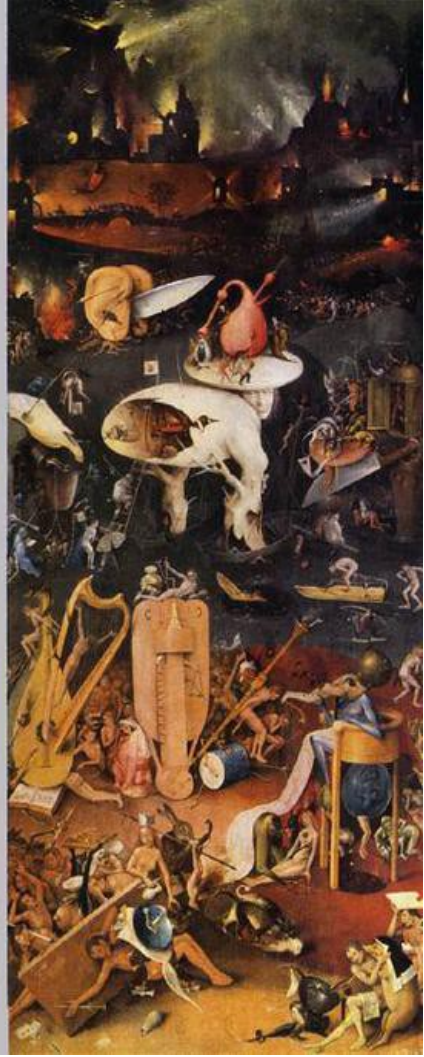
Mass-radius sequences for different model equations of state (EoS) illustrate how the **three major problems** in the theory of exotic matter in compact stars (left panel) can be solved (right panel) by taking into account the baryon size effect within a excluded volume approximation (EVA). Due to the EVA both, the nucleonic (N-EVA) and hyperonic (B-EVA) EoS get sufficiently stiffened to describe high-mass pulsars so that the hyperon puzzle gets solved which implies a removal of the reconfinement problem. Since the EVA does not apply to the quark matter EoS it shall be always sufficiently different from the hadronic one so that the masquerade problem is solved.

2. Microphysical approach to strong 1st order PT

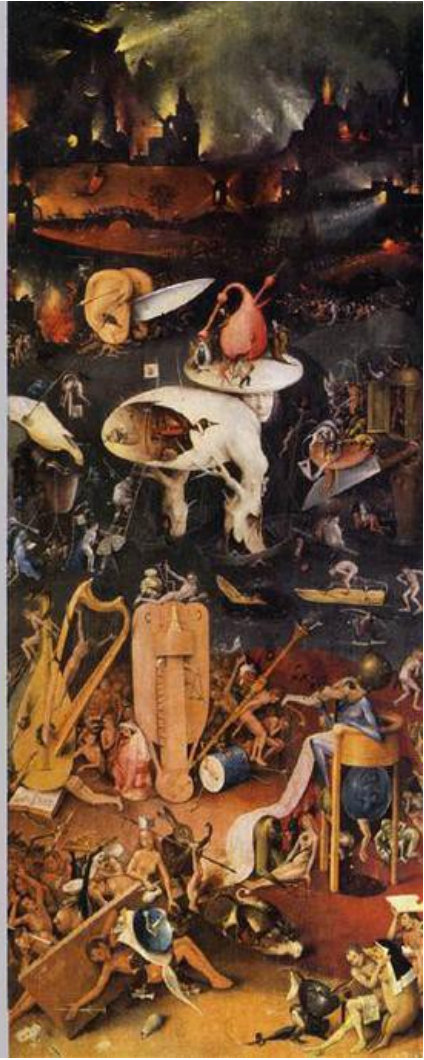
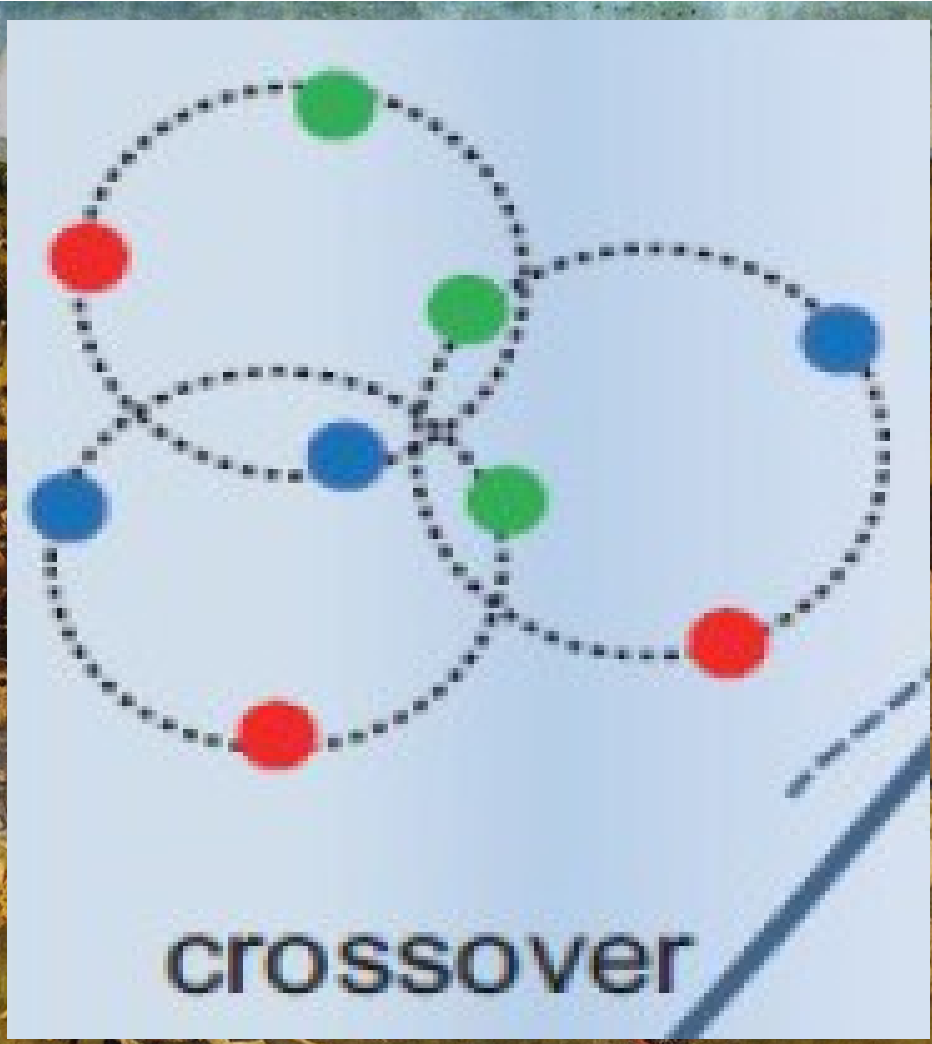
2. Story “Three-window picture of dense matter”



2. Story “Three-window picture of dense matter”

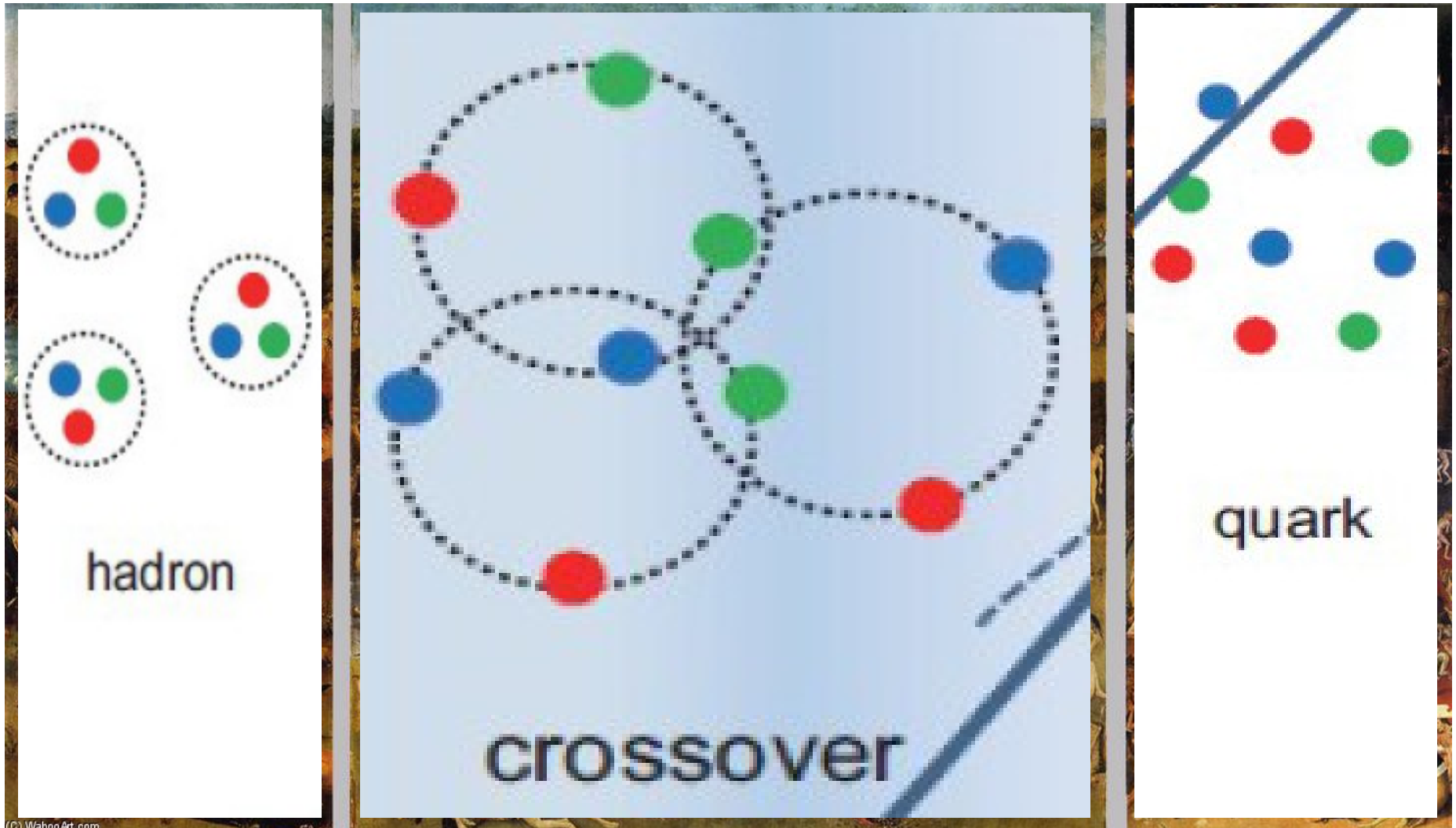


2. Story “Three-window picture of dense matter”



(C) WahooArt.com

2. Story “Three-window picture of dense matter”



Hadron-Quark Crossover and Massive Hybrid Stars

Kota Masuda^{1,2,*}, Tetsuo Hatsuda², and Tatsuyuki Takatsuka^{3†}

¹*Department of Physics, The University of Tokyo, Tokyo 113-0033, Japan*

²*Theoretical Research Division, Nishina Center, RIKEN, Wako 351-0198, Japan*

³*Iwate University, Morioka 020-8550, Japan*

**E-mail: masuda@nt.phys.s.u-tokyo.ac.jp*

.....
On the basis of the percolation picture from the hadronic phase with hyperons to the quark phase with strangeness, we construct a new equation of state (EOS) with the pressure interpolated as a function of the baryon density. The maximum mass of neutron stars can exceed $2M_{\odot}$ if the following two conditions are satisfied; (i) the crossover from the hadronic matter to the quark matter takes place at around three times the normal nuclear matter density, and (ii) the quark matter is strongly interacting in the crossover region. This is in contrast to the conventional approach assuming the first order phase transition in which the EOS becomes always soft due to the presence of the quark matter at high density. Although the choice of the hadronic EOS does not affect the above conclusion on the maximum mass, the three-body force among nucleons and hyperons plays an essential role for the onset of the hyperon mixing and the cooling of neutron stars.
.....

Subject Index Neutron stars, Nuclear matter aspects in nuclear astrophysics, Hadrons and quarks in nuclear matter, Quark matter

1. Introduction

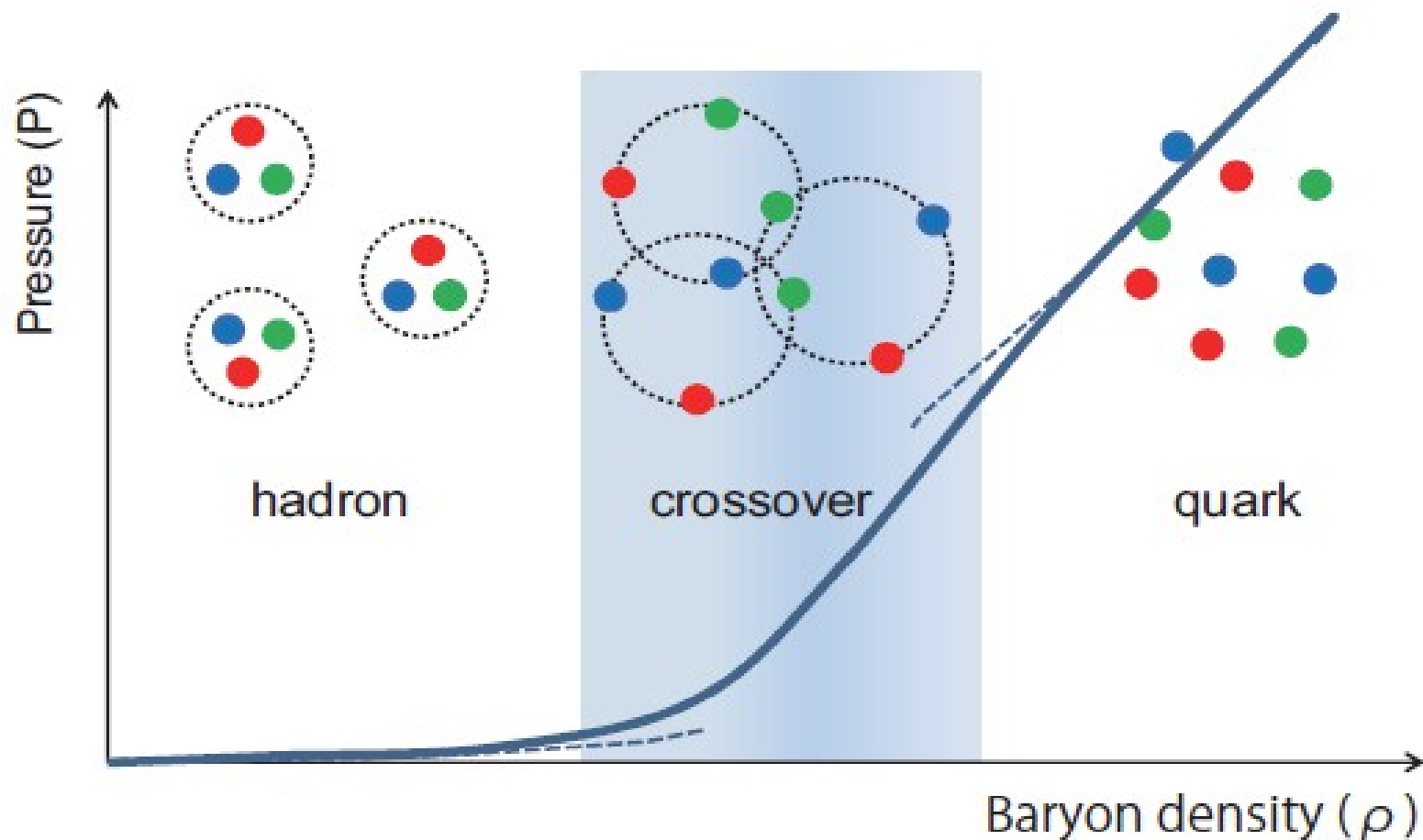
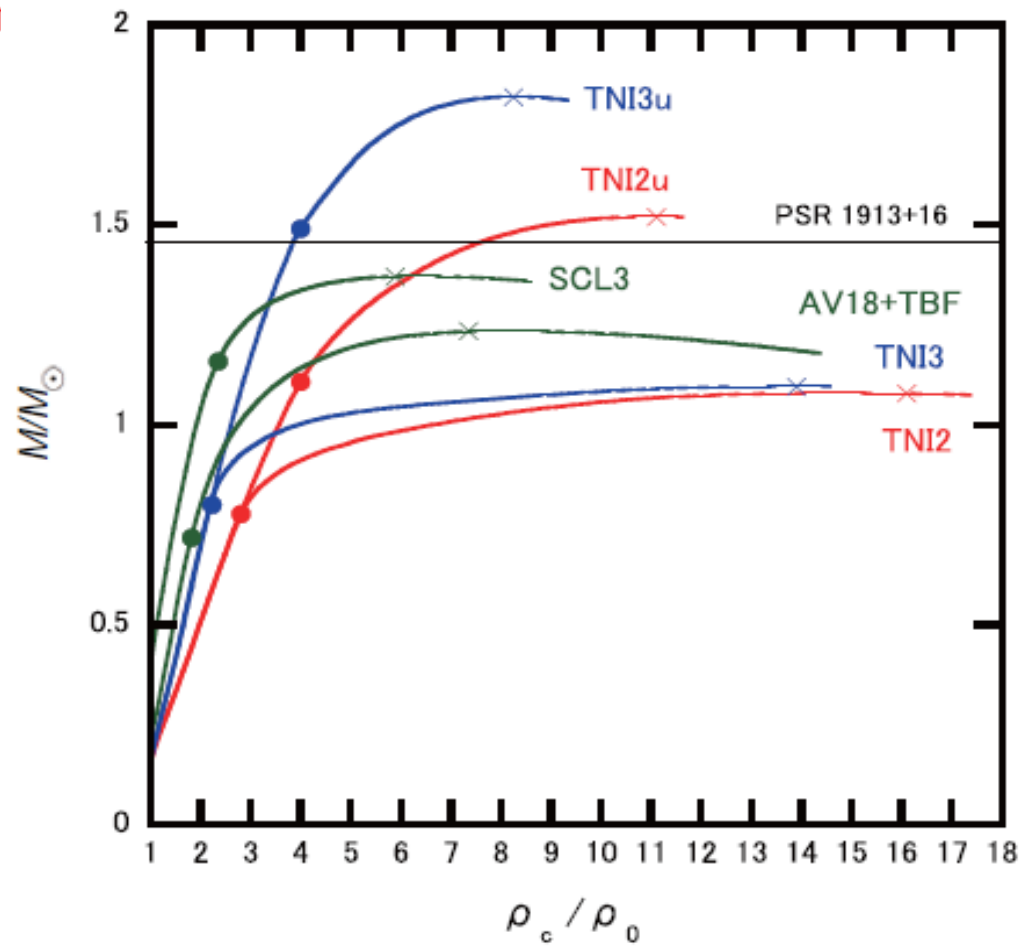
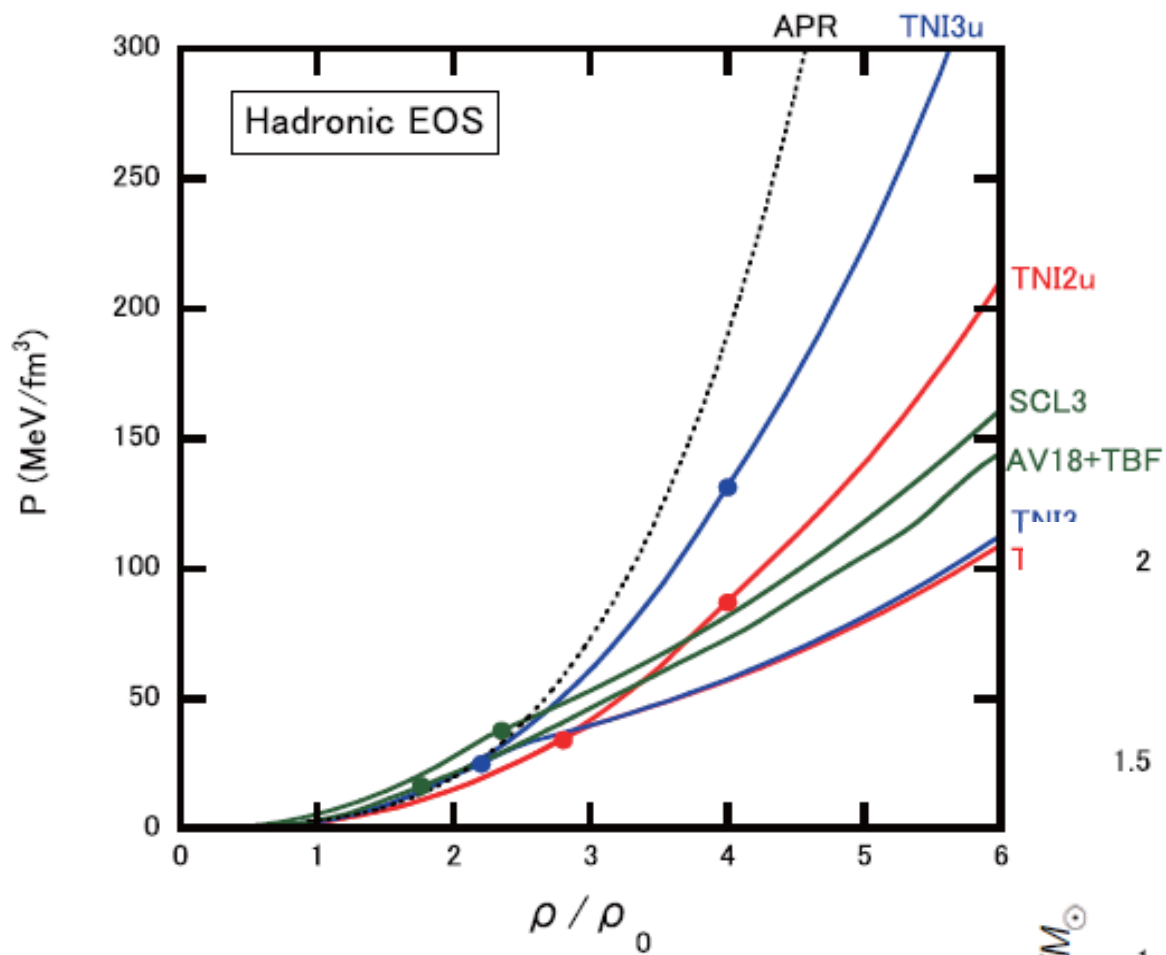


Fig. 1 Schematic picture of the QCD pressure (P) as a function of the baryon density (ρ) under the assumption of the hadron-quark crossover. The crossover region where finite-size hadrons start to overlap and percolate is shown by the shaded area. The pressure calculated on the basis of the point-like hadrons (shown by the dashed line at low density) and that calculated on the basis of weakly interacting quarks (shown by the dashed line at high density) lose their validity in the crossover region, so that the naive use of the Gibbs conditions by extrapolating the dashed lines is not justified in general.

2. Hadronic EOS (H-EOS)

Table 1 Properties of various hadronic EOSs with hyperons; TNI2, TNI3, TNI2u, TNI3u [33, 34], Paris+TBF, AV18+TBF [36–38] and SCL3 $\Lambda\Sigma$ [39]. κ is the nuclear incompressibility and ρ_{th} is the threshold density of hyperon-mixing with ρ_0 ($=0.17/\text{fm}^3$) being the normal nuclear density. R and ρ_c denote the radius and central density for the maximum mass (M_{max}) NS, respectively. The numbers in the parentheses are those without hyperons. *s indicate that the numbers are read from the figures in [36].

EOS	TNI2	TNI3	TNI2u	TNI3u	Paris+TBF	AV18+TBF	SCL3 $\Lambda\Sigma$
κ (MeV)	250	300	250	300	281	192	211
$\rho_{\text{th}}(\Lambda)/\rho_0$	2.95	2.45	4.01	4.01	2.9*	2.8*	2.24
$\rho_{\text{th}}(\Sigma^-)/\rho_0$	2.83	2.23	4.06	4.01	1.9*	1.8*	2.24
M_{max}/M_{\odot}	1.08 (1.62)	1.10 (1.88)	1.52	1.83	1.26 (2.06)	1.22 (2.00)	1.36 (1.65)
R(km)	7.70 (8.64)	8.28 (9.46)	8.43	9.55	10.46 (10.50)	10.46 (10.54)	11.42 (10.79)
ρ_c/ρ_0	16.10 (9.97)	13.90 (8.29)	11.06	8.26	7.35 (6.47)	7.35 (6.53)	6.09 (6.85)



3. Quark EOS (Q-EOS)

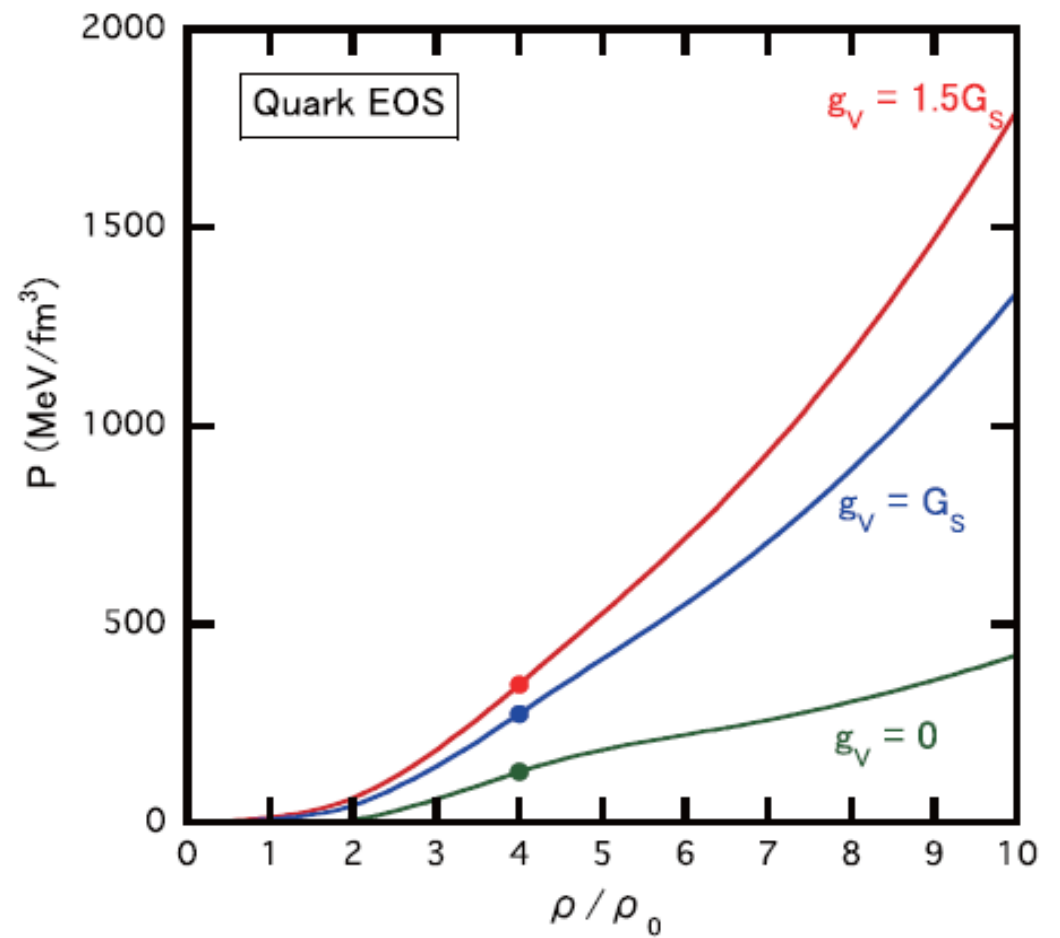
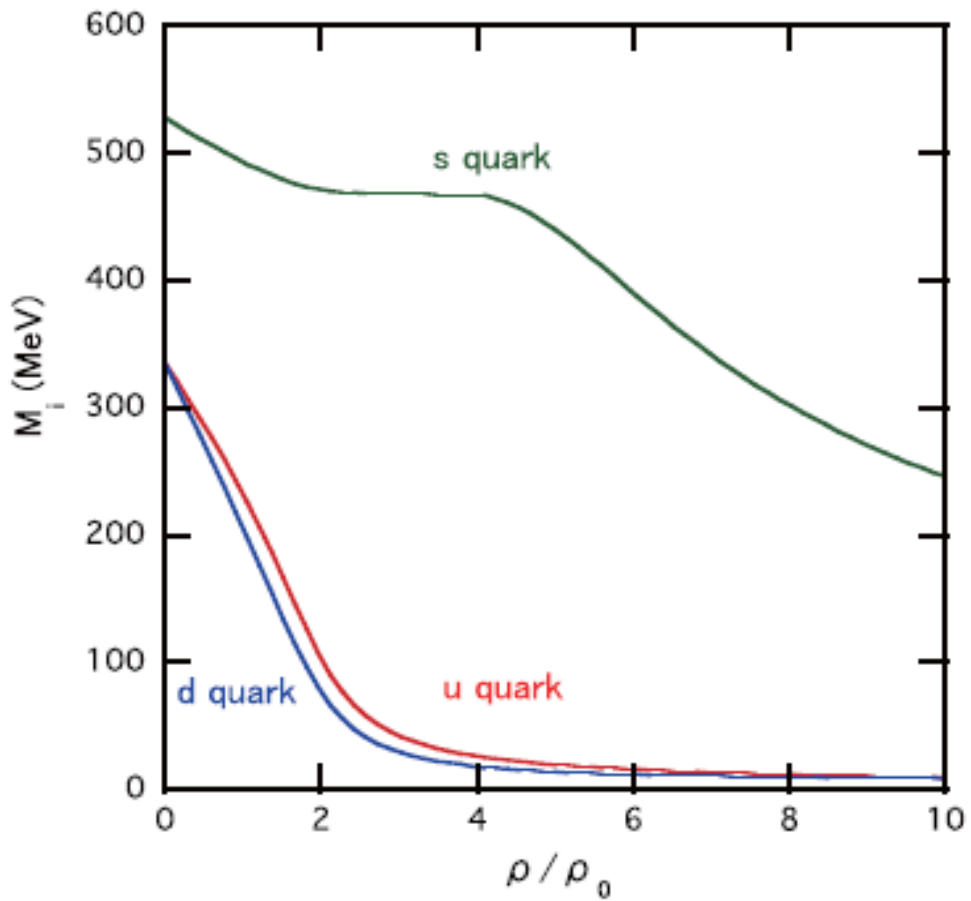
$$\mathcal{L}_{\text{NJL}} = \bar{q}(i\not{\partial} - m)q + \frac{1}{2}G_s \sum_{a=0}^8 [(\bar{q}\lambda^a q)^2 + (\bar{q}i\gamma_5\lambda^a q)^2] - G_D [\det\bar{q}(1 + \gamma_5)q + \text{h.c.}]$$

$$- \left\{ \begin{array}{l} \frac{1}{2}g_v (\bar{q}\gamma^\mu q)^2 \\ \frac{1}{2}G_v \sum_{a=0}^8 [(\bar{q}\gamma^\mu\lambda^a q)^2 + (\bar{q}i\gamma^\mu\gamma_5\lambda^a q)^2] \end{array} \right.$$

$$P(T, \mu_{u,d,s}) = T \sum_i \sum_\ell \int \frac{d^3p}{(2\pi)^3} \text{Tr} \ln \left(\frac{S_i^{-1}(i\omega_\ell, \mathbf{p})}{T} \right) - G_s \sum_i \sigma_i^2 - 4G_D \sigma_u \sigma_d \sigma_s + \left\{ \begin{array}{l} \frac{1}{2}g_v (\sum_i n_i)^2 \\ \frac{1}{2}G_v \sum_i n_i^2 \end{array} \right.$$

$$S_i^{-1} = \not{p} - M_i - \gamma^0 \mu_i^{\text{eff}}, \quad \mu_i^{\text{eff}} \equiv \begin{cases} \mu_i - g_v \sum_j n_j \\ \mu_i - G_v n_i \end{cases}$$

	$\Lambda(\text{MeV})$	$G_s \Lambda^2$	$G_D \Lambda^5$	$m_{u,d}(\text{MeV})$	$m_s(\text{MeV})$
HK	631.4	3.67	9.29	5.5	135.7
RKH	602.3	3.67	12.36	5.5	140.7
LKW	750	3.64	8.9	3.6	87



4. Hadron-Quark crossover

As discussed in §1, treating the point-like hadron as an independent degree of freedom loses its validity as the baryon density approaches to the percolation region. In other words, the system cannot be described neither by an extrapolation of the hadronic EOS from the low-density side nor by an extrapolation of the quark EOS from the high-density side. Under such situation, it does not make much sense to apply the Gibbs criterion of two phases I and II, $P_I(T_c, \mu_c) = P_{II}(T_c, \mu_c)$ since P_I and P_{II} are not reliable in the transition region.

we will consider a phenomenological “interpolation” between the H-EOS and Q-EOS as a first step. Such an interpolation is certainly not unique, but we adopt a simplest

$$P(\rho) = P_H(\rho)f_-(\rho) + P_Q(\rho)f_+(\rho),$$
$$f_{\pm}(\rho) = \frac{1}{2} \left(1 \pm \tanh \left(\frac{\rho - \bar{\rho}}{\Gamma} \right) \right),$$

where P_H and P_Q are the pressure in the hadronic matter and that in the quark matter,

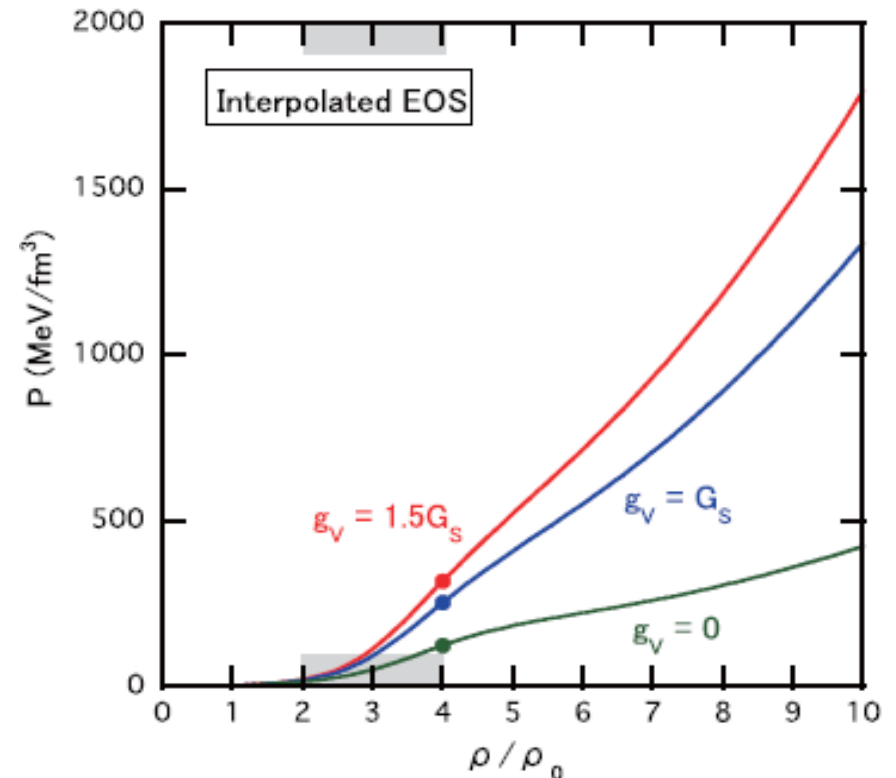
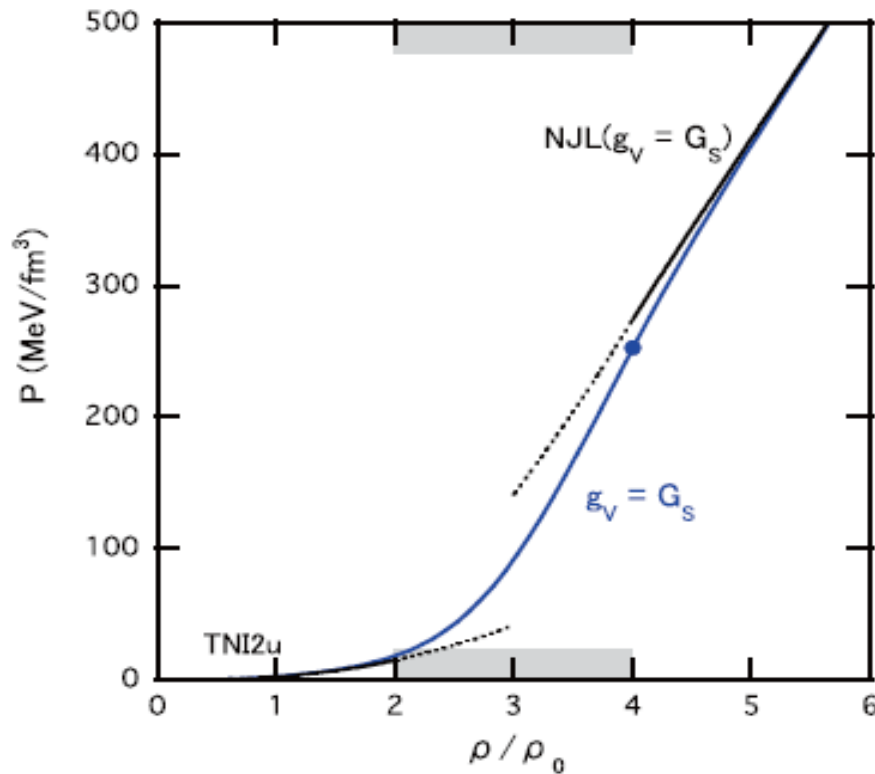
One should not confuse Eq.(7) with the pressure in the mixed phase associated with the first-order phase transition in which f_{\pm} is considered to the volume fraction of each phase. In our crossover picture, the system is always uniform and f_- (f_+) should be interpreted as the degree of reliability of H-EOS (Q-EOS) at given baryon density.

To calculate the energy density ε as a function of ρ in thermodynamically consistent way, we integrate the thermodynamical relation, $P = \rho^2 \partial(\varepsilon/\rho)/\partial\rho$ and obtain

$$\varepsilon(\rho) = \varepsilon_H(\rho)f_-(\rho) + \varepsilon_Q(\rho)f_+(\rho) + \Delta\varepsilon$$

$$\Delta\varepsilon = \rho \int_{\bar{\rho}}^{\rho} (\varepsilon_H(\rho') - \varepsilon_Q(\rho')) \frac{g(\rho')}{\rho'} d\rho'$$

with $g(\rho) = \frac{2}{\Gamma}(e^X + e^{-X})^{-2}$ and $X = (\rho - \bar{\rho})/\Gamma$. Here ε_H (ε_Q) is the energy density obtained from H-EOS (Q-EOS). $\Delta\varepsilon$ is an extra term which guarantees the thermodynamic consistency.



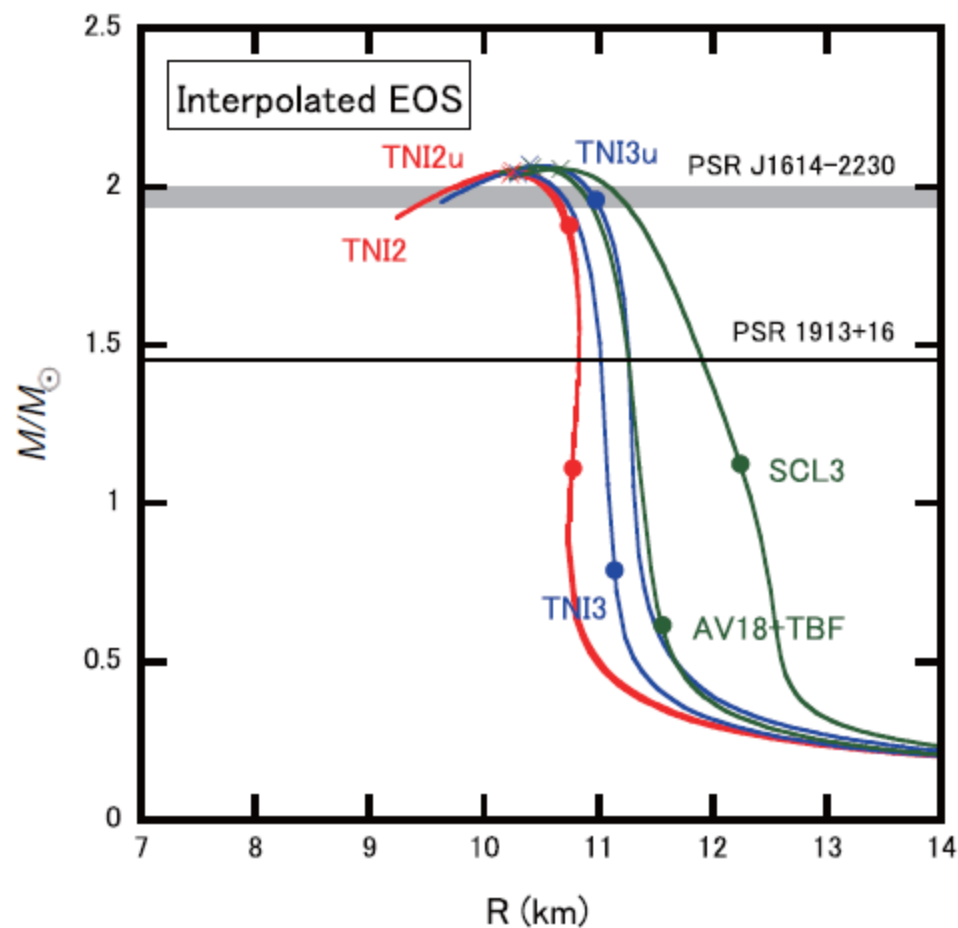
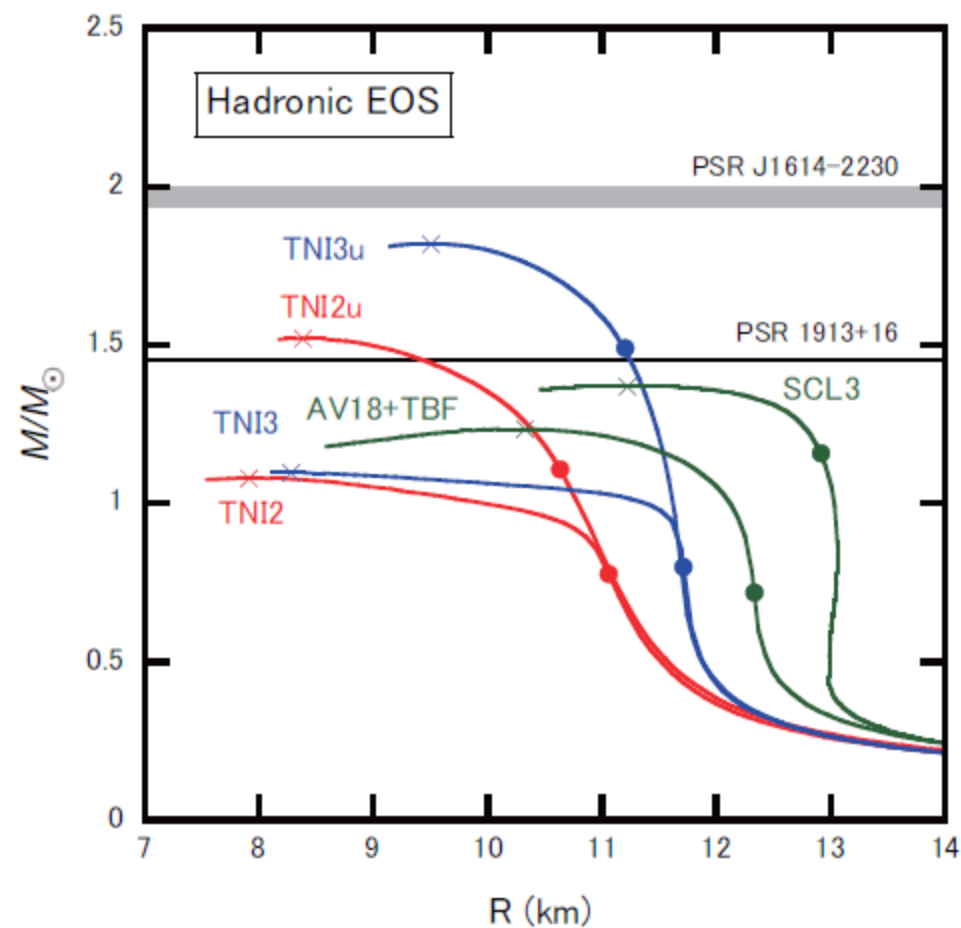
5. Numerical results and discussions

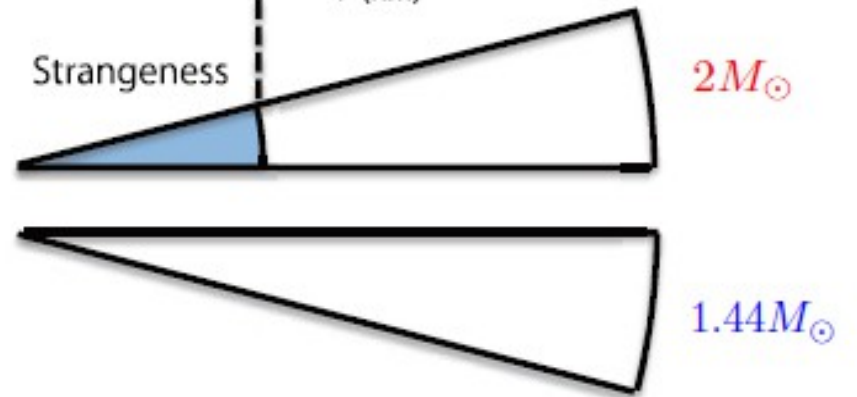
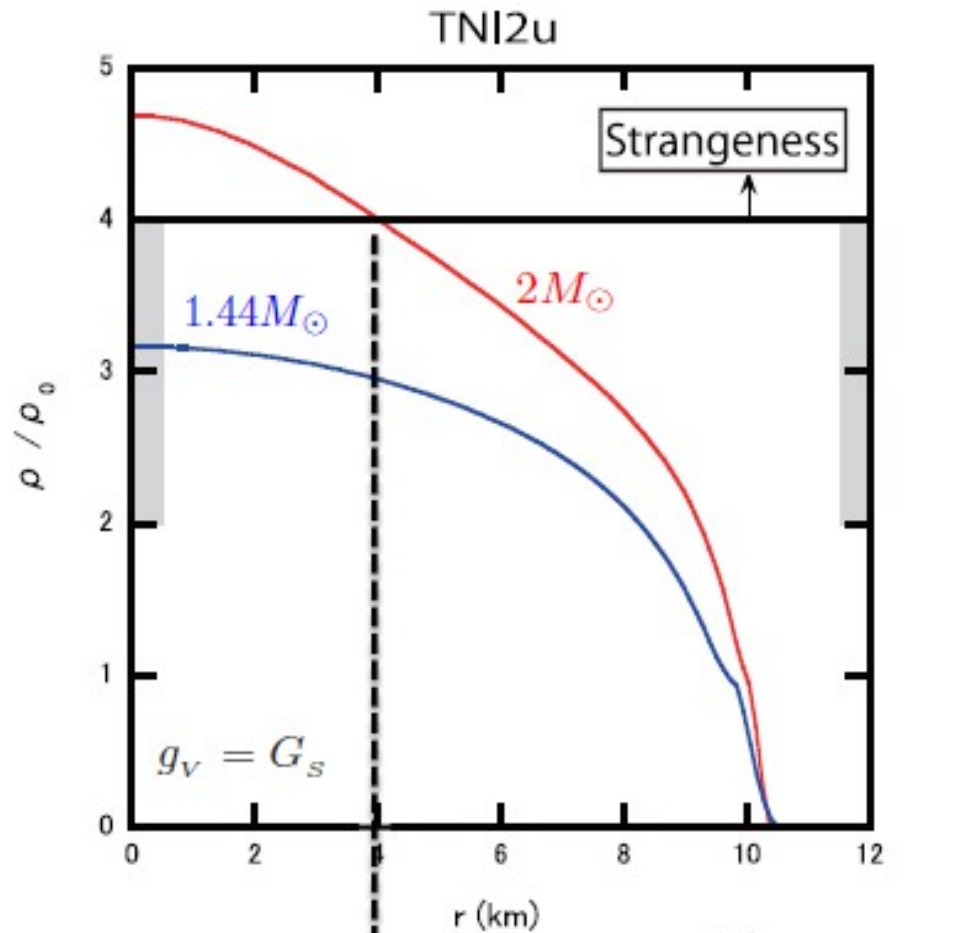
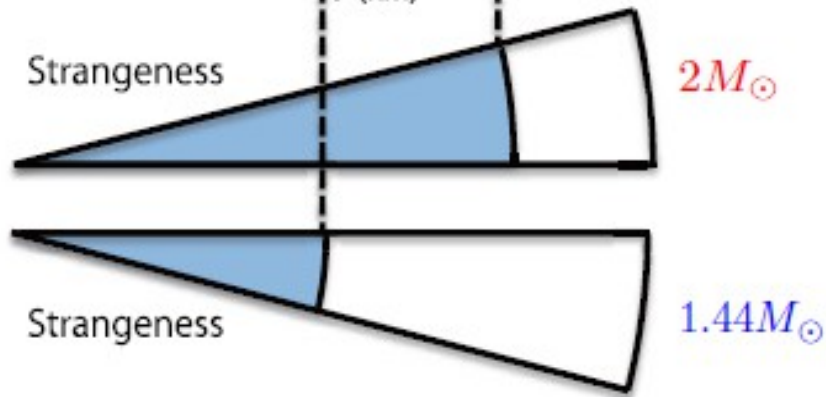
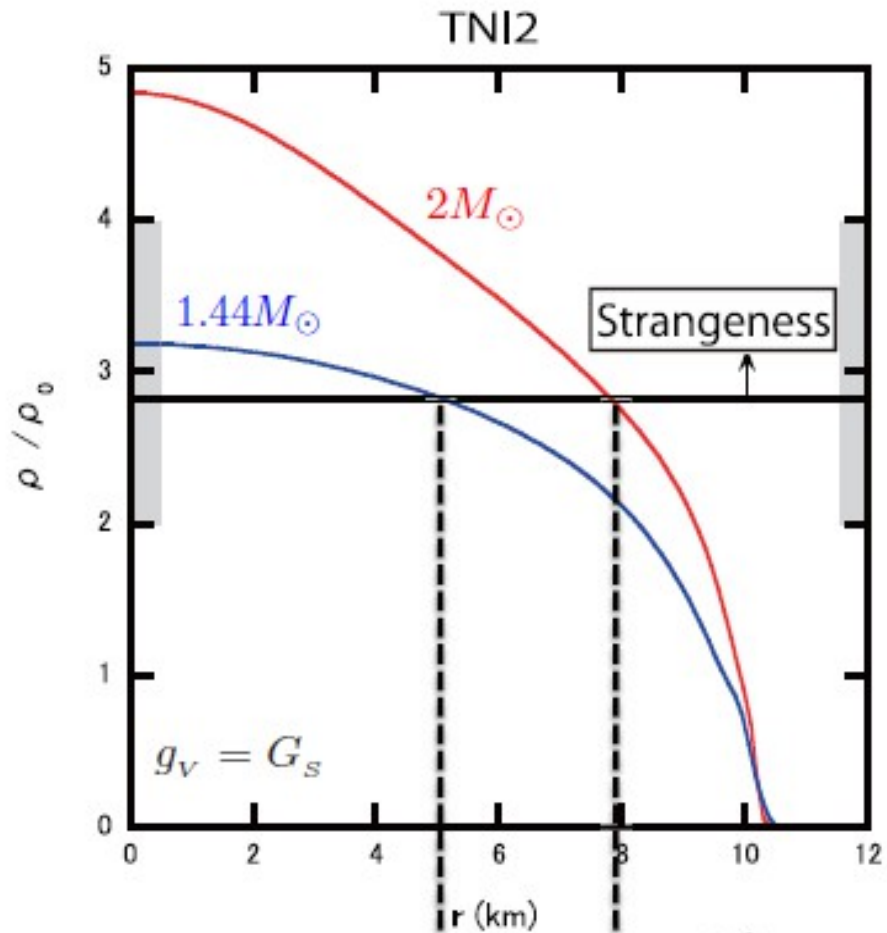
5.1. Massive hybrid star with strangeness

We now solve the following Tolman-Oppenheimer-Volkov (TOV) equation to obtain M - R relationship by using the EOSs with and without the hadron-quark crossover:

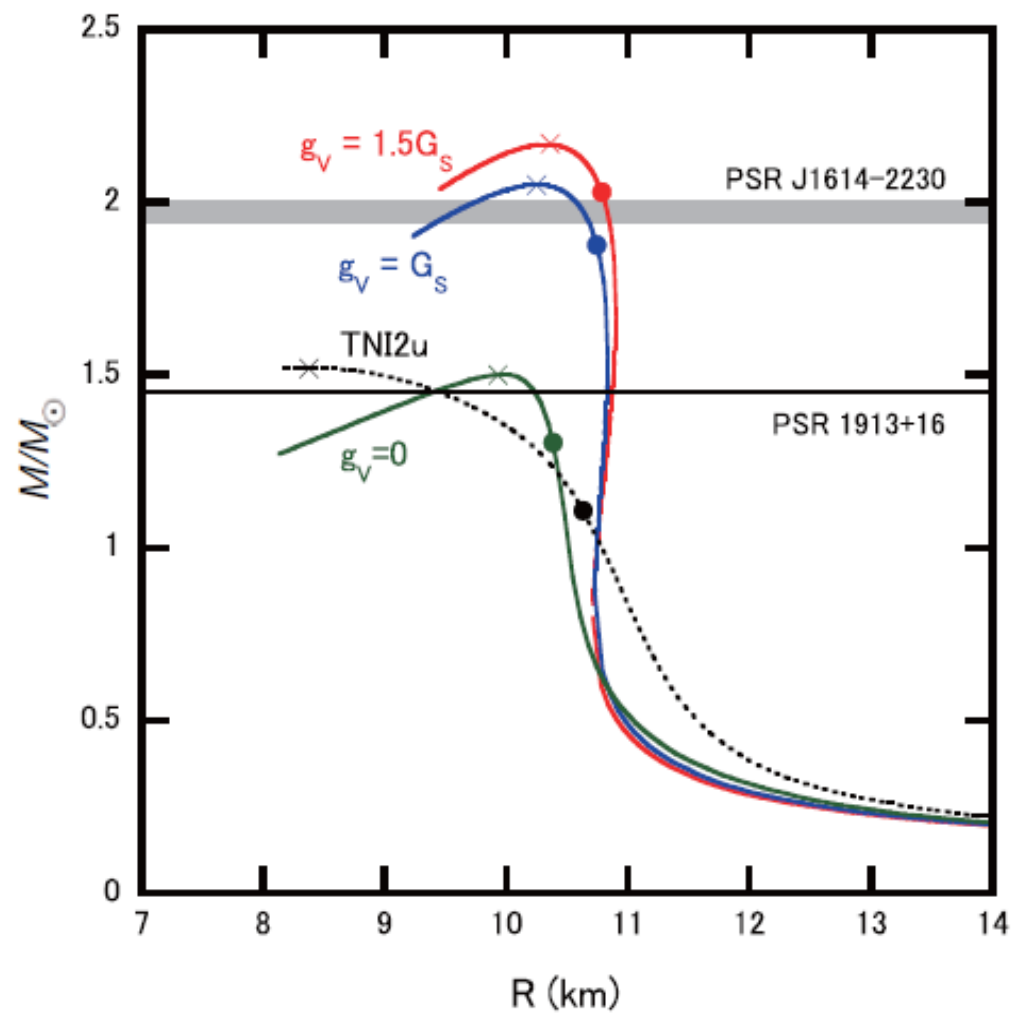
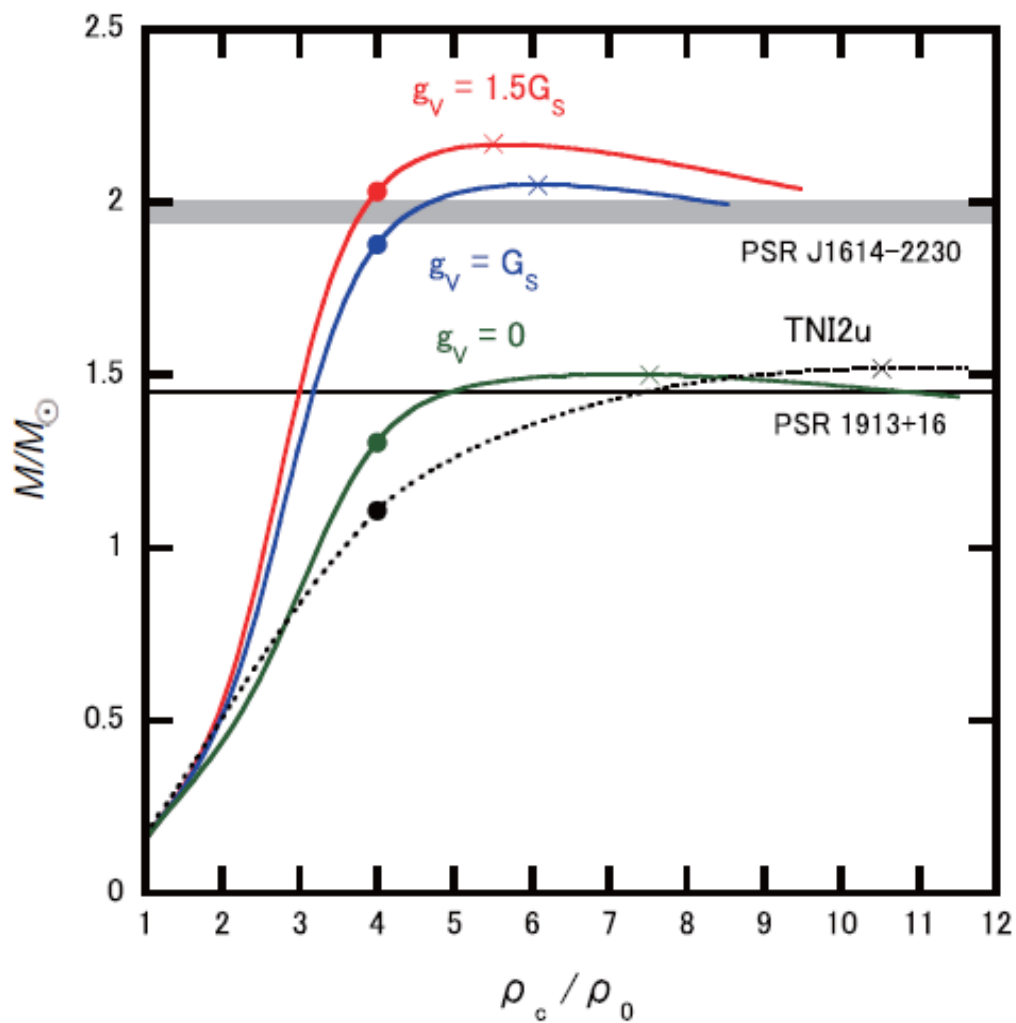
$$\frac{dP}{dr} = -\frac{G}{r^2} (M(r) + 4\pi Pr^3) (\varepsilon + P) (1 - 2GM(r)/r)^{-1},$$

$$M(r) = \int_0^r 4\pi r'^2 \varepsilon(r') dr',$$



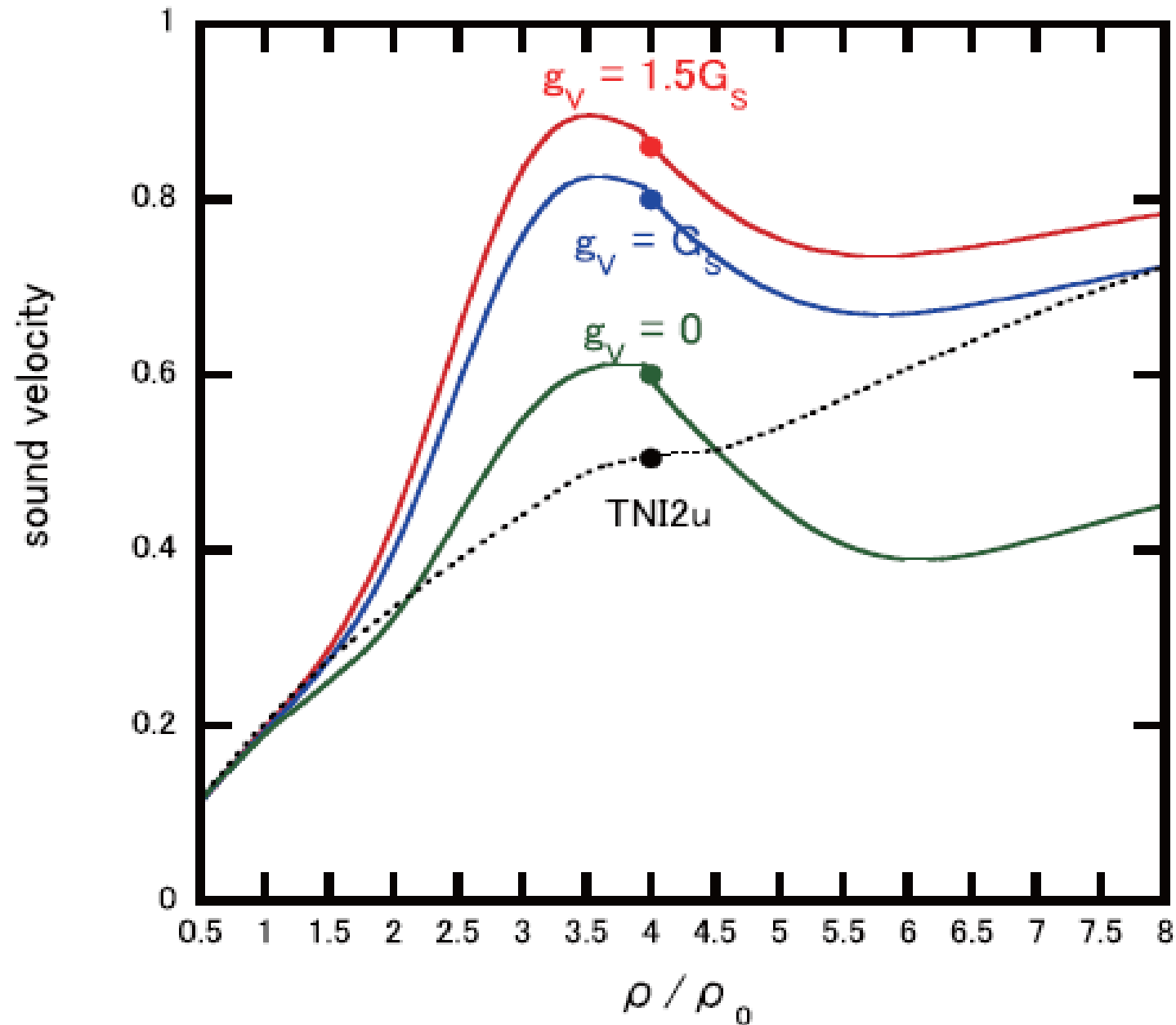


5.2. Dependence on Q-EOS



5.4. Sound velocity of interpolated EOS

One of the measures to quantify the stiffness of EOS is the sound velocity $v_s = \sqrt{dP/d\varepsilon}$.



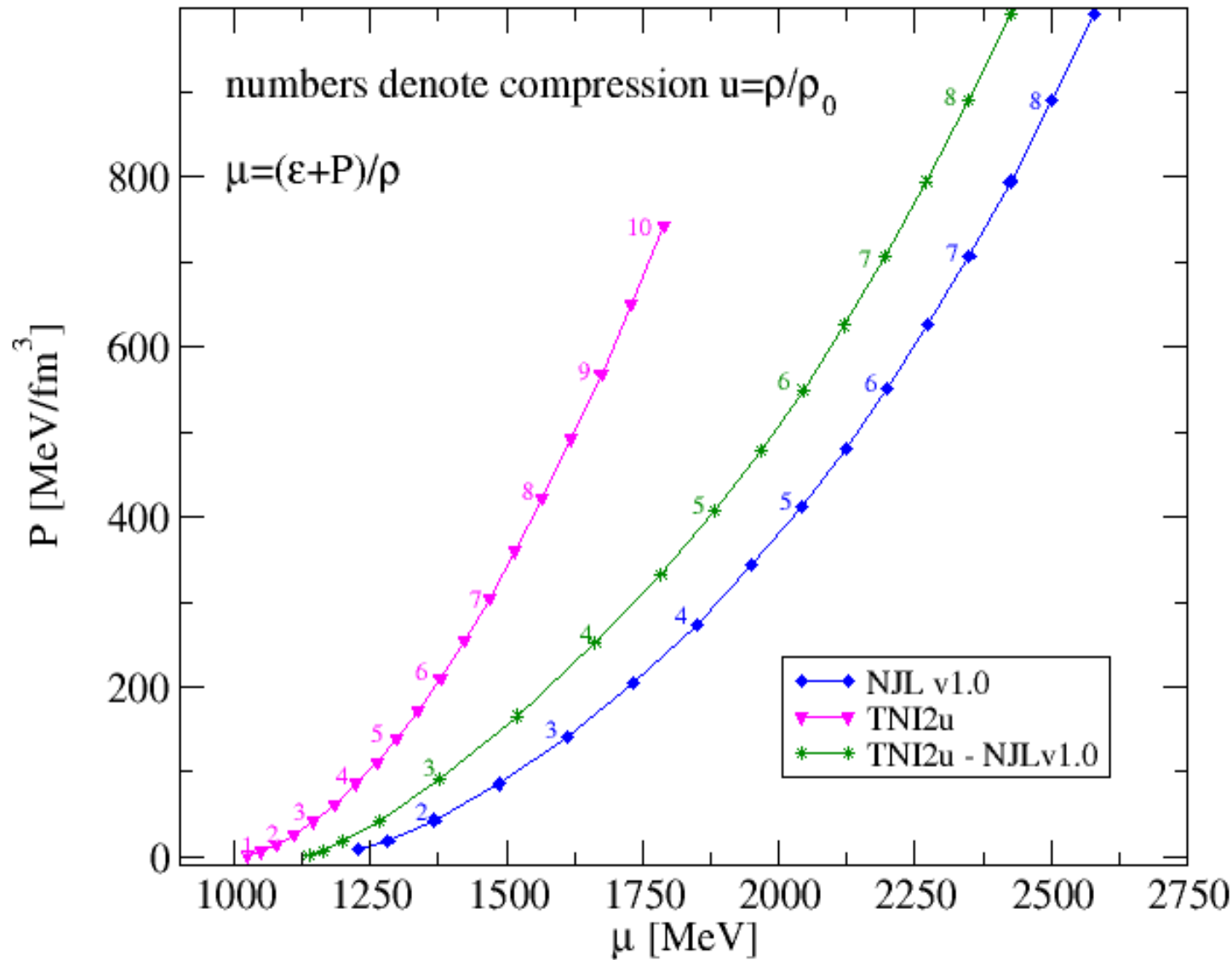
6. Summary and concluding remarks

We have constructed an EOS by the interpolation between the H-EOS at lower densities and the Q-EOS at higher densities, and found that the hybrid stars could have $M_{\text{max}} \sim 2M_{\odot}$, compatible with the observation. This conclusion is in contrast to the conventional EOS for hybrid stars derived through the Gibbs construction in which the resultant EOS becomes always softer than hadronic EOS and thereby leads to smaller M_{max} .

The idea of rapid stiffening of the EOS starting from $2\rho_0$ opens a possibility that the experimental nuclear incompressibility $\kappa = (240 \pm 20)\text{MeV}$ at $\rho \sim \rho_0$ is compatible with the existence of massive neutron stars. Also, the idea may well be checked by independent laboratory experiments with medium-energy heavy-ion collisions.

Finally, we remark that the crossover region may contain richer non-perturbative phases such as color superconductivity, inhomogeneous structures and so on [1]. How these structures as well as the associated cooling processes affect the results of the present paper would be an interesting future problem to be examined.

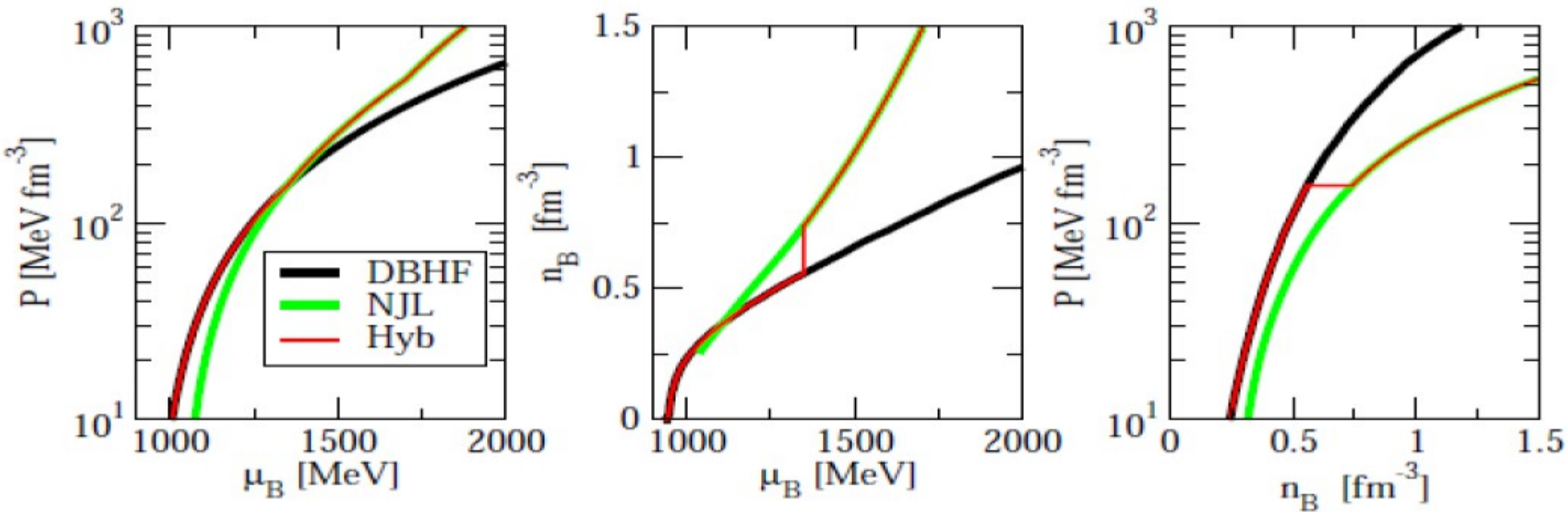
Pressure vs. chem. Potential for H-EoS, Q-EoS and hybrid EoS with “Crossover”



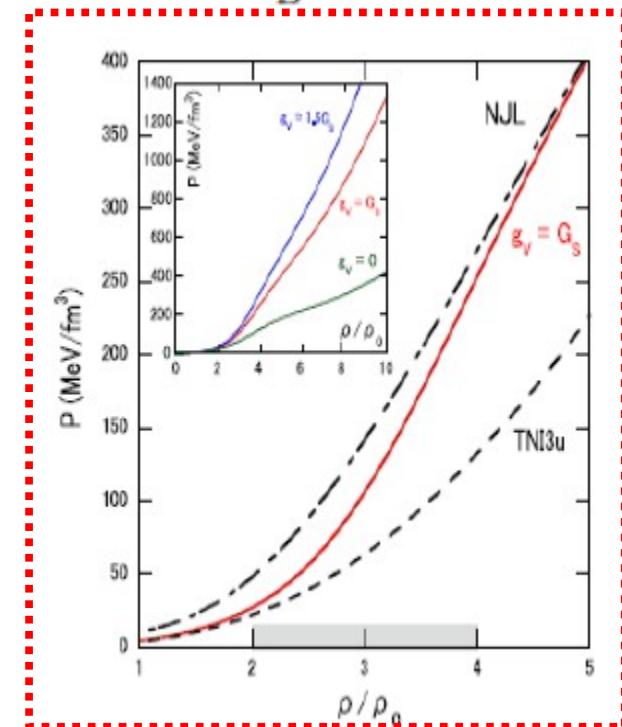
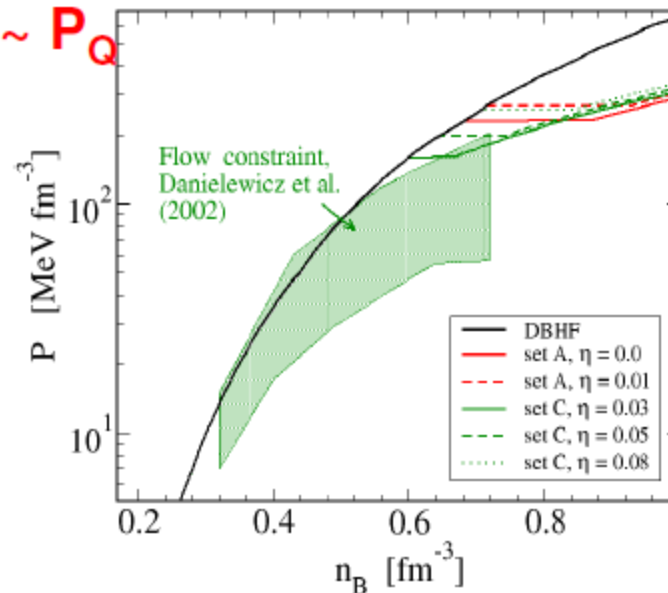
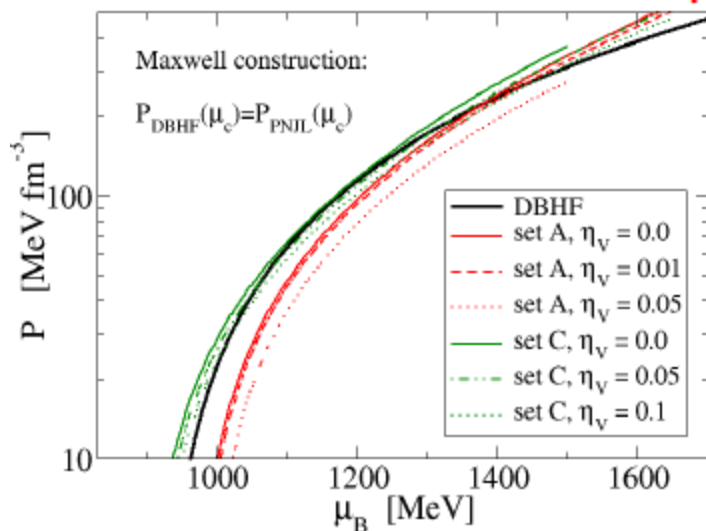
PROBLEM:
 The interpolation in $P(\rho)$ is not a “crossover”, since thermodynamic consistency requires a shift $\Delta\epsilon$ which isolates the resulting hybrid EoS (green) from the hadronic (magenta) and quark (blue) asymptotes.

Figure prepared with data from arxiv:1212.6803v1

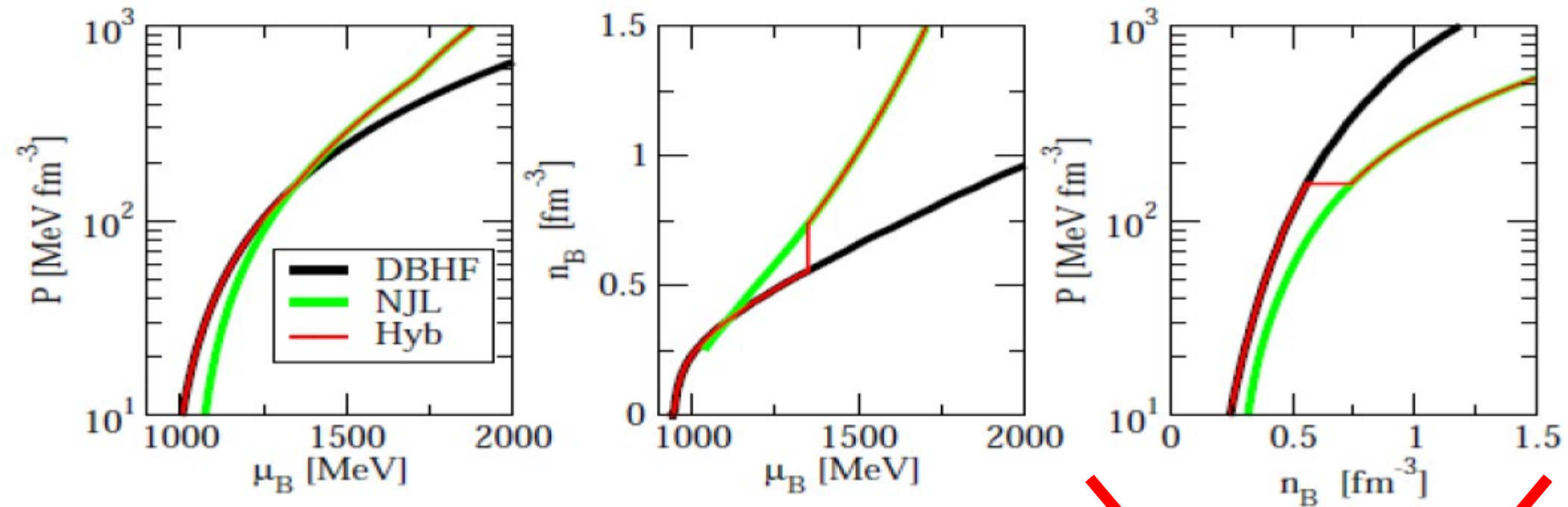
Traditional: Pressure vs. chem. Potential for H-EoS, Q-EoS and hybrid EoS



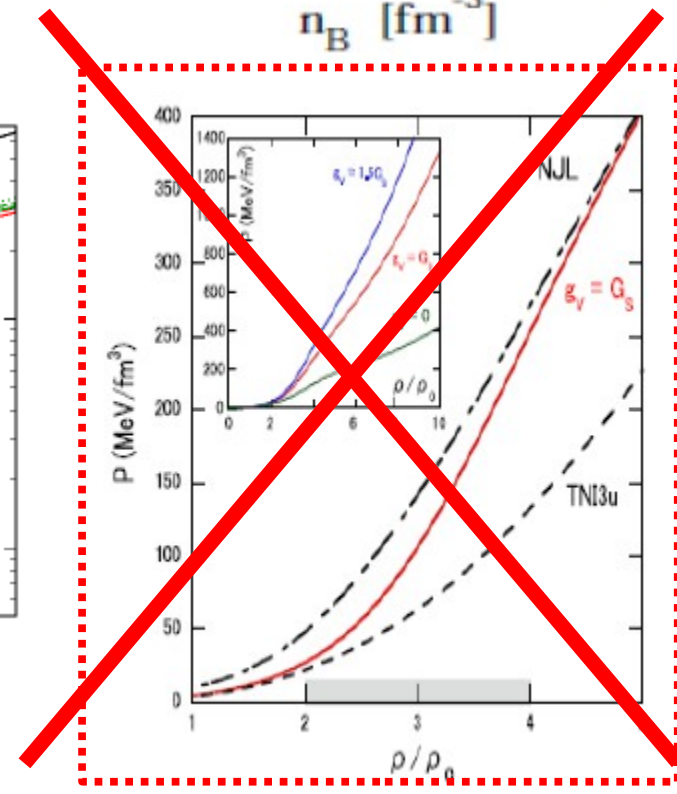
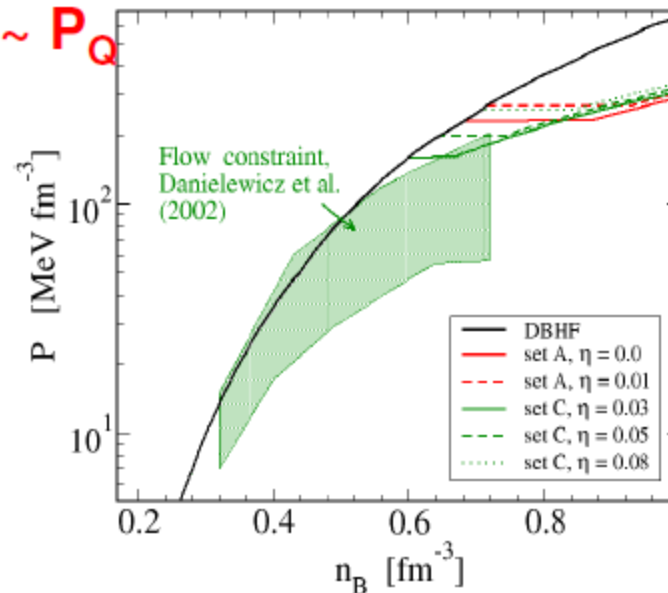
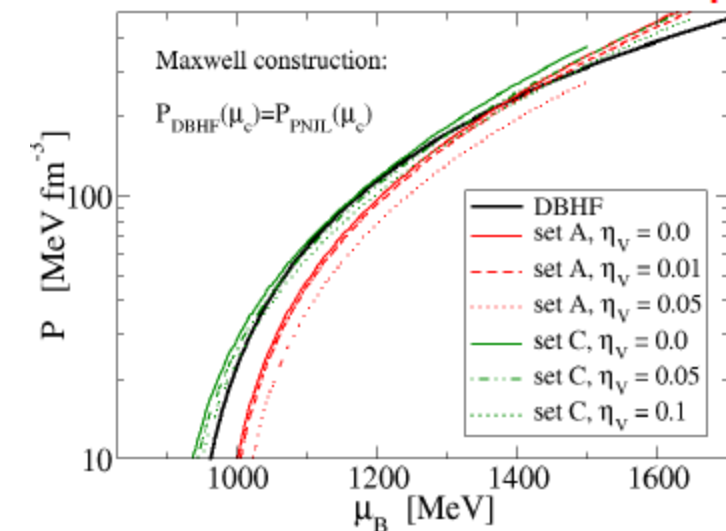
Masquerade problem: $P_H \sim P_Q$



Traditional: Pressure vs. chem. Potential for H-EoS, Q-EoS and hybrid EoS



Masquerade problem: $P_H \sim P_Q$



Maximum mass of neutron stars with a quark core

G.F. Burgio^a, M. Baldo^a, P.K. Sahu^a, A.B. Santra^b, H.-J. Schulze^c

^a *Istituto Nazionale di Fisica Nucleare, Sezione di Catania, Corso Italia 57, I-95129 Catania, Italy*

^b *Nuclear Physics Division, Bhabha Atomic Research Center, Mumbai 400 085, India*

^c *Departament d'Estructura i Constituents de la Matèria, Universitat de Barcelona, Av. Diagonal 647, E-08028 Barcelona, Spain*

Received 22 April 2001; received in revised form 28 September 2001; accepted 16 December 2001

Editor: J.-P. Blaizot

PHYSICAL REVIEW C 66, 025802 (2002)

Hadron-quark phase transition in dense matter and neutron stars

G. F. Burgio,¹ M. Baldo,¹ P. K. Sahu,² and H.-J. Schulze¹

HADRONIC PHASE

$$\epsilon = \frac{1}{2} m_\omega^2 \bar{\omega}_0^2 + \frac{1}{2} m_\rho^2 (\bar{\rho}_0^3)^2 + \frac{1}{2} m_\sigma^2 \bar{\sigma}^2 + \frac{1}{3} b m_N (g_{\sigma N} \bar{\sigma})^3$$

$$+ \frac{1}{4} c (g_{\sigma N} \bar{\sigma})^4 + \sum_i \epsilon_{\text{FG}}(\bar{m}_i, \bar{\mu}_i) + \sum_l \epsilon_{\text{FG}}(m_l, \mu_l),$$

$$P = \frac{1}{2} m_\omega^2 \bar{\omega}_0^2 + \frac{1}{2} m_\rho^2 (\bar{\rho}_0^3)^2 - \frac{1}{2} m_\sigma^2 \bar{\sigma}^2 - \frac{1}{3} b m_N (g_{\sigma N} \bar{\sigma})^3$$

$$- \frac{1}{4} c (g_{\sigma N} \bar{\sigma})^4 + \sum_i P_{\text{FG}}(\bar{m}_i, \bar{\mu}_i) + \sum_l P_{\text{FG}}(m_l, \mu_l)$$

QUARK PHASE

$$\epsilon_Q = \sum_q (\Omega_q + \mu_q \rho_q) + B, \quad P_Q = - \sum_q \Omega_q - B,$$

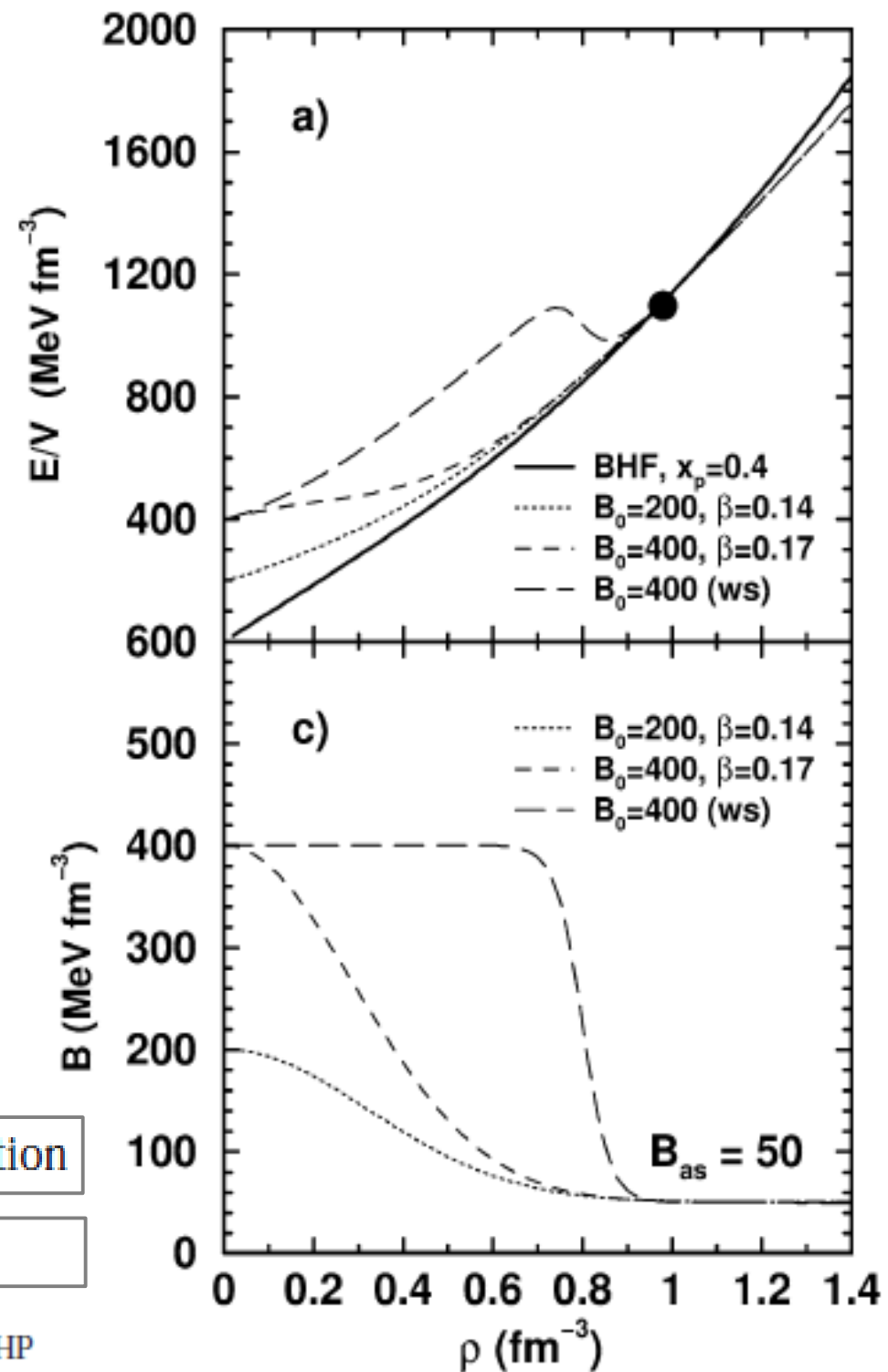
$$B(\rho) = B_{\text{as}} + (B_0 - B_{\text{as}}) \left[1 + \exp\left(\frac{\rho - \bar{\rho}}{\rho_d}\right) \right]^{-1}$$

Phase transition in β -stable neutron star matter

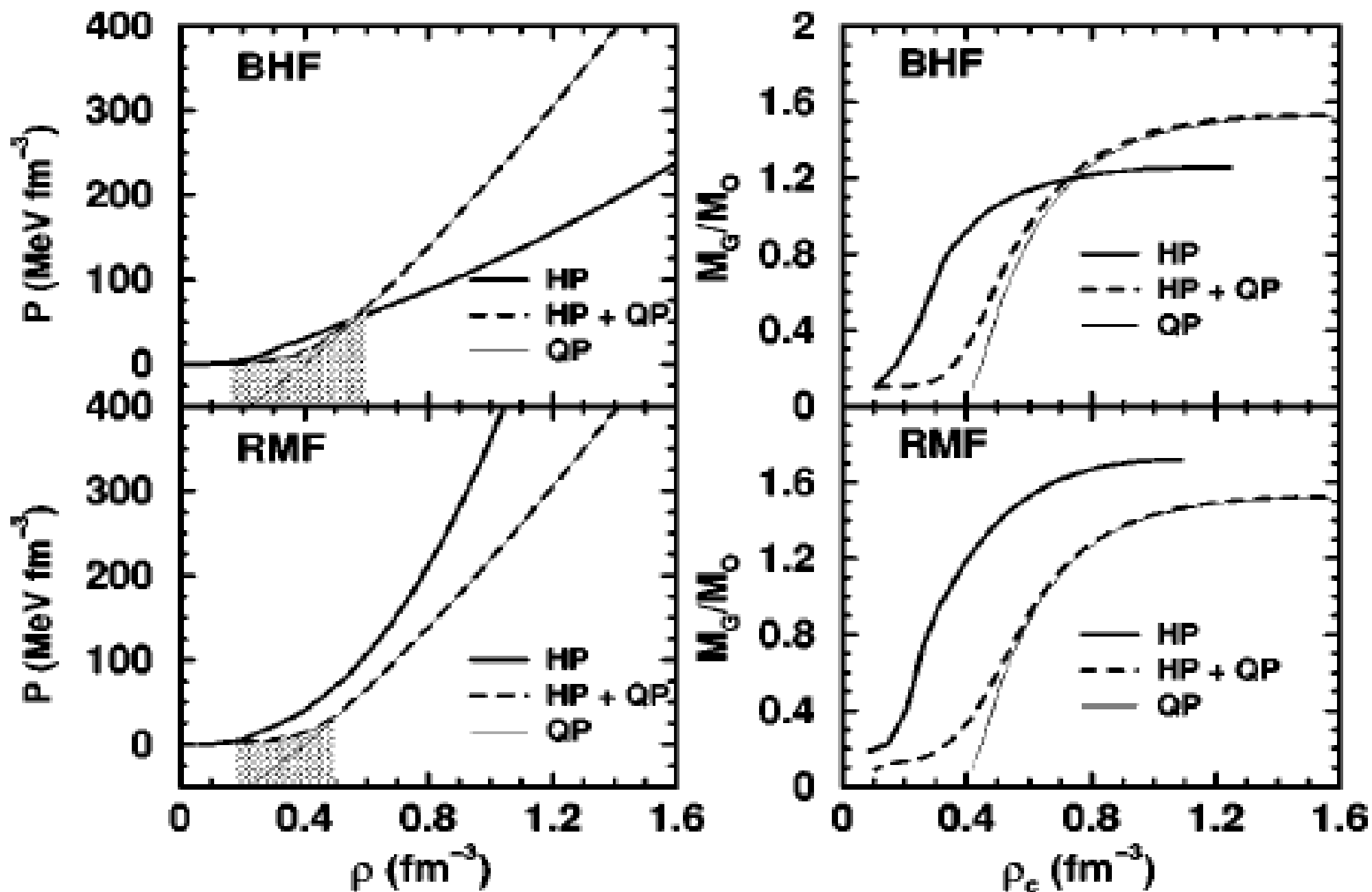
$$P_{\text{HP}}(\mu_e, \mu_n) = P_{\text{QP}}(\mu_e, \mu_n) = P_{\text{MP}} \quad \boxed{\text{Gibbs condition}}$$

$$\chi \rho_c^{\text{QP}} + (1 - \chi) \rho_c^{\text{HP}} = 0. \quad \boxed{\text{Global charge conservation}}$$

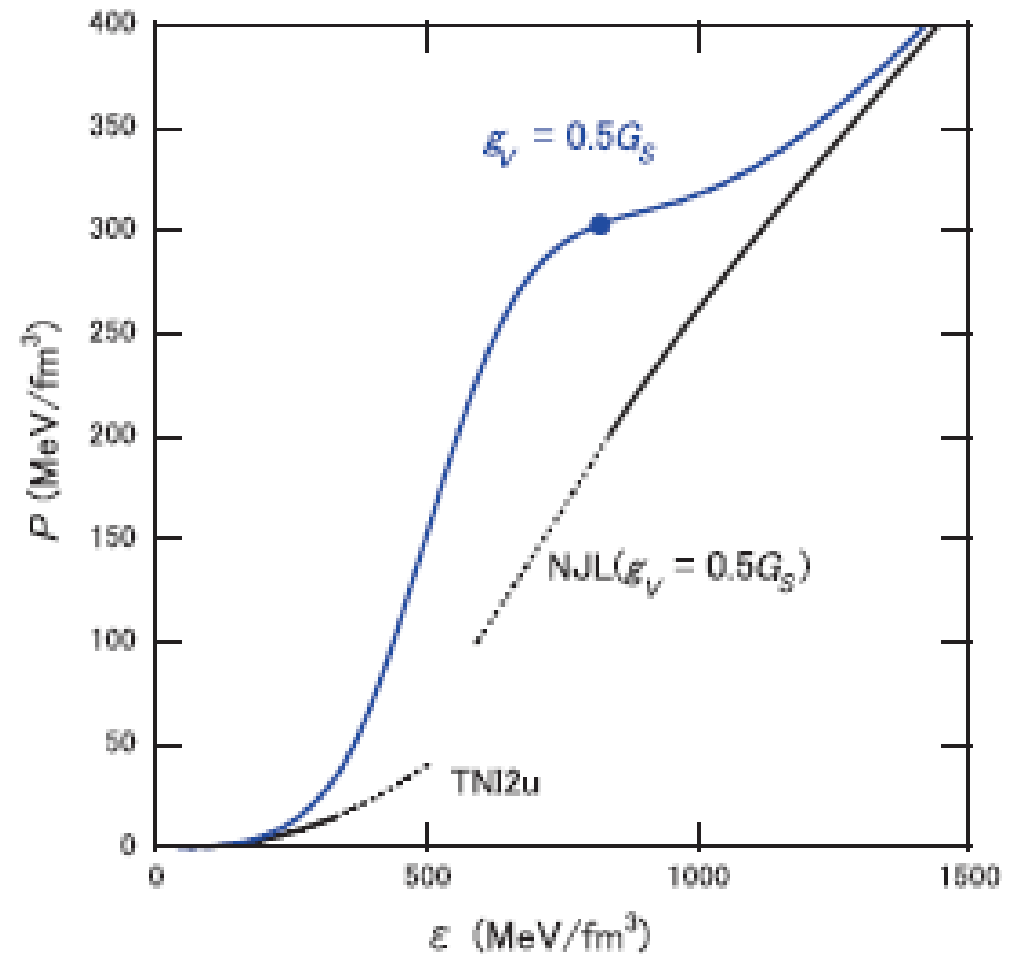
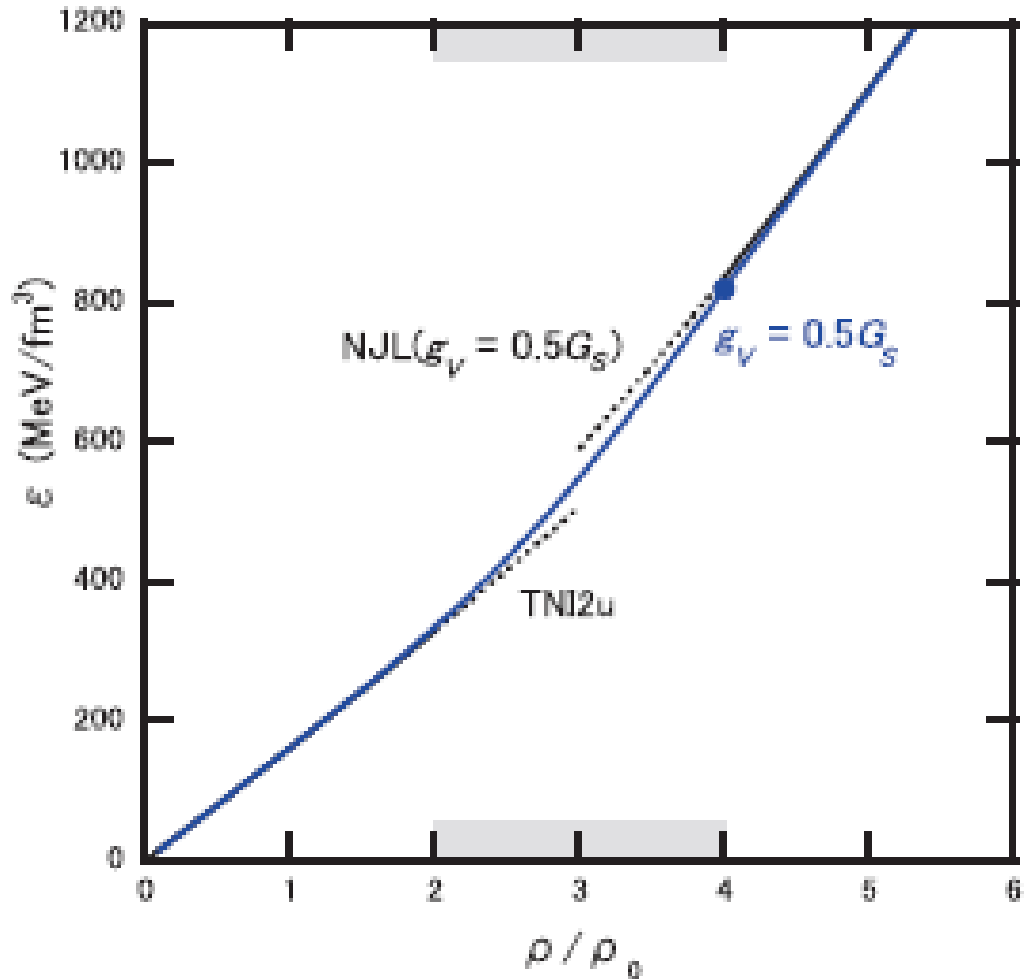
$$\epsilon_{\text{MP}} = \chi \epsilon_{\text{QP}} + (1 - \chi) \epsilon_{\text{HP}}, \quad \rho_{\text{MP}} = \chi \rho_{\text{QP}} + (1 - \chi) \rho_{\text{HP}}$$



Gibbs Phase transition \rightarrow Mixed phase, Softening the EoS; Quark Phase: stiff

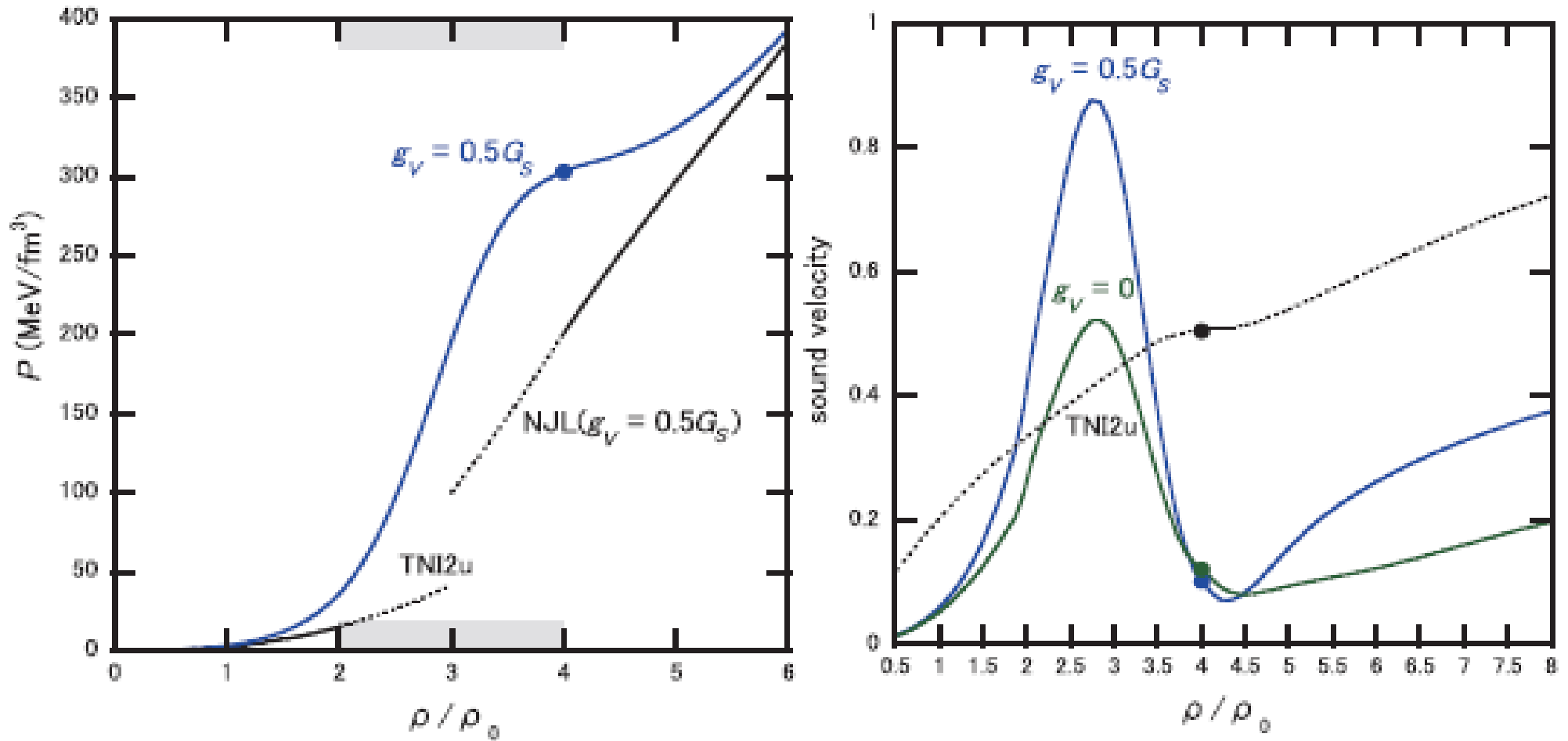


2nd attempt: interpolation between energy densities $\varepsilon(\rho)$



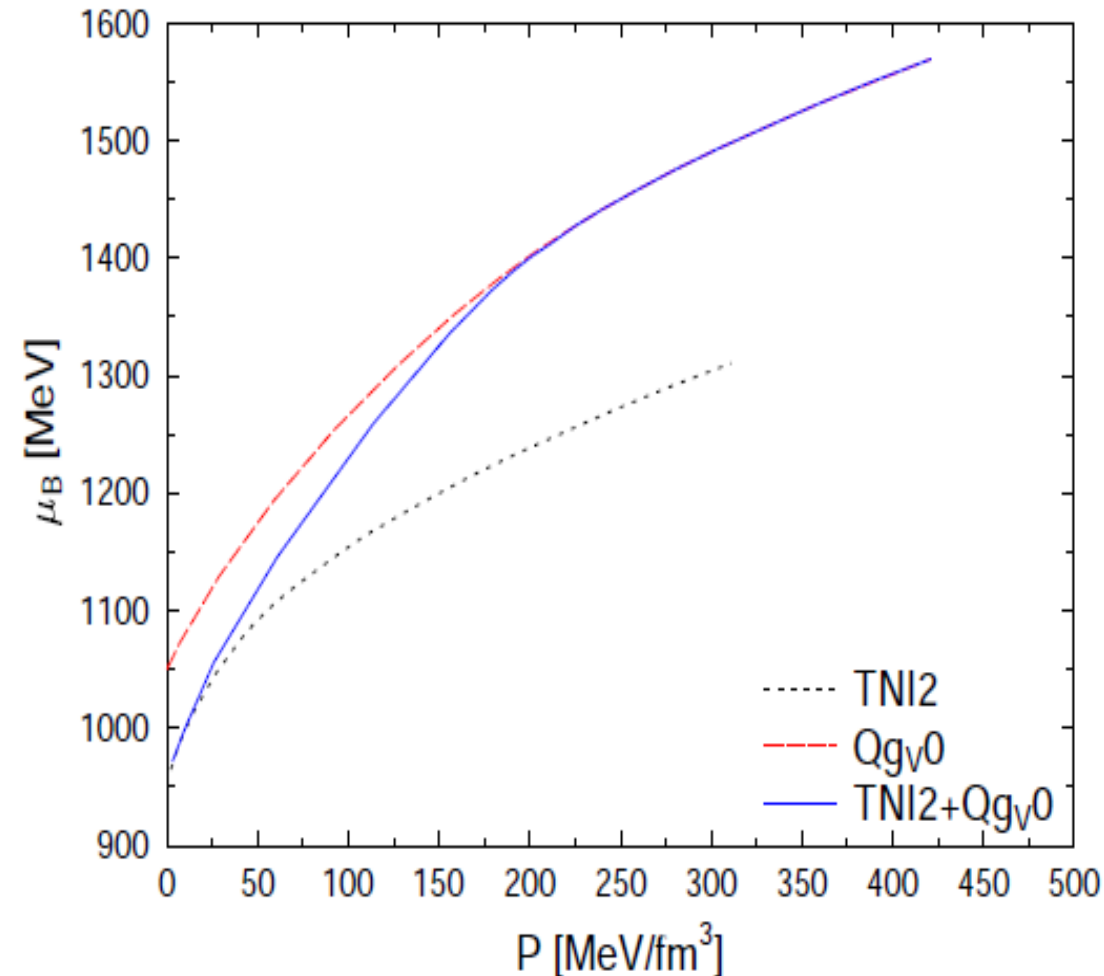
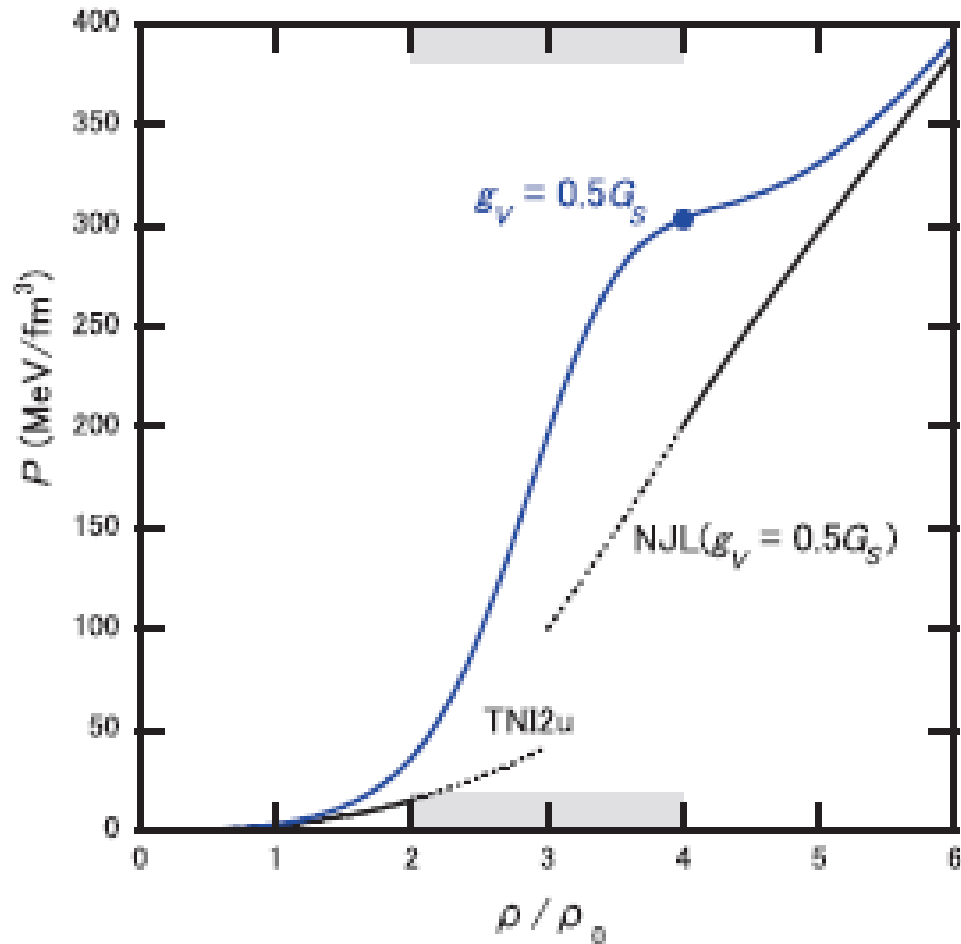
Masuda, Hatsuda, Takatsuka, PTP 073D01 (2013); [arxiv:1212.6803v2]

2nd attempt: interpolation between energy densities $\varepsilon(\rho)$



NOTE: After a strong stiffening one observes the “dip” in the speed of sound which is typical for a phase transition and corresponds to the “plateau” in $P(\rho)$

2nd attempt: interpolation between energy densities $\varepsilon(\rho)$

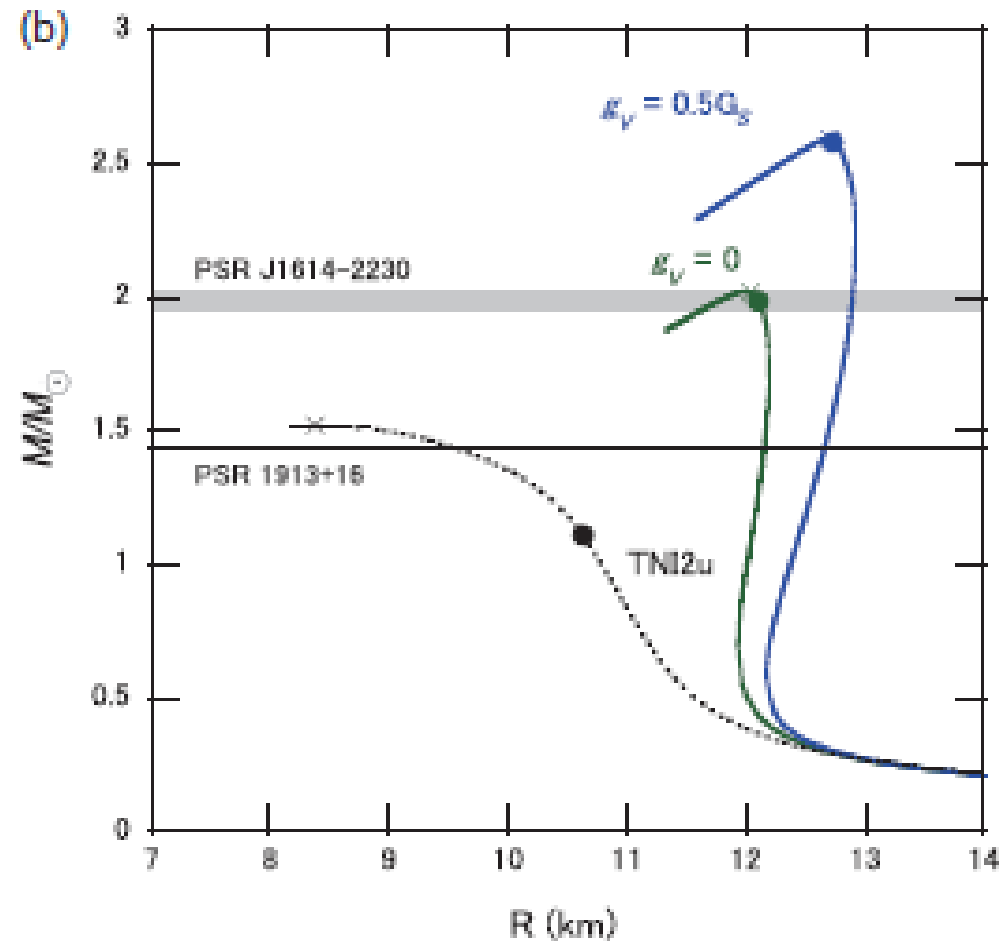
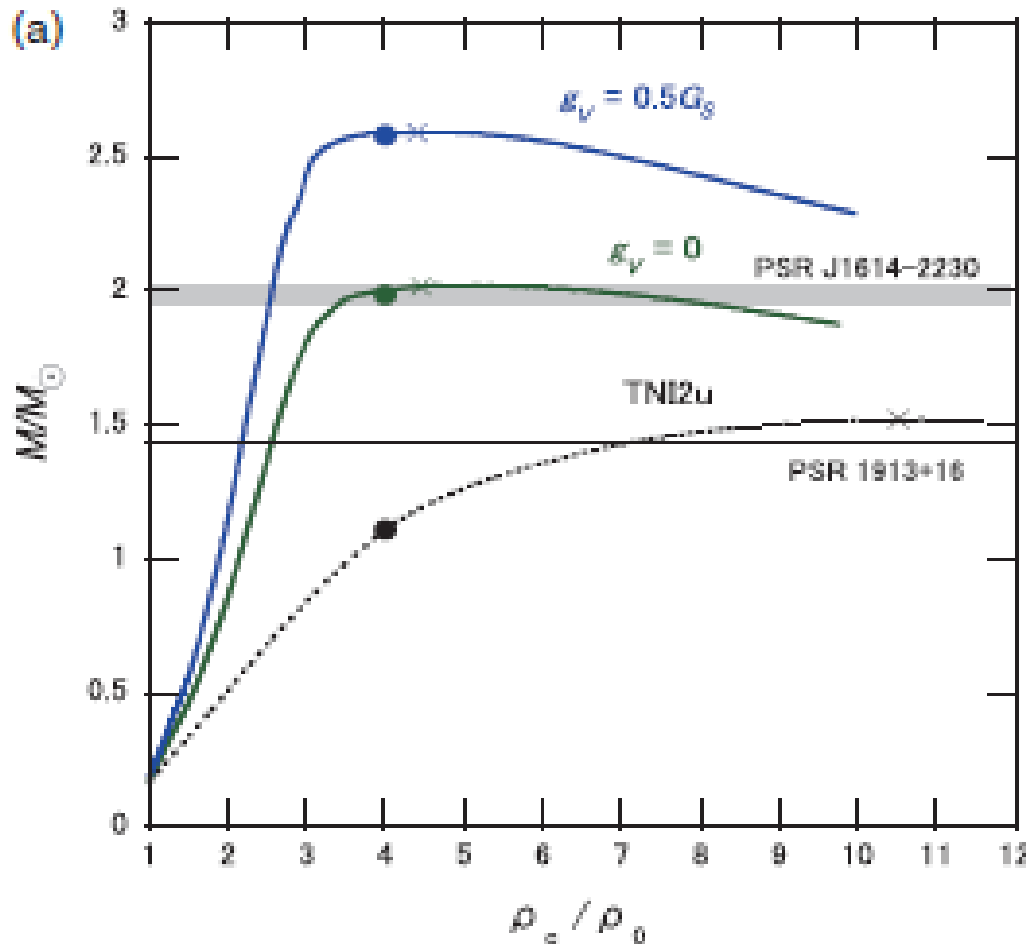


NOTE: This interpolation procedure in $\varepsilon(\rho)$ is not only thermodynamically consistent, but also a true interpolation, as can be seen from $P(\mu)$ or its inversion $\mu(P)$.

Courtesy: Matthias Hempel, using data from arxiv:1212.6803v2

For hybrid star EoS with interpolation in $P(\mu)$, see arxiv:1302.6275; arxiv:1310.3803

2nd attempt: interpolation between energy densities $\epsilon(\rho)$



Attention:

Results with interpolation between energy densities $\epsilon(\rho)$ are different from those with interpolation in pressures $P(\rho)$

Which one is correct? ...

2. Microphysical approach to strong 1st order PT

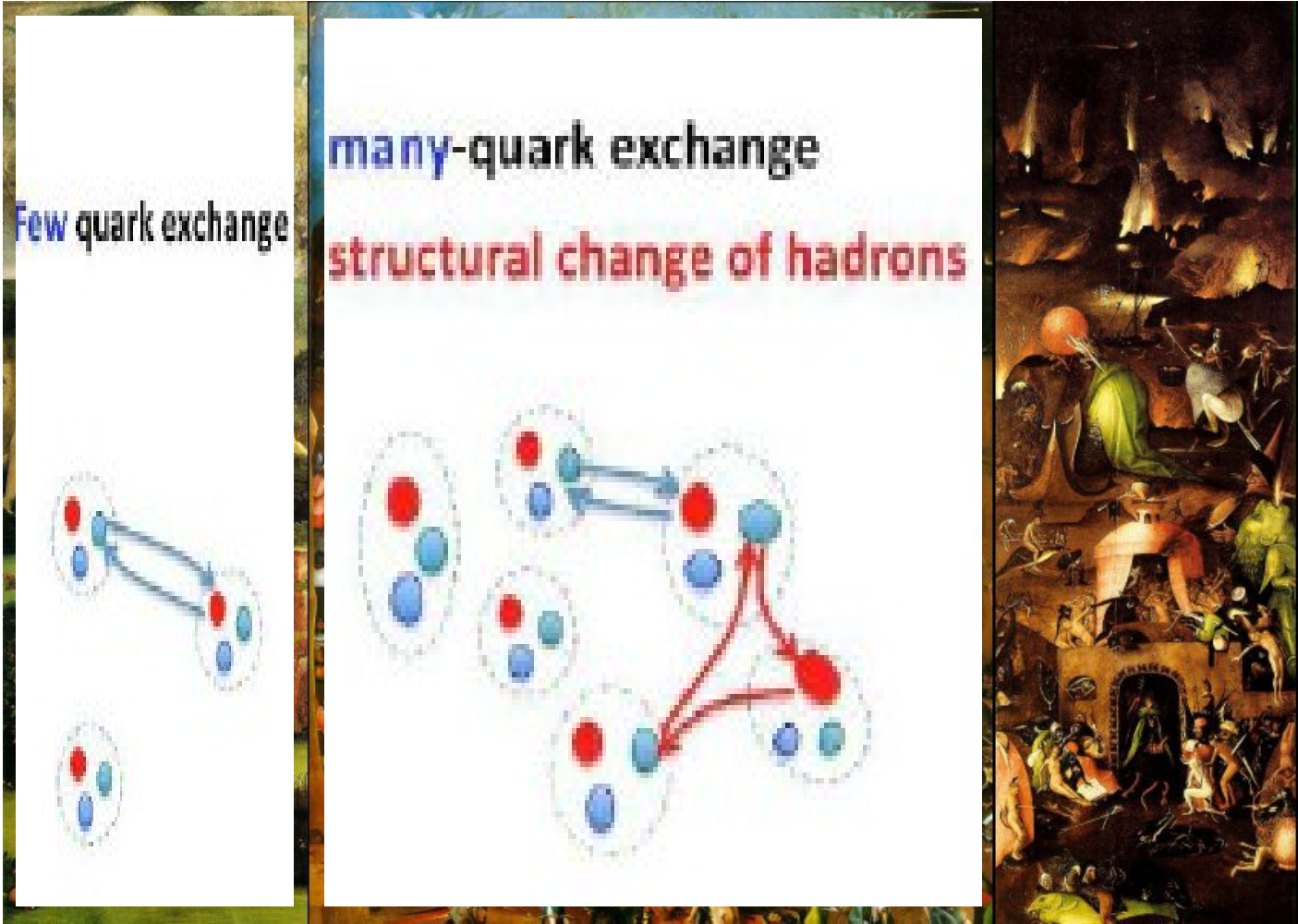
2. Another “three-window picture of dense matter”



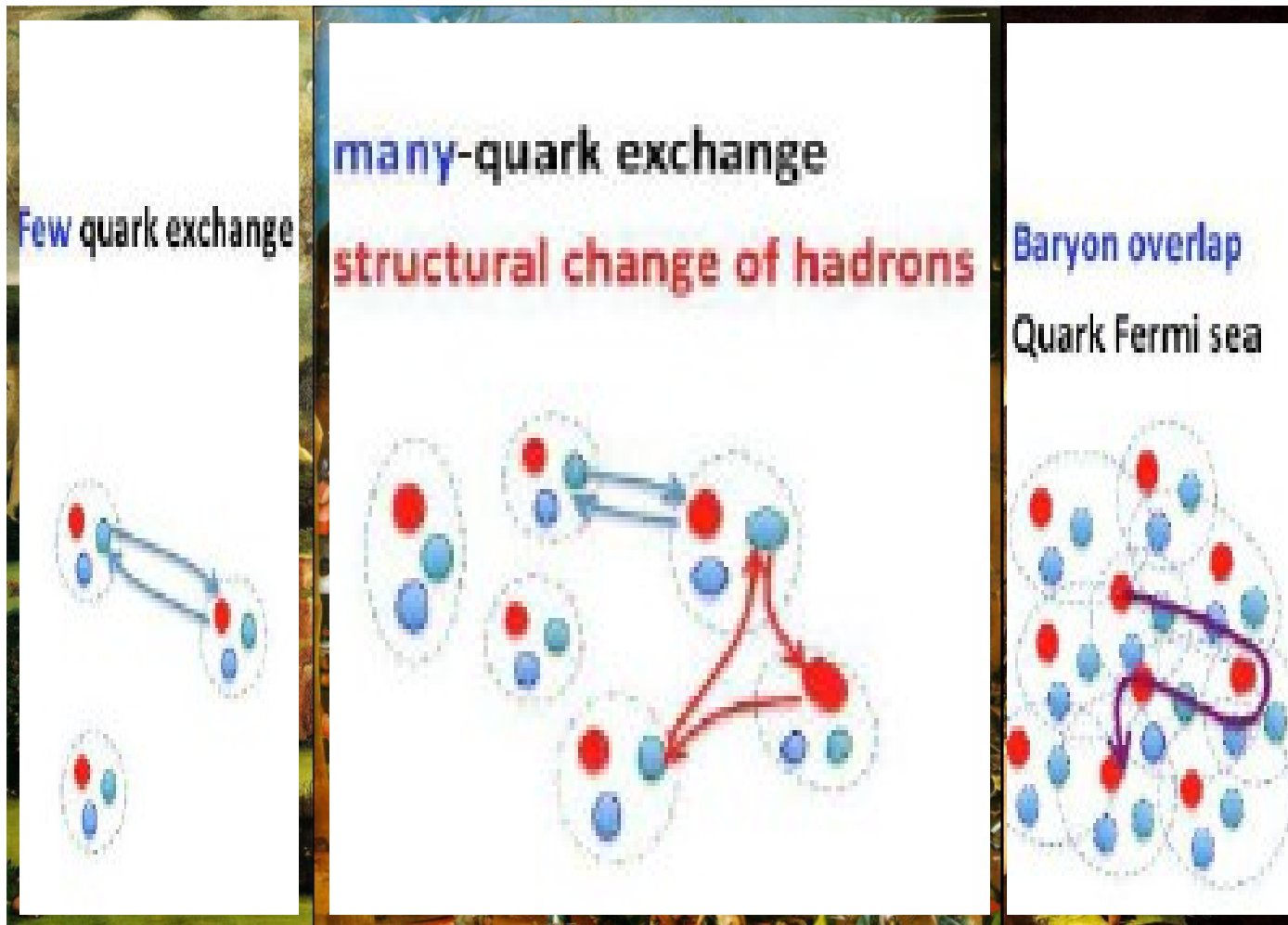
2. Another “three-window picture of dense matter”



2. Another “three-window picture of dense matter”

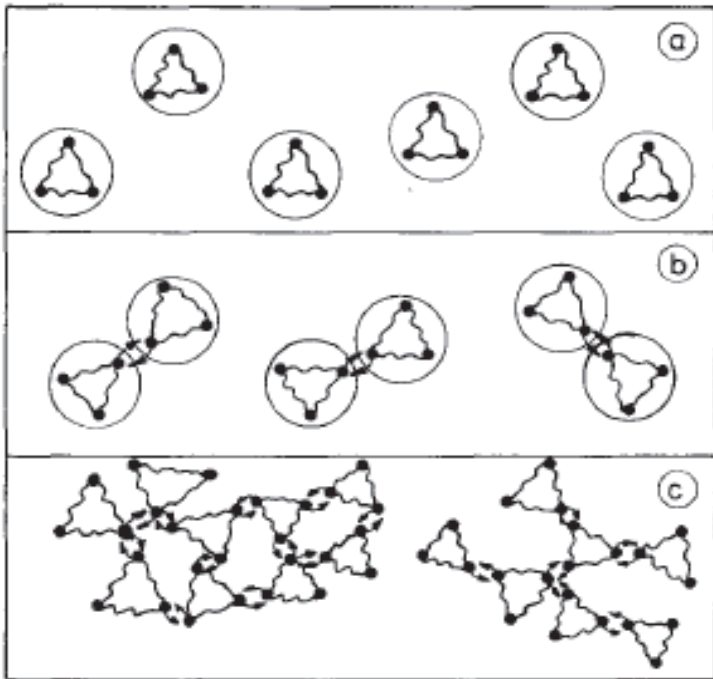


2. Another “three-window picture of dense matter”



Toru Kojo,
EPJA 52,
51 (2016)

2.1. Pauli blocking among baryons

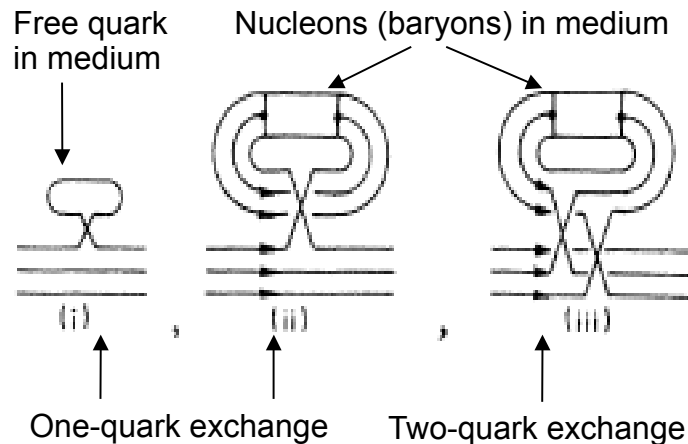


a) Low density: Fermi gas of nucleons (baryons)

b) ~ saturation: Quark exchange interaction and Pauli blocking among nucleons (baryons)

c) high density: Quark cluster matter (string-flip model ...)

Roepke & Schulz, Z. Phys. C 35, 379 (1987); Roepke, DB, Schulz, PRD 34, 3499 (1986)



Nucleon (baryon) self-energy --> Energy shift

$$\Delta E_{\nu P}^{\text{Pauli}} = \sum_{123} |\psi_{\nu P}(123)|^2 [E(1) + E(2) + E(3) - E_{\nu P}^0] [f_{\alpha_1}(1) + f_{\alpha_2}(2) + f_{\alpha_3}(3)]$$

$$+ \sum_{123} \sum_{456} \sum_{\nu P'} \psi_{\nu P}^*(123) \psi_{\nu P'}(456) f_3(E_{\nu P'}^0) \{ \delta_{36} \psi_{\nu P}(123) \psi_{\nu P'}^*(456) - \psi_{\nu P}(453) \psi_{\nu P'}^*(126) \}$$

$$\times [E(1) + E(2) + E(3) + E(4) + E(5) + E(6) - E_{\nu P}^0 - E_{\nu P'}^0]$$

$$= \Delta E_{\nu P}^{\text{Pauli, free}} + \Delta E_{\nu P}^{\text{Pauli, bound}}$$



PHYSICAL REVIEW D

VOLUME 34, NUMBER 11

1 DECEMBER 1986

Pauli quenching effects in a simple string model of quark/nuclear matter

G. Röpke and D. Blaschke

Department of Physics, Wilhelm-Pieck-Universität, 2500 Rostock, German Democratic Republic

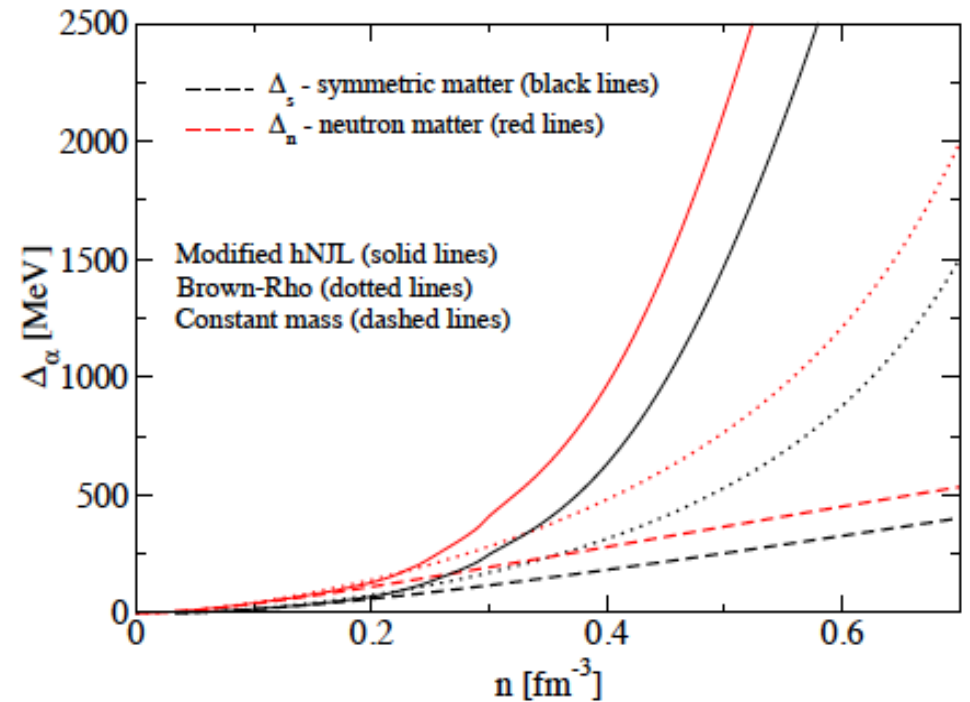
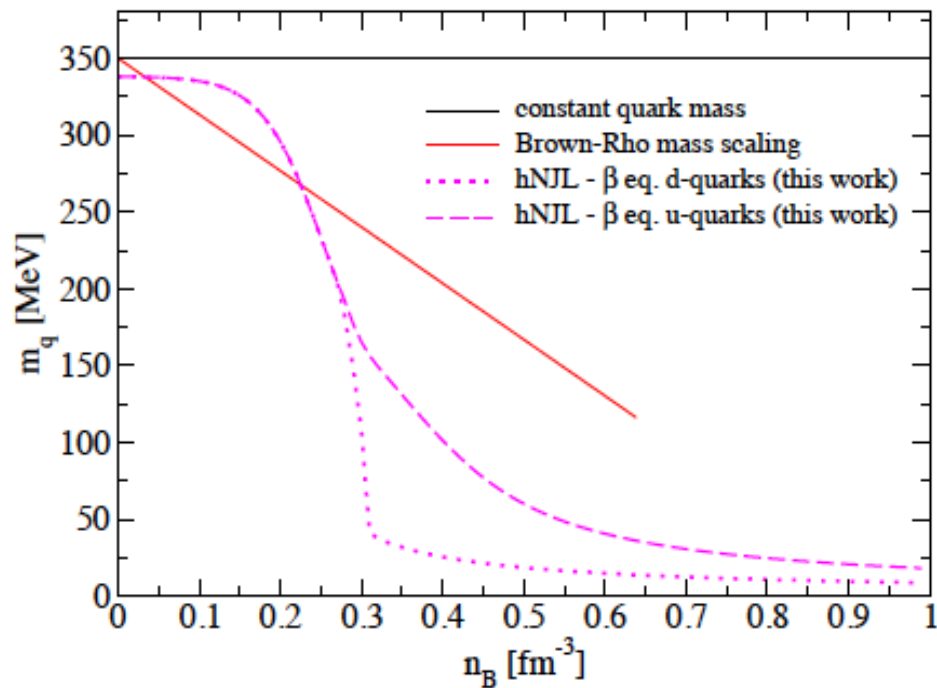
H. Schulz

*Central Institute for Nuclear Research, Rossendorf, 8051 Dresden, German Democratic Republic
and The Niels Bohr Institute, 2100 Copenhagen, Denmark*

(Received 16 December 1985)

2.1. Pauli blocking among baryons – details

New aspect: chiral restoration --> dropping quark mass



**Increased baryon swelling at supersaturation densities:
--> dramatic enhancement of the Pauli repulsion !!**

2.2. Pauli blocking among baryons – results

New EoS: Joining RMF (Linear Walecka) for pointlike baryons with chiral Pauli blocking

$$p = \frac{1}{4\pi^2} \sum_{\nu} \left[-E_{\nu}^* m_{\nu}^{*2} p_{F\nu} + \frac{2}{3} E_{\nu}^* p_{F\nu}^3 + m_{\nu}^{*4} \log \left(\frac{E_{\nu}^* + p_{F\nu}}{m_{\nu}^*} \right) \right]$$

$$+ \frac{1}{2} \left(\frac{g_{\omega}}{m_{\omega}} \right)^2 n^2 - \frac{1}{2} \left(\frac{g_{\sigma}}{m_{\sigma}} \right)^2 n_s^2 + p_{ex};$$

$$\epsilon = \frac{1}{4\pi^2} \sum_{\nu} \left[2 E_{\nu}^{*3} p_{F\nu} - E_{\nu}^* m_{\nu}^{*2} p_{F\nu} - m_{\nu}^{*4} \log \left(\frac{E_{\nu}^* + p_{F\nu}}{m_{\nu}^*} \right) \right]$$

$$+ \frac{1}{2} \left(\frac{g_{\omega}}{m_{\omega}} \right)^2 n^2 + \frac{1}{2} \left(\frac{g_{\sigma}}{m_{\sigma}} \right)^2 n_s^2 + \epsilon_{ex},$$

$$\mu_{ex,\nu} = \Delta_{\nu}(n, x) = \Sigma_{\nu}(p_{F,\nu}; p_{Fn}, p_{Fp}),$$

$$\epsilon_{ex} = \sum_{\nu} \int_0^n dn' \{ x \Delta_p(n', x) + (1-x) \Delta_n(n', x) \},$$

$$p_{ex} = \sum_{\nu} \mu_{ex,\nu} n_{\nu} - \epsilon_{ex},$$

$$n_{s,\nu} = \frac{m_{\nu}^*}{\pi^2} \left[E_{\nu}^* p_{F\nu} - m_{\nu}^{*2} \log \left(\frac{E_{\nu}^* + p_{F\nu}}{m_{\nu}^*} \right) \right],$$

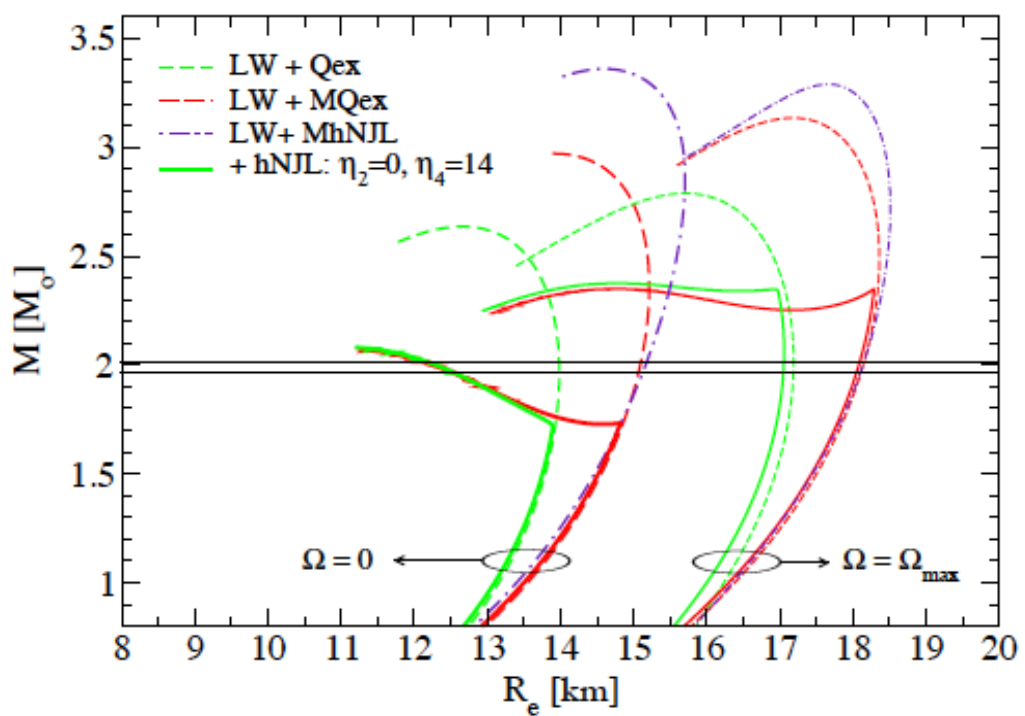
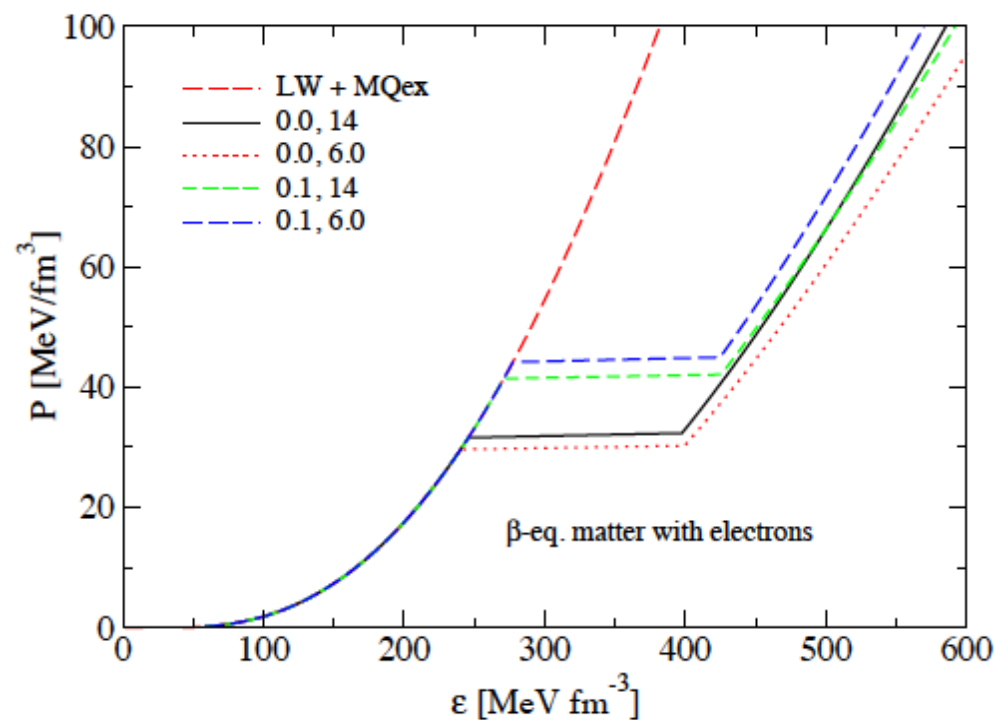
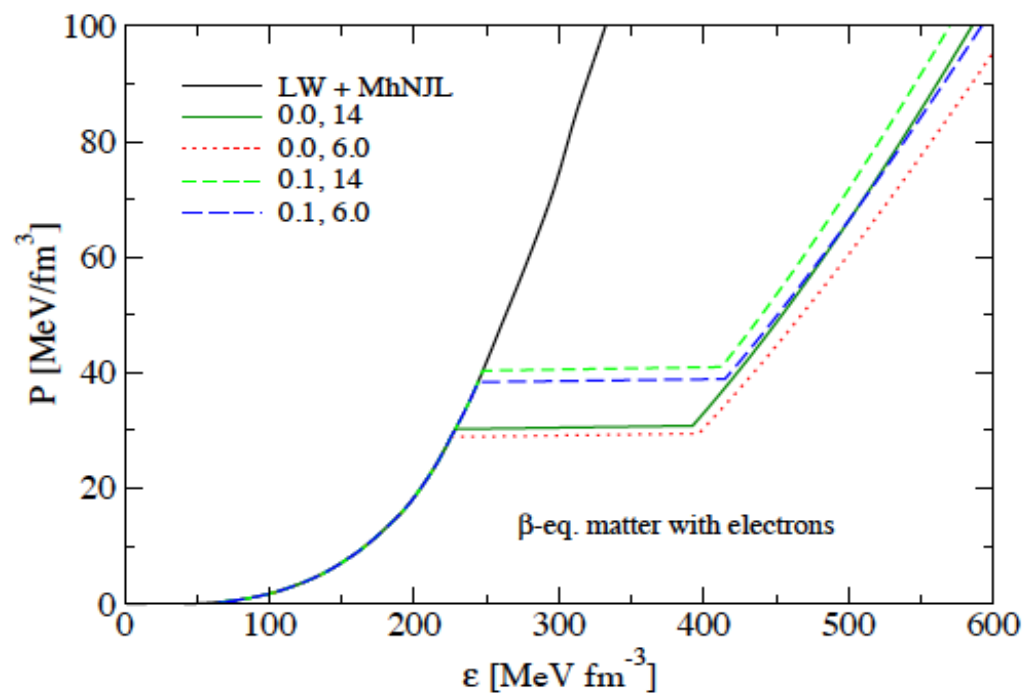
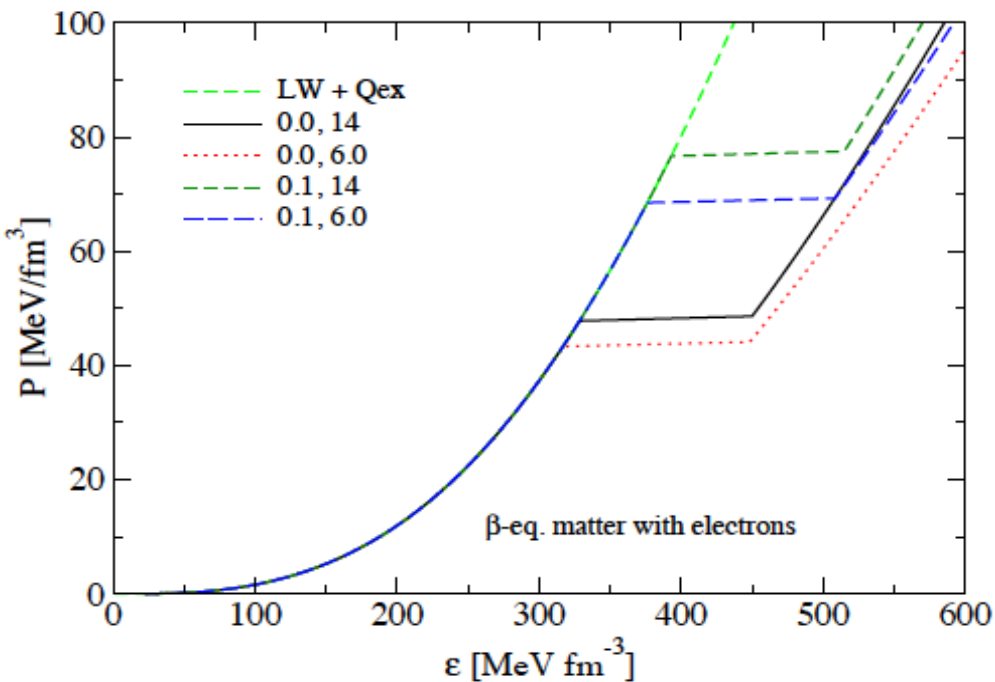
$$E_{\nu}^* = \sqrt{m_{\nu}^{*2} + p_{F\nu}^2}$$

$$n_{\nu} = \frac{p_{F\nu}^3}{3\pi^2},$$

$$m_{\nu}^* = m_{\nu} - \left(\frac{g_{\sigma}}{m_{\sigma}} \right)^2 n_{s,\nu},$$

$$\mu_{\nu} = E_{\nu}^* + \left(\frac{g_{\omega}}{m_{\omega}} \right)^2 n_{\nu} + \mu_{ex,\nu}.$$

2.2. Pauli blocking among baryons – results



2.3. Pauli blocking among baryons – Summary

Pauli blocking selfenergy (cluster meanfield) calculable in potential models for baryon structure

Partial replacement of other short-range repulsion mechanisms (vector meson exchange)

Modern aspects:

- onset of chiral symmetry restoration enhances nucleon swelling and Pauli blocking at high n
- quark exchange among baryons \rightarrow six-quark wavefunction \rightarrow “bag melting” \rightarrow deconfinement

Chiral stiffening of nuclear matter \rightarrow reduces onset density for deconfinement

Hybrid EoS:

Convenient generalization of RMF models,

Take care: eventually aspects of quark exchange already in density dependent vertices!

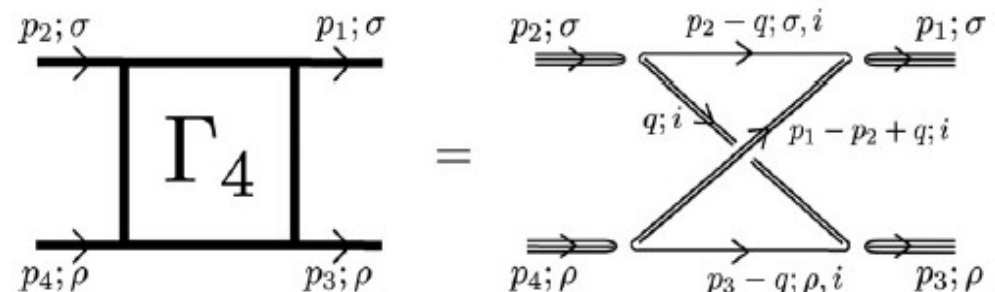
Other baryons:

- hyperons
- deltas

Again calculable, partially done in nonrelativistic quark exchange models, chiral effects not yet!

Relativistic generalization:

Box diagrams of quark-diquark model ...



2.4. Pauli blocking effect → Excluded volume

Well known from modeling dissociation of clusters in the supernova EoS:

- excluded volume: Lattimer-Swesty (1991), Shen-Toki-Oyamatsu-Sumiyoshi (1996), ...
- Pauli blocking: Roepke-Grigo-Sumiyoshi-Shen (2003), Typel et al. PRC 81 (2010)
- excl. Vol. vs. Pauli blocking: Hempel, Schaffner-Bielich, Typel, Roepke PRC 84 (2011)

Here: nucleons as quark clusters with finite size --> excluded volume effect !

Available volume fraction: $\Phi = V_{av}/V = 1 - v \sum_{i=n,p} n_i$, $v = \frac{1}{2} \frac{4\pi}{3} (2r_{nuc})^3 = 4V_{nuc}$

Equations of state for T=0 nuclear matter: $p_{tot}(\mu_n, \mu_p) = \frac{1}{\Phi} \sum_{i=n,p} p_i + p_{mes}$,

$$\mathcal{E}_{tot}(\mu_n, \mu_p) = -p_{tot} + \sum_{i=n,p} \mu_i n_i$$

$$p_i = \frac{1}{4} (E_i n_i - m_i^* n_i^{(s)}),$$

$$n_i = \frac{\Phi}{3\pi^3} k_i^3,$$

$$n_i^{(s)} = \frac{\Phi m_i^*}{2\pi^2} \left[E_i k_i - (m_i^*)^2 \ln \frac{k_i + E_i}{m_i^*} \right],$$

$$E_i = \sqrt{k_i^2 + (m_i^*)^2} = \mu_i - V_i - \frac{v}{\Phi} \sum_{j=p,n} p_j,$$

Effective mass: $m_i^* = m_i - S_i$.

Scalar meanfield: $S_i \sim n_i^{(s)}$

Vector meanfield: $V_i \sim n_i$

2.5. Stiff quark matter at high densities

S. Benic, Eur. Phys. J. A 50, 111 (2014)

$$\mathcal{L} = \bar{q}(i\cancel{\partial} - m)q + \mu_q \bar{q}\gamma^0 q + \mathcal{L}_4 + \mathcal{L}_8, \quad \mathcal{L}_4 = \frac{g_{20}}{\Lambda^2} [(\bar{q}q)^2 + (\bar{q}i\gamma_5\tau q)^2] - \frac{g_{02}}{\Lambda^2} (\bar{q}\gamma_\mu q)^2,$$

$$\mathcal{L}_8 = \frac{g_{40}}{\Lambda^8} [(\bar{q}q)^2 + (\bar{q}i\gamma_5\tau q)^2]^2 - \frac{g_{04}}{\Lambda^8} (\bar{q}\gamma_\mu q)^4 - \frac{g_{22}}{\Lambda^8} (\bar{q}\gamma_\mu q)^2 [(\bar{q}q)^2 + (\bar{q}i\gamma_5\tau q)^2]$$

Meanfield approximation: $\mathcal{L}_{\text{MF}} = \bar{q}(i\cancel{\partial} - M)q + \tilde{\mu}_q \bar{q}\gamma^0 q - U,$

$$M = m + 2\frac{g_{20}}{\Lambda^2} \langle \bar{q}q \rangle + 4\frac{g_{40}}{\Lambda^8} \langle \bar{q}q \rangle^3 - 2\frac{g_{22}}{\Lambda^8} \langle \bar{q}q \rangle \langle q^\dagger q \rangle^2,$$

$$\tilde{\mu}_q = \mu_q - 2\frac{g_{02}}{\Lambda^2} \langle q^\dagger q \rangle - 4\frac{g_{04}}{\Lambda^8} \langle q^\dagger q \rangle^3 - 2\frac{g_{22}}{\Lambda^8} \langle \bar{q}q \rangle^2 \langle q^\dagger q \rangle,$$

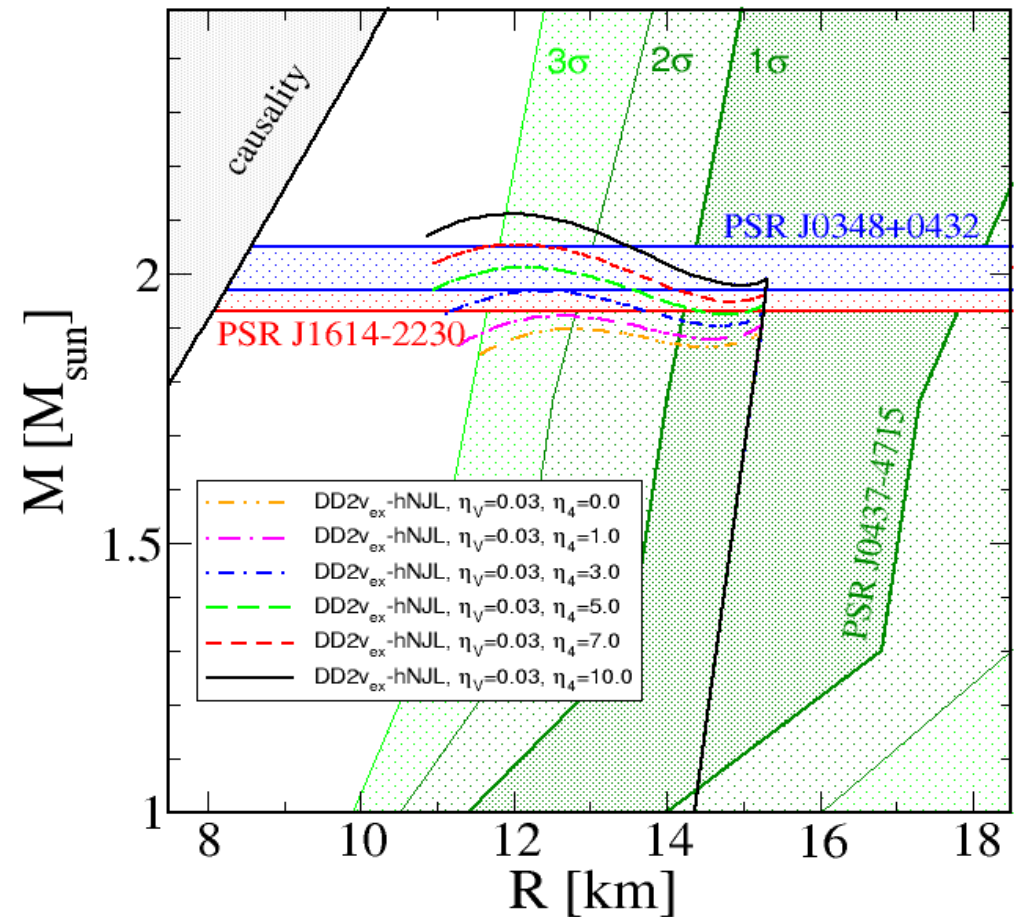
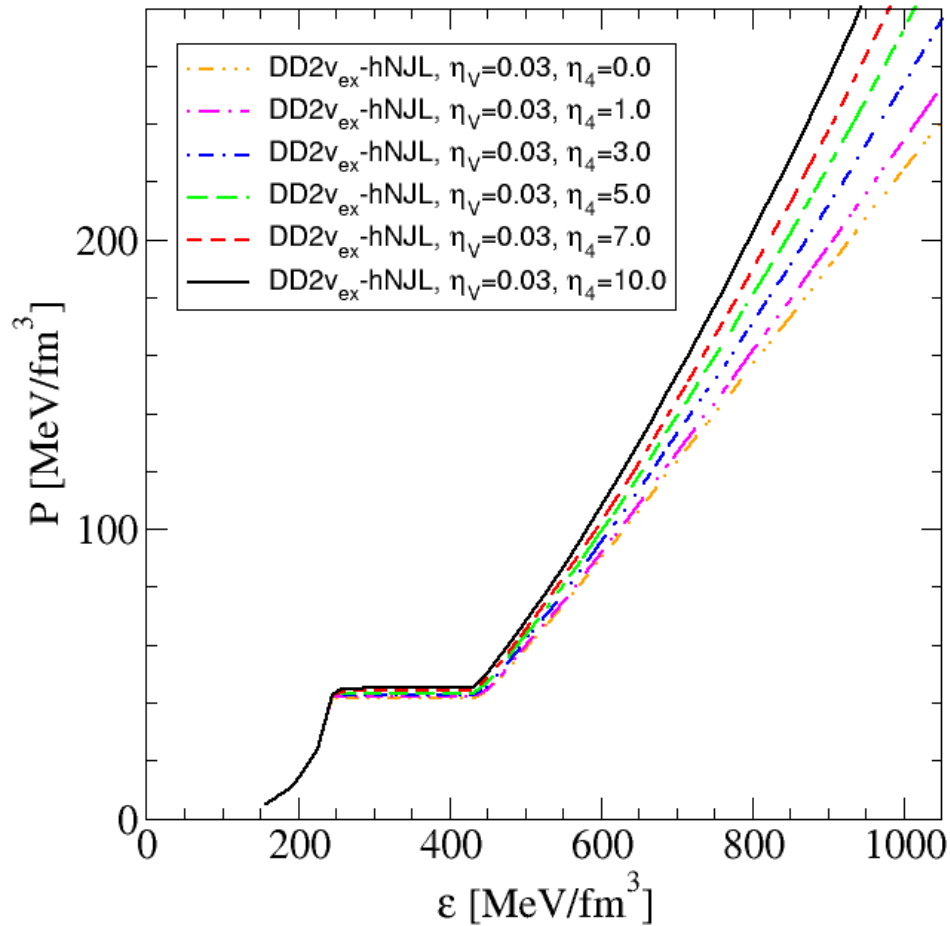
$$U = \frac{g_{20}}{\Lambda^2} \langle \bar{q}q \rangle^2 + 3\frac{g_{40}}{\Lambda^8} \langle \bar{q}q \rangle^4 - 3\frac{g_{22}}{\Lambda^8} \langle \bar{q}q \rangle^2 \langle q^\dagger q \rangle^2 - \frac{g_{02}}{\Lambda^2} \langle q^\dagger q \rangle^2 - 3\frac{g_{04}}{\Lambda^8} \langle q^\dagger q \rangle^4.$$

Thermodynamic Potential:

$$\Omega = U - 2N_f N_c \int \frac{d^3 p}{(2\pi)^3} \left\{ E + T \log[1 + e^{-\beta(E - \tilde{\mu}_q)}] + T \log[1 + e^{-\beta(E + \tilde{\mu}_q)}] \right\} + \Omega_0$$

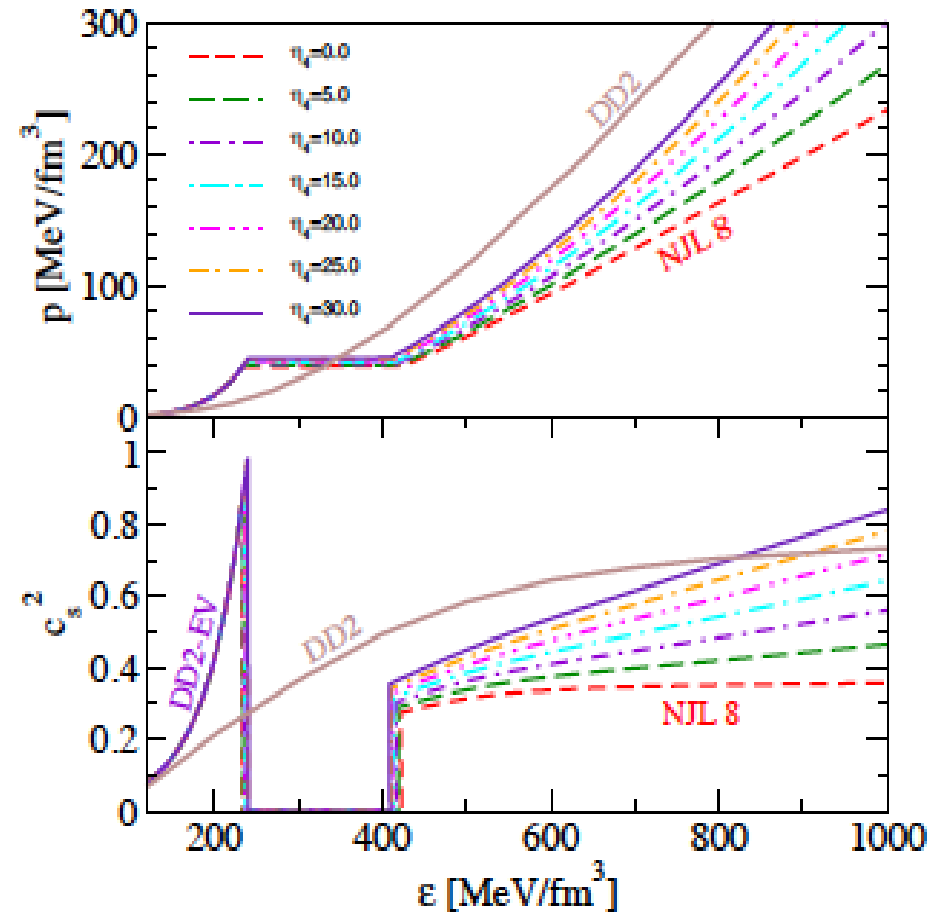
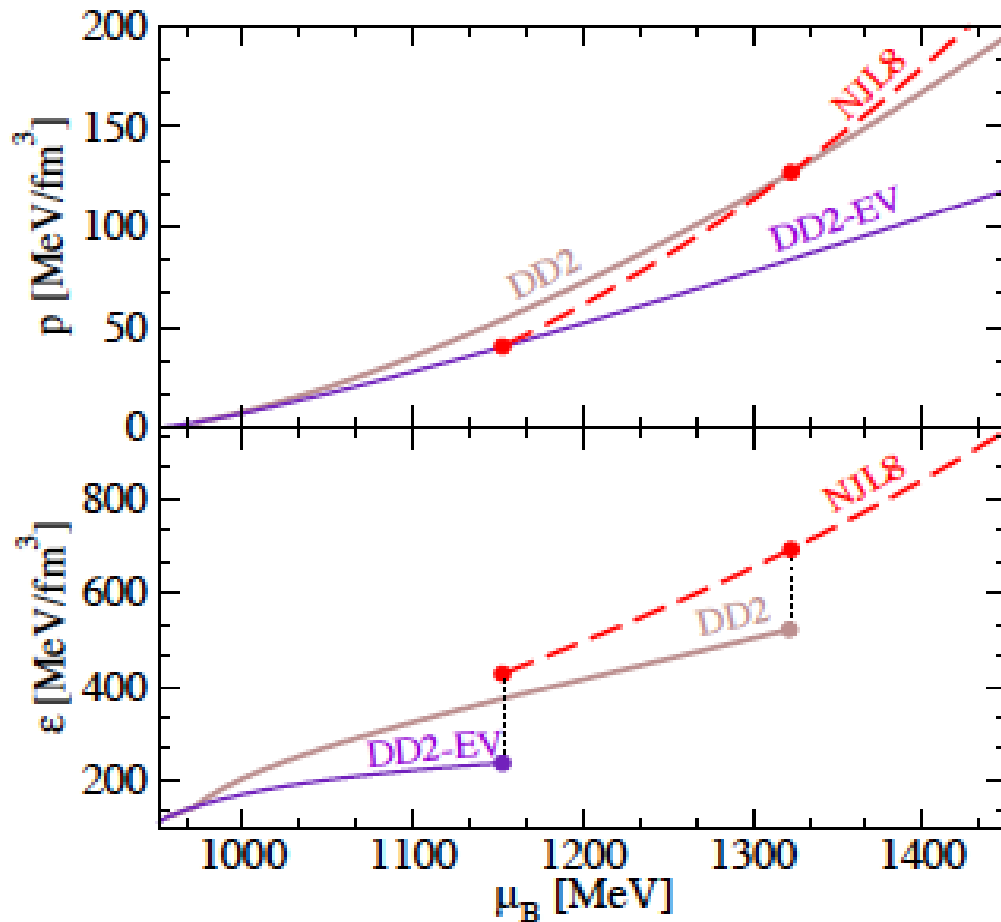
Result: high-mass twins \leftrightarrow 1st order PT

S. Benic, D. Blaschke, D. Alvarez-Castillo, T. Fischer, S. Typel, arxiv:1411.2856



Hybrid EoS supports M - R sequences with high-mass twin compact stars

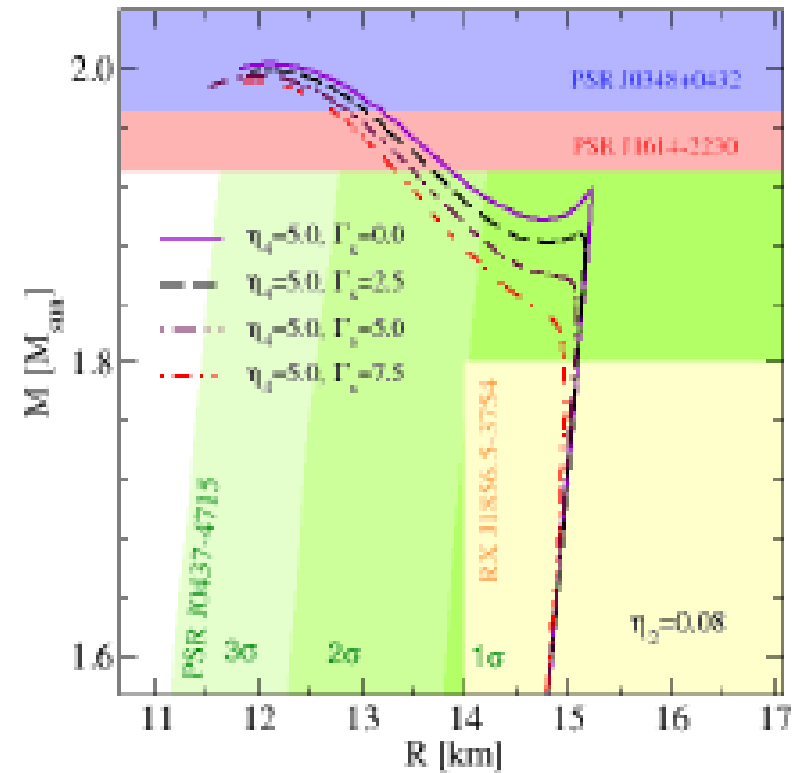
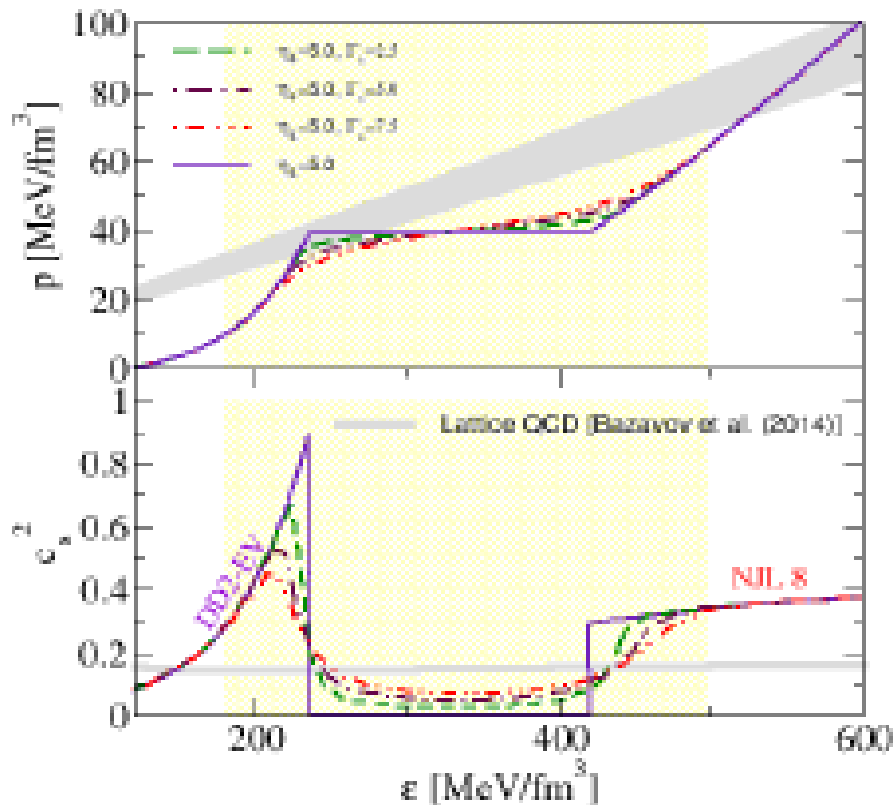
2.5. Stiff quark matter at high densities



Here: Stiffening of dense hadronic matter by excluded volume in density-dependent RMF

2.5. Stiff quark matter at high densities

Estimate effects of structures in the phase transition region (“pasta”)



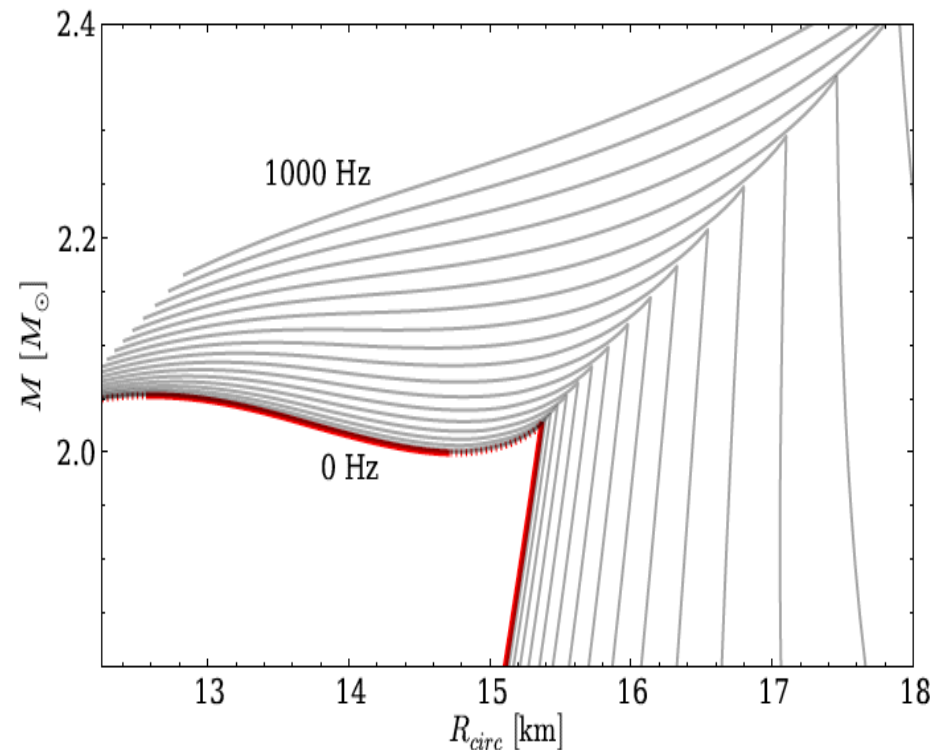
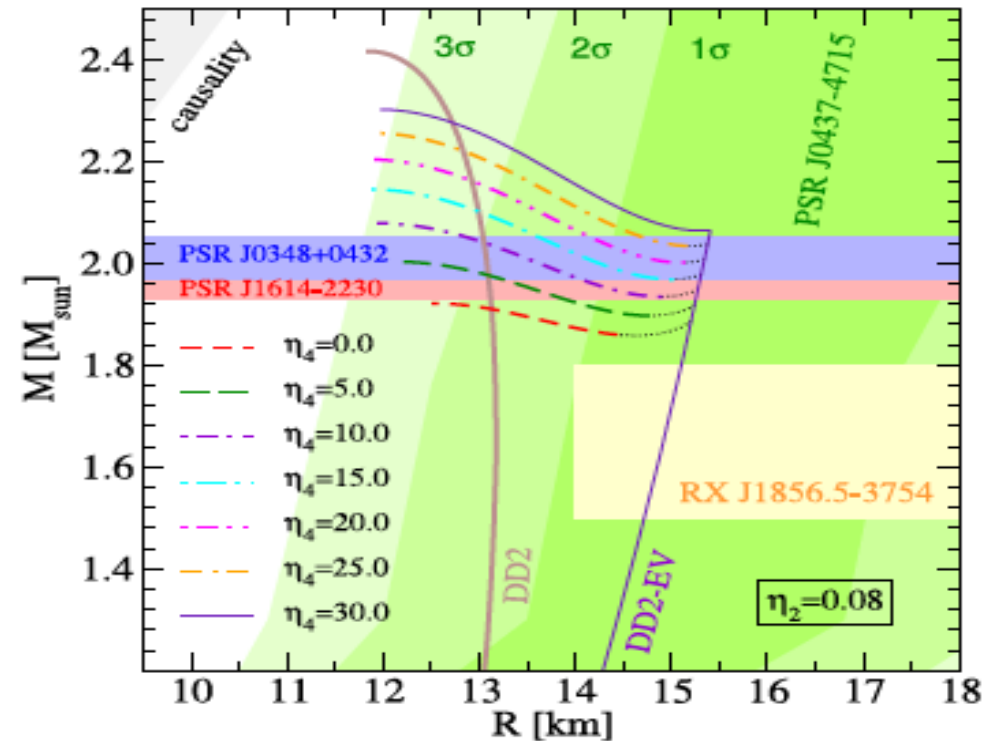
High-mass Twins relatively robust against “smoothing” the Maxwell transition construction

D. Alvarez-Castillo, D.B., arxiv:1412.8463; Phys. Part. Nucl. 46 (2015) 846

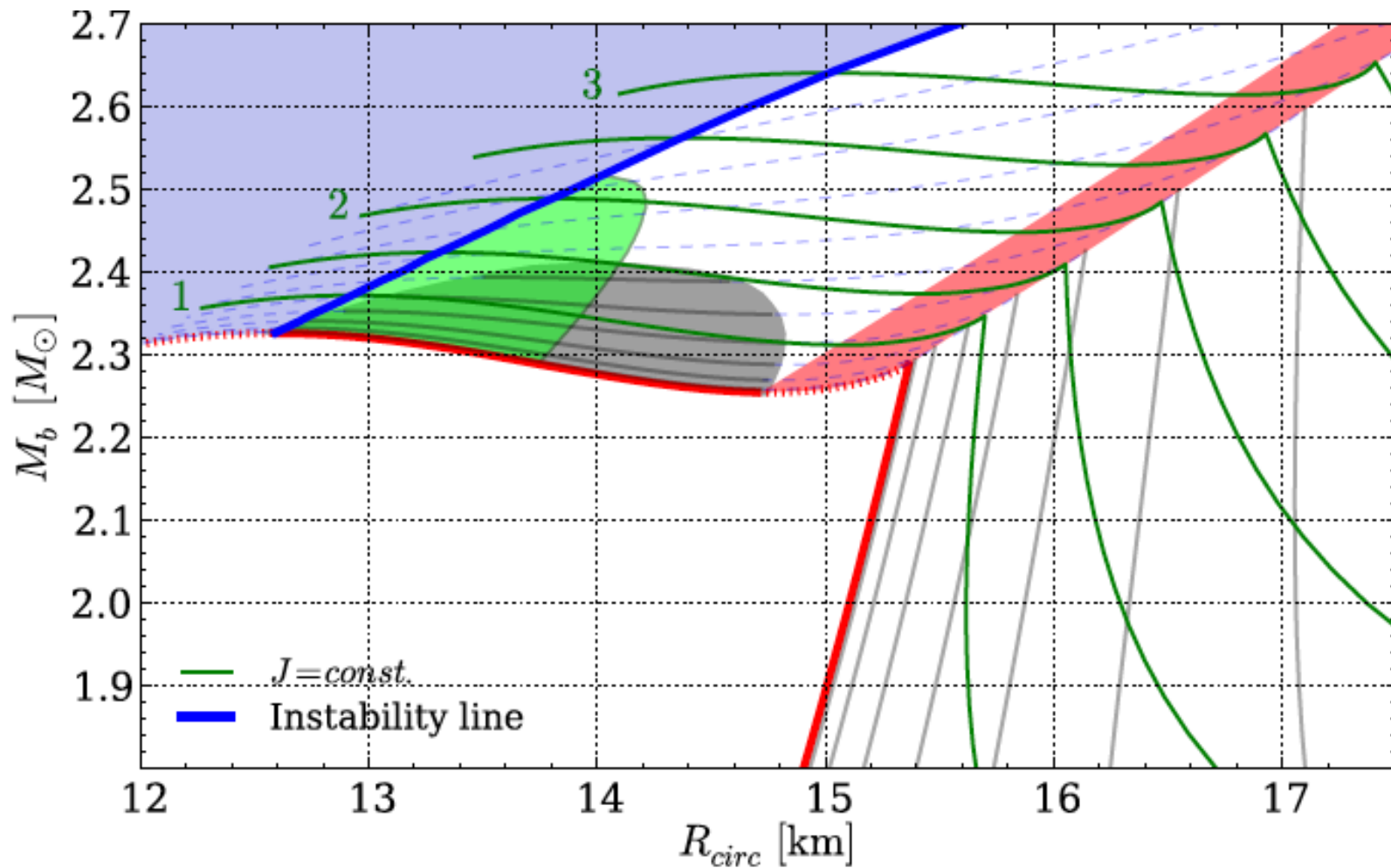
2.6. Rotation

- existence of 2 M_{sun} pulsars and possibility of high-mass twins raises question for their inner structure: (Q)uark or (N)ucleon core ??
 - > degenerate solutions
 - > transition from N to Q branch
 - PSR J1614-2230 is millisecond pulsar, period $P = 3.41$ ms, consider rotation !
 - transitions N --> Q must be considered for rotating configurations:
 - > how fast can they be?
- (angular momentum J and baryon mass should be conserved simultaneously)
- similar scenario as fast radio bursts (Falcke-Rezzolla, 2013) or braking index (Glendenning-Pei-Weber, 1997)

M. Bejger, D.B. et al., arxiv:1608.07049



2.6. Rotation and stability



Red region - strong phase-transition instability,

Blue region - unstable w.r.t axisymmetric oscillations,

Grey region - no back-bending,

Green region - stable twin branch reached after the mini-collapse from the tip of $J = const.$ curve, along $M_b = const.$

2.6. Rotation - summary

This type of instability EOS provides a "natural" explanation for:

- ★ Lack of back-bending in radiopulsar timing,
- ★ Spin frequency cut-off at some moderate (but >716 Hz) frequency,
- ★ Falcke & Rezzolla Fast Radio Burst (FRB) engine
 - ★ catastrophic mini-collapse to the second branch (or to a black hole),
 - ★ massive rearrangement of the magnetic field \rightarrow energy emission.

Astrophysical predictions:

- ★ Way to constraint on M_b , J , I , core EOS etc.,
- ★ Specific shape of NS-BH mass function (no mass gap?)
- \rightarrow population of massive, low B-field NSs (radio-dead?),
- \rightarrow population of massive, high B-field NSs (collapse enhances the field?),
- ★ Characteristic burst-like signature in GW emission during the mini-collapse.

3. New Bayesian Analysis scheme

Measure the cold EoS by Bayesian TOV!

Bayesian TOV analysis:

Steiner, Lattimer, Brown, ApJ 722 (2010) 33

Most Probable Values for Masses and Radii for Neutron Stars Constrained to Lie on One Mass Versus Radius Curve

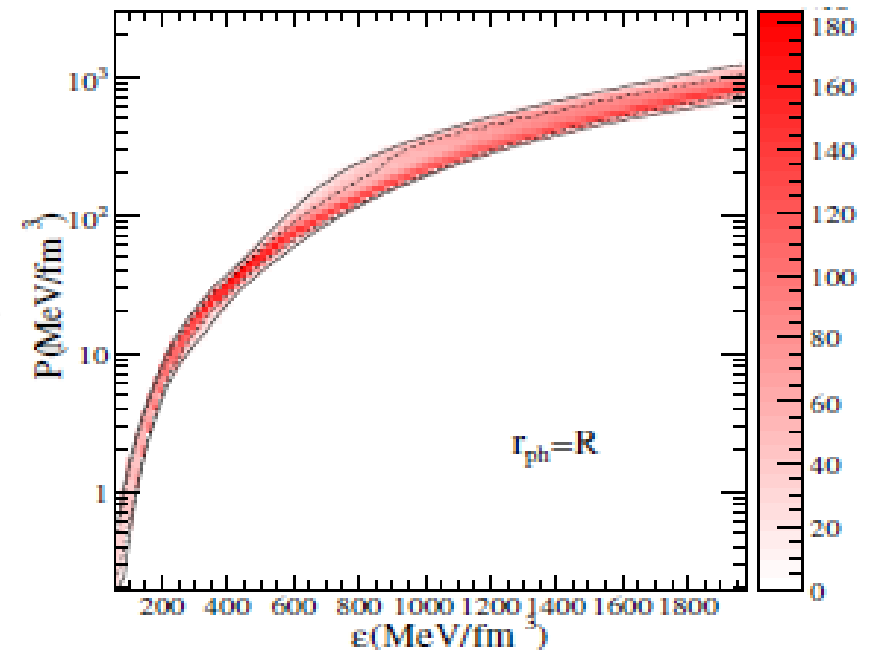
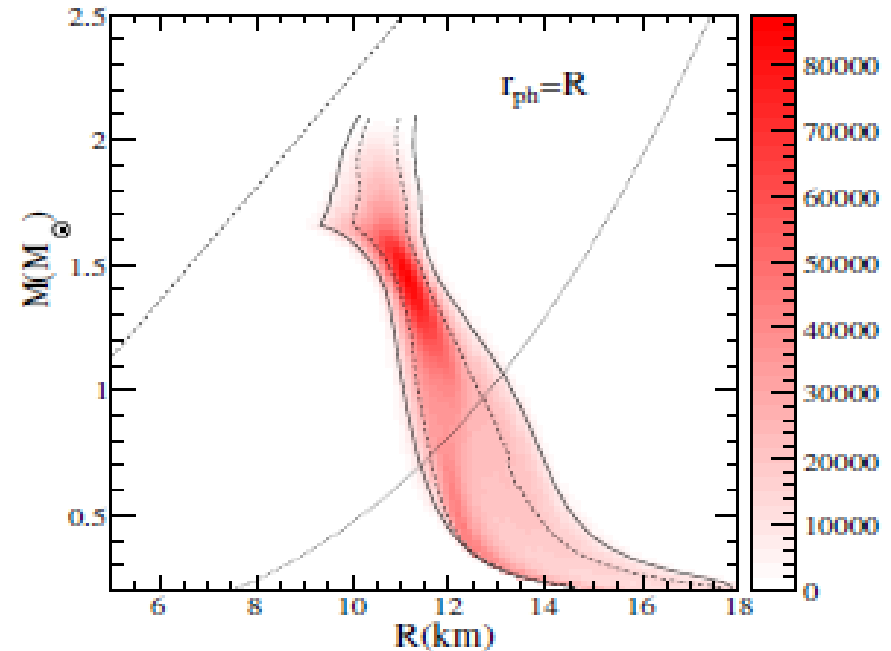
Object	$r_{\text{ph}} = R$		$r_{\text{ph}} \gg R$	
	$M (M_{\odot})$	$R \text{ (km)}$	$M (M_{\odot})$	$R \text{ (km)}$
4U 1608–522	$1.52^{+0.22}_{-0.18}$	$11.04^{+0.53}_{-1.50}$	$1.64^{+0.34}_{-0.41}$	$11.82^{+0.42}_{-0.89}$
EXO 1745–248	$1.55^{+0.12}_{-0.36}$	$10.91^{+0.86}_{-0.65}$	$1.34^{+0.450}_{-0.28}$	$11.82^{+0.47}_{-0.72}$
4U 1820–30	$1.57^{+0.13}_{-0.15}$	$10.91^{+0.39}_{-0.92}$	$1.57^{+0.37}_{-0.31}$	$11.82^{+0.42}_{-0.82}$
M13	$1.48^{+0.21}_{-0.64}$	$11.04^{+1.00}_{-1.28}$	$0.901^{+0.28}_{-0.12}$	$12.21^{+0.18}_{-0.62}$
ω Cen	$1.43^{+0.26}_{-0.61}$	$11.18^{+1.14}_{-1.27}$	$0.994^{+0.51}_{-0.21}$	$12.09^{+0.27}_{-0.66}$
X7	$0.832^{+1.19}_{-0.051}$	$13.25^{+1.37}_{-3.50}$	$1.98^{+0.10}_{-0.36}$	$11.3^{+0.95}_{-1.03}$

Caution:

If optical spectra are not measured, the observed X-ray spectrum may not come from the entire surface
But from a hot spot at the magnetic pole!

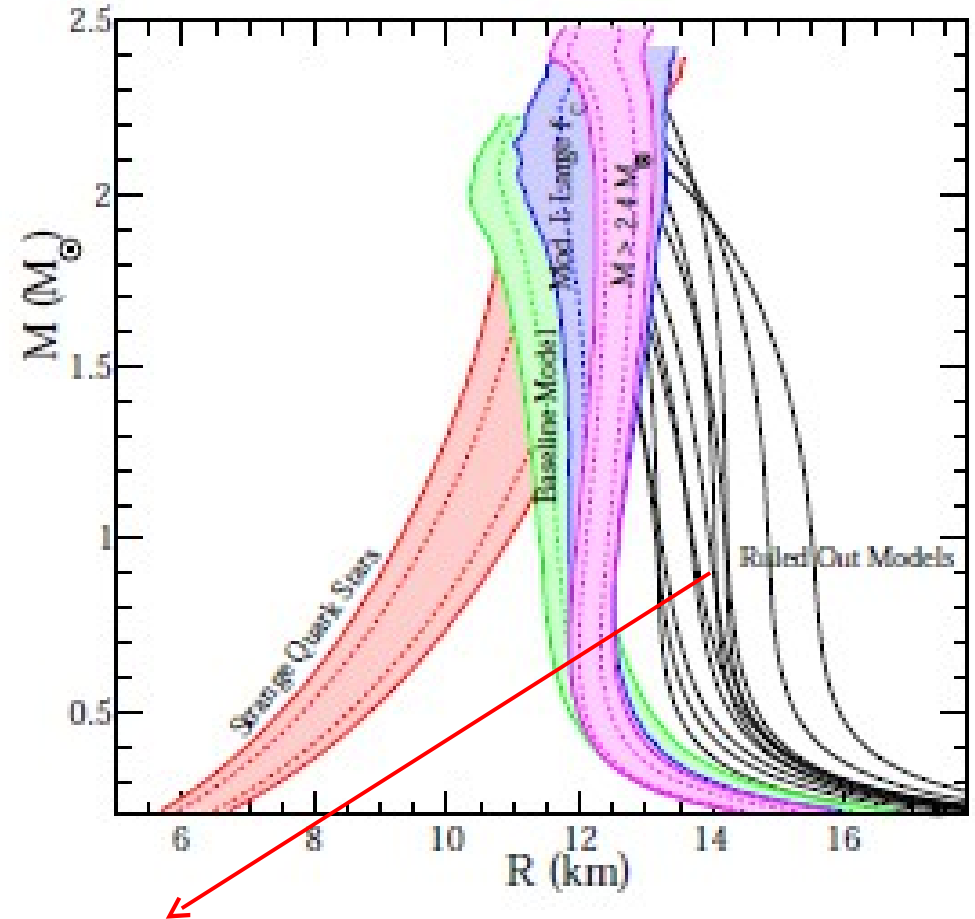
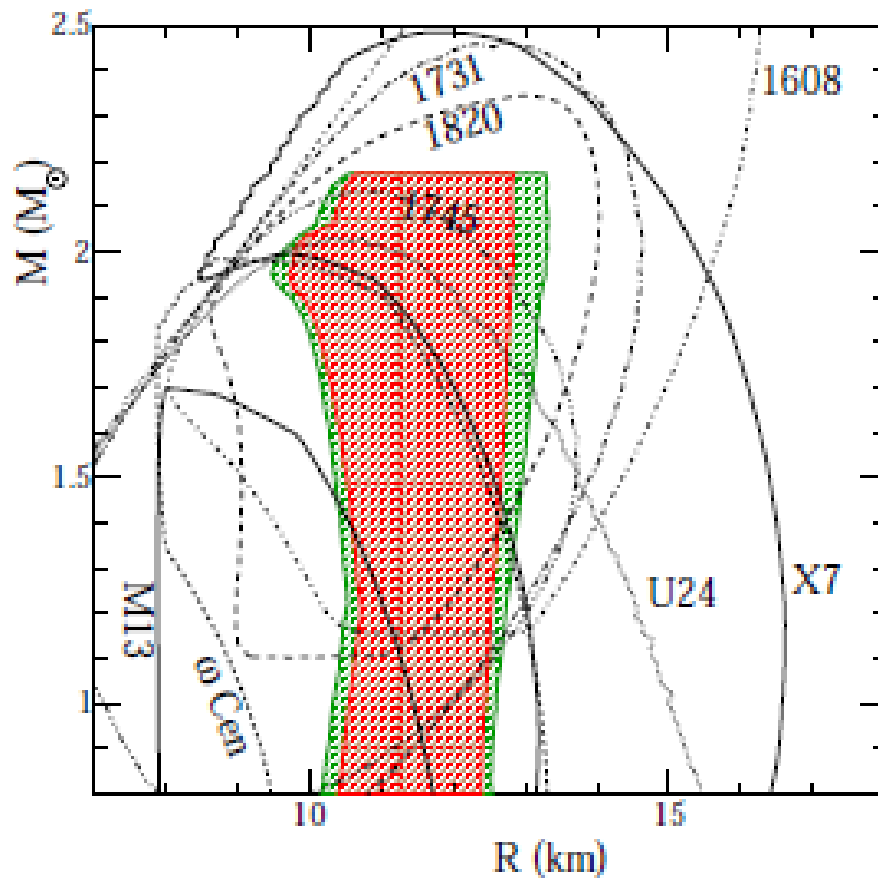
J. Trumper, Prog. Part. Nucl. Phys. 66 (2011) 674

Such systematic errors are not accounted for in Steiner et al. \rightarrow $M(R)$ is a lower limit \rightarrow softer EoS



Which constraints require caution ?

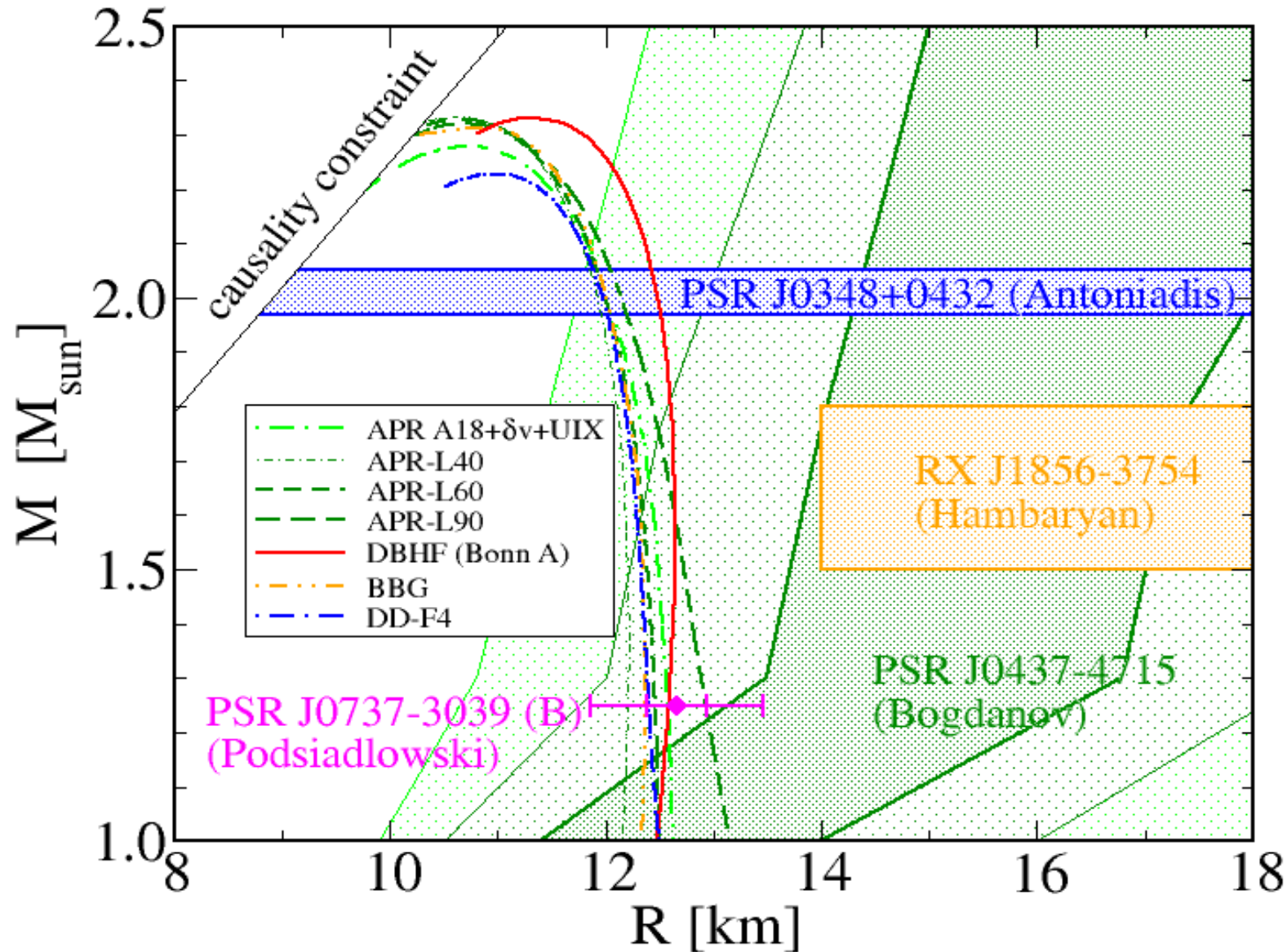
A. Steiner, J. Lattimer, E. Brown, ApJ Lett. 765 (2013) L5



“Ruled out models” - too strong a conclusion!

$M(R)$ constraint is a lower limit, which is itself included in that from RX J1856, which is one of the best known sources.

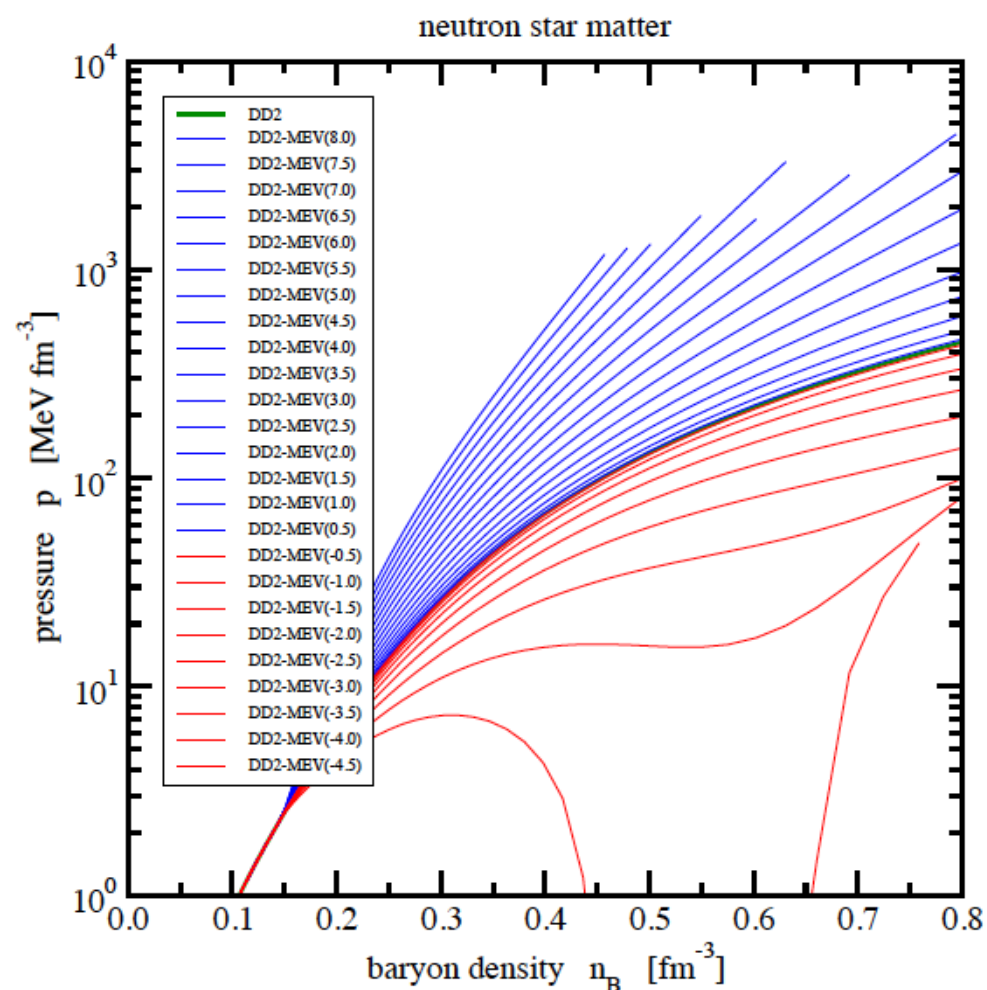
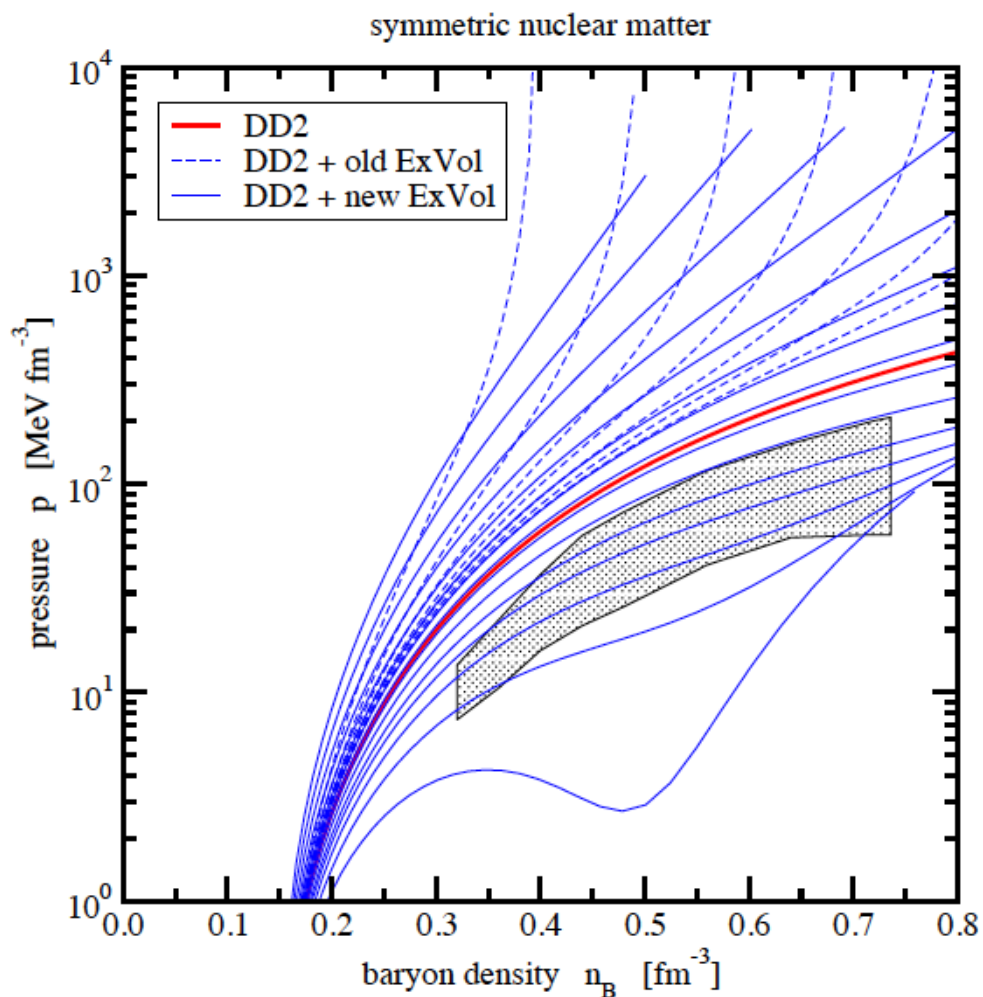
Disjunct M-R constraints for Bayesian analysis !



3.1. Equation of state

- excluded volume corrections in the hadronic EoS,

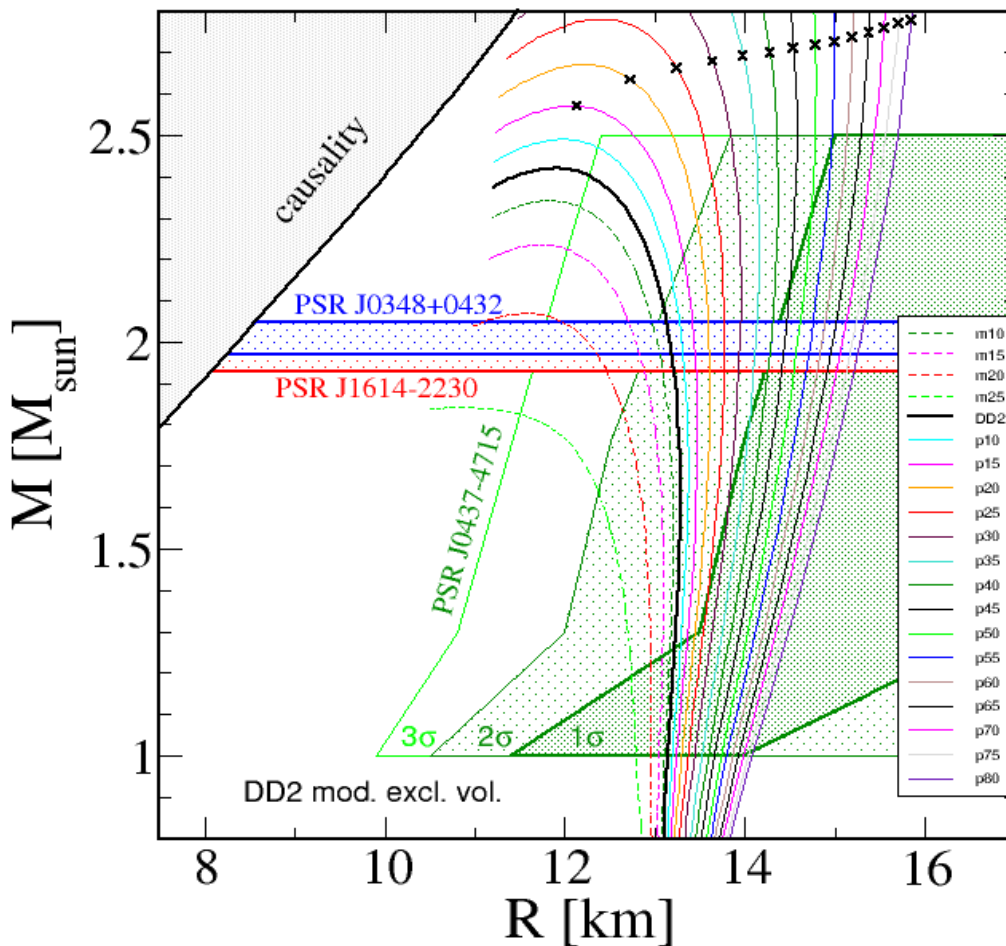
$$\Phi_N = \begin{cases} 1, & \text{if } n \leq n_{\text{sat}} \\ \exp[-v|v|(n - n_{\text{sat}})^2/2], & \text{if } n > n_{\text{sat}} \end{cases}$$



1. Equation of state <--> M-R relation

- excluded volume corrections in the hadronic EoS,

$$\Phi_N = \begin{cases} 1, & \text{if } n \leq n_{\text{sat}} \\ \exp[-v|v|(n - n_{\text{sat}})^2/2], & \text{if } n > n_{\text{sat}} \end{cases}$$

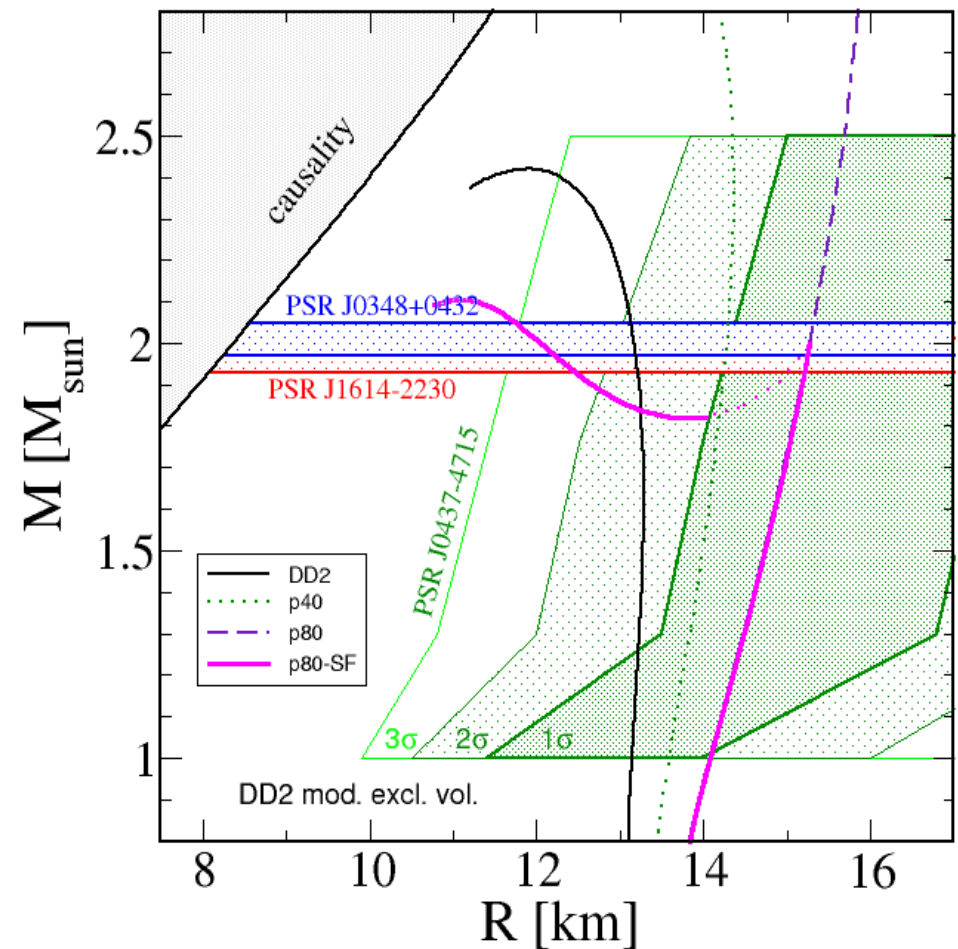
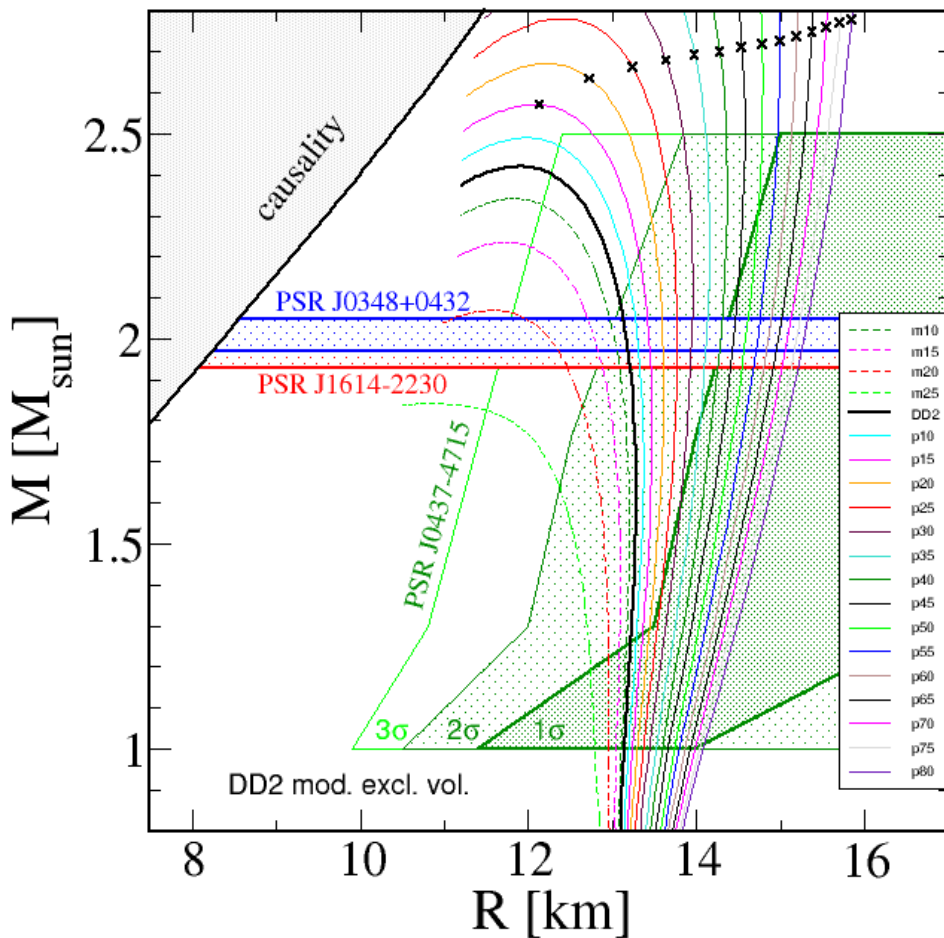


- crosses: violation of causality!
- consider phase transition to quark matter!

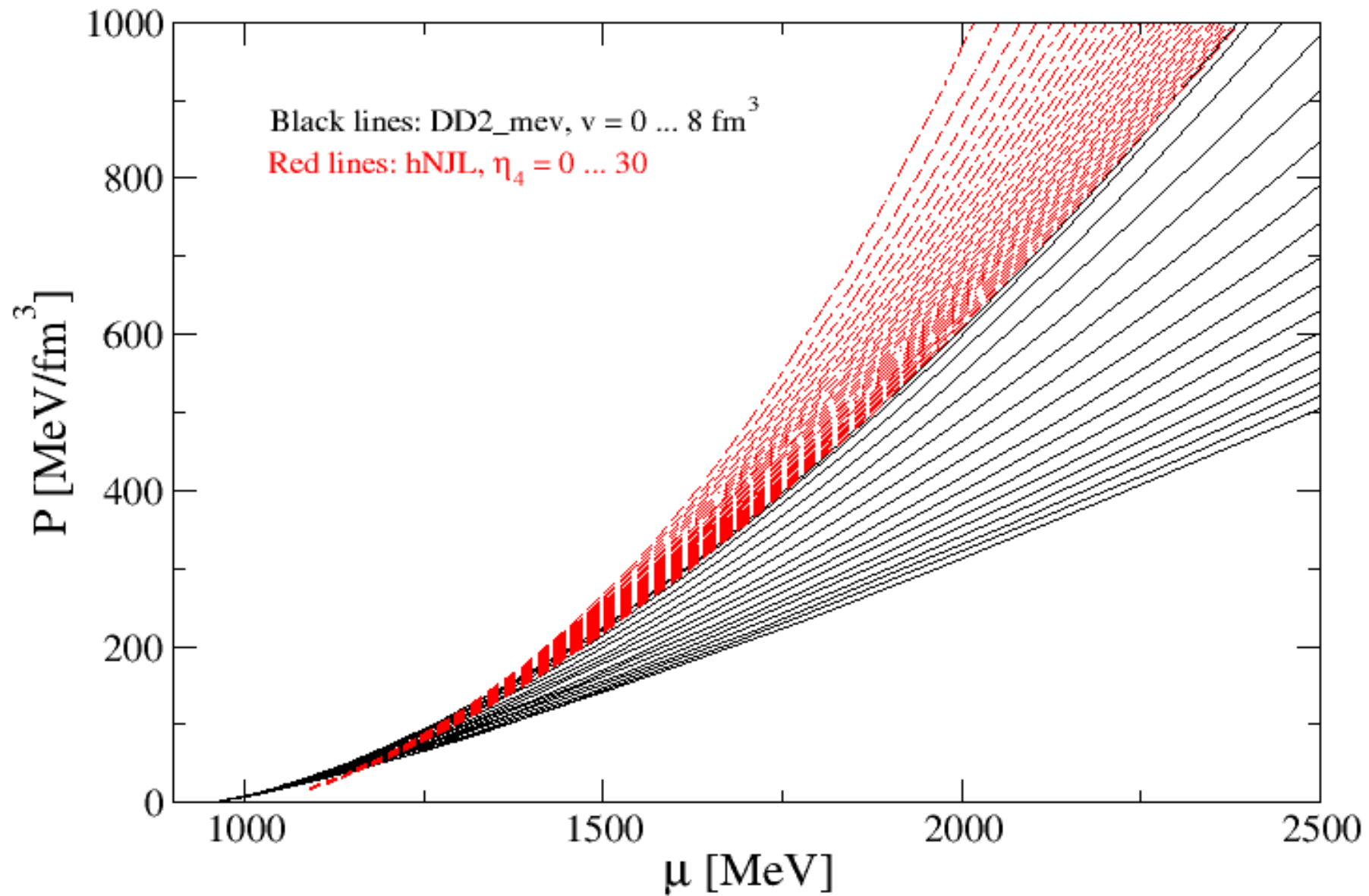
3.1. Equation of state <--> M-R relation

--> Phase transition removes problem with causality ...

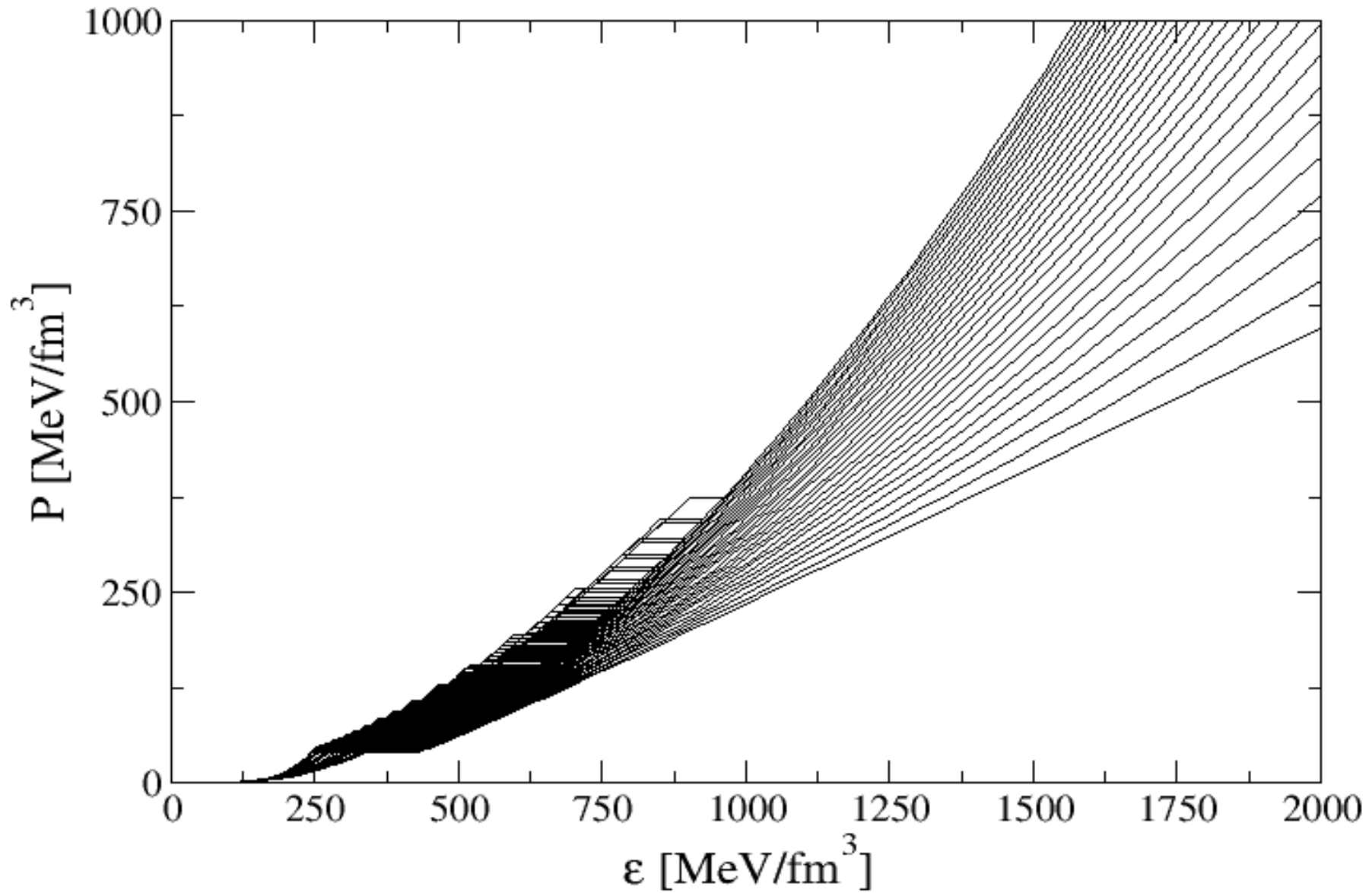
--> Example: See Alvarez, Kaltenborn, Blaschke [arxiv:1511.05873] (magenta line)



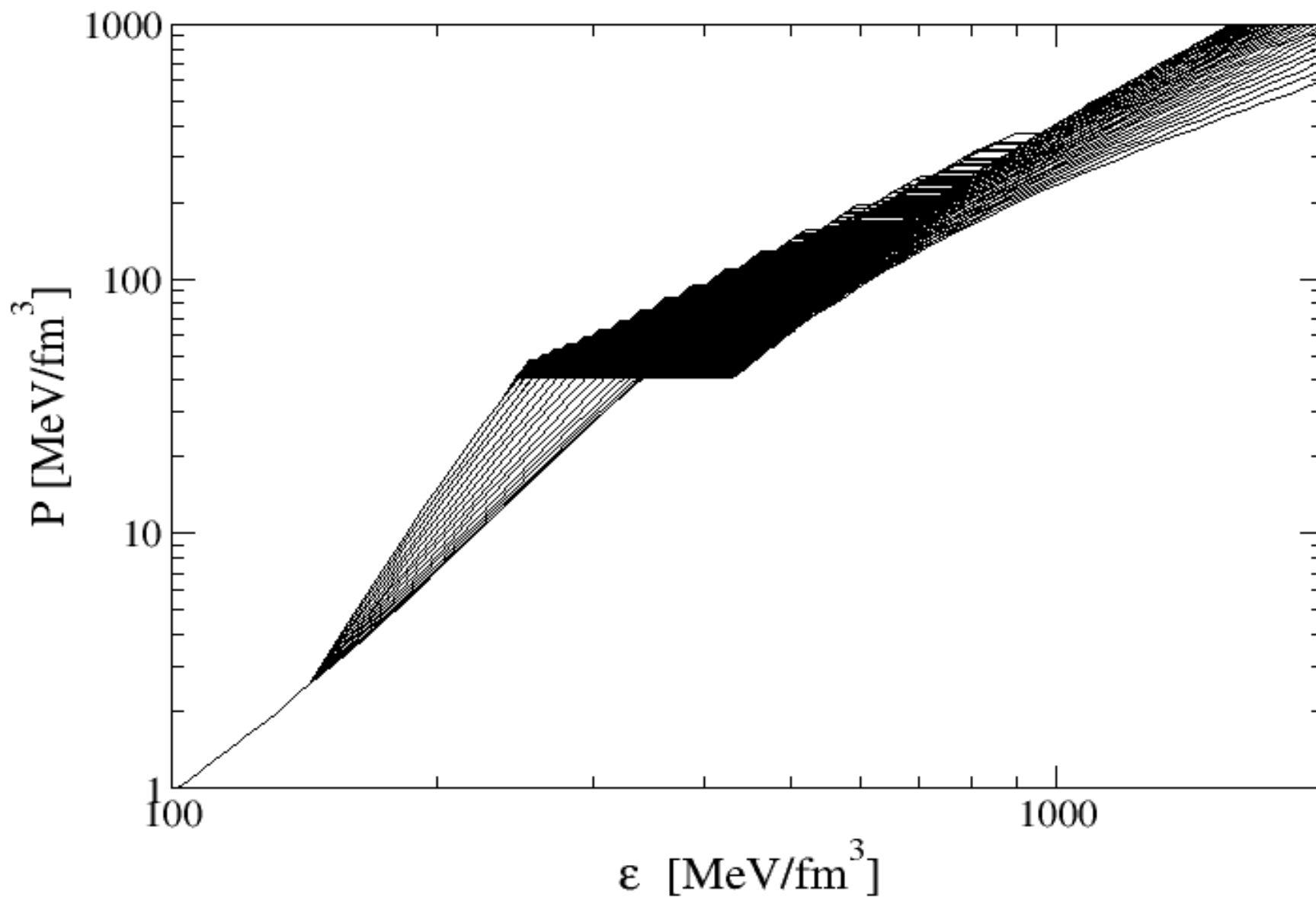
3.1. Equation of state



3.1. Equation of state

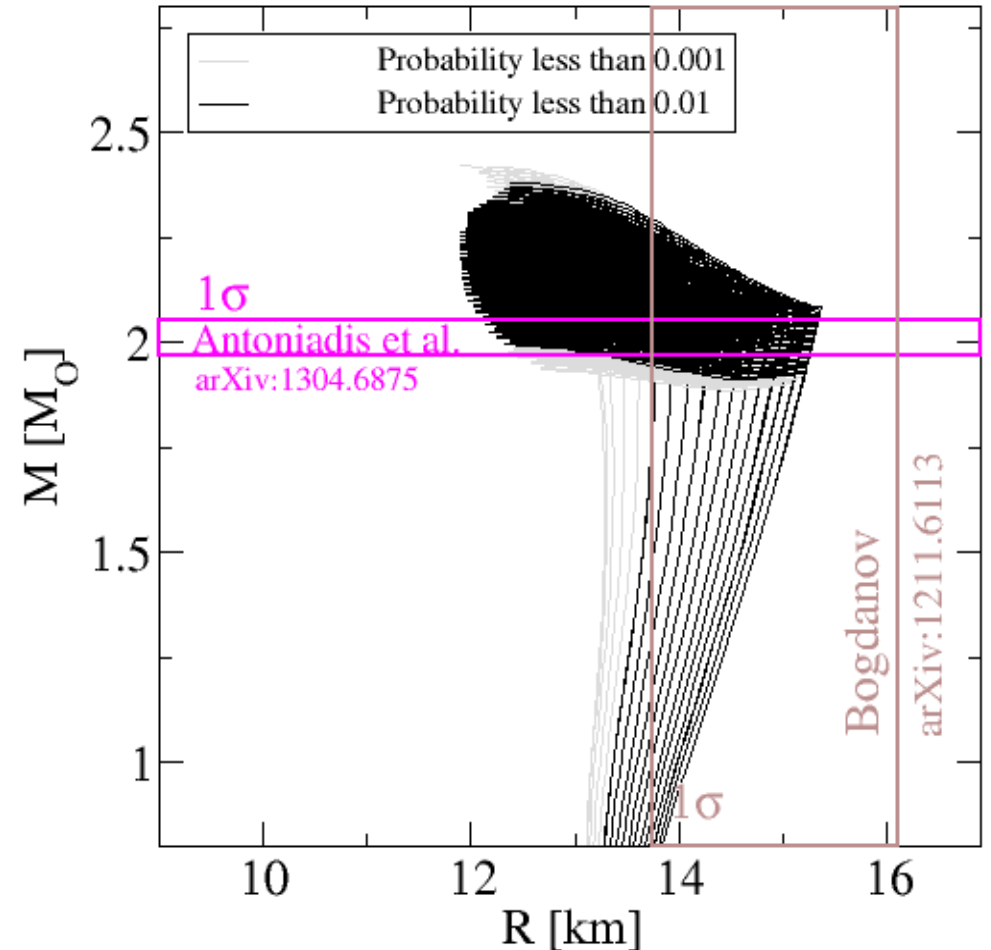
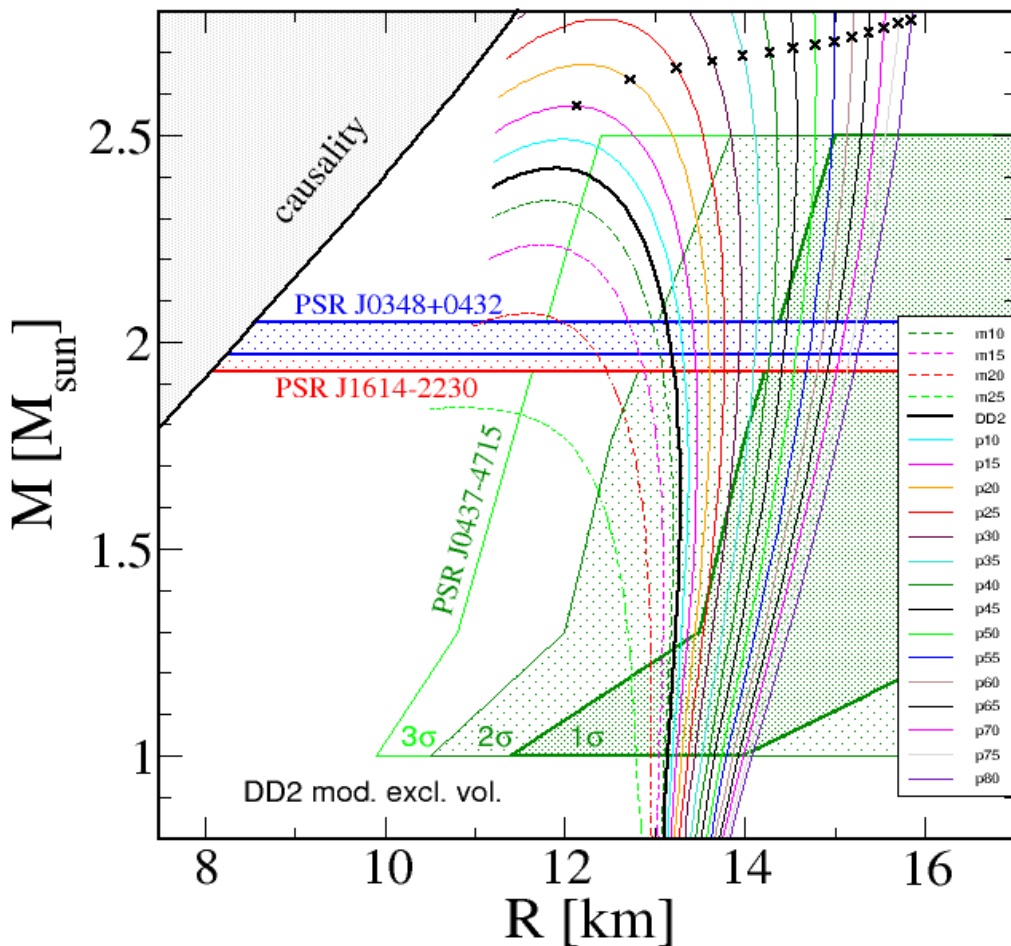


3.1. Equation of state



3.1. Equation of state <--> M-R relation

- excluded volume corrections in the hadronic EoS,
- multi-quark interactions for quark matter EoS.



3.2. New Bayesian analysis scheme

For the BA of the most probable EoS for given prior from (real or fictitious) observations, we start by defining a vector of free parameters $\vec{\pi}(p, \eta_A)$, which correspond to all the possible models with phase transition from nuclear to quark matter using the EoS described above. The way we sample these parameters is

$$\pi_i = \vec{\pi}(p(k), \eta_A(l)), \quad (2)$$

where $i = 0, 1, \dots, N - 1$ with $N = N_1 \times N_2$ such that $i = N_2 \times k + l$ and $k = 0, 1, \dots, N_1 - 1$, $l = 0, 1, \dots, N_2 - 1$, with N_1 and N_2 as the total number of parameters p_k and $\eta_{(4)l}$ respectively. The goal is to find the set π_i corresponding to an EoS and thus a sequence of configurations which contains the most probable one based on the given constraints using BA. For initializing the BA we propose that *a priori* each vector of parameters π_i has the same probability: $P(\pi_i) = 1/N$ for $\forall i$. We can calculate probability of π_i using Bayes' theorem [13]

$$P(\pi_i | E) = \frac{P(E | \pi_i) P(\pi_i)}{\sum_{j=0}^{N-1} P(E | \pi_j) P(\pi_j)}. \quad (3)$$

D. E. Alvarez-Castillo, A. Ayriyan, D. Blaschke and H. Grigorian, arXiv:1506.07755

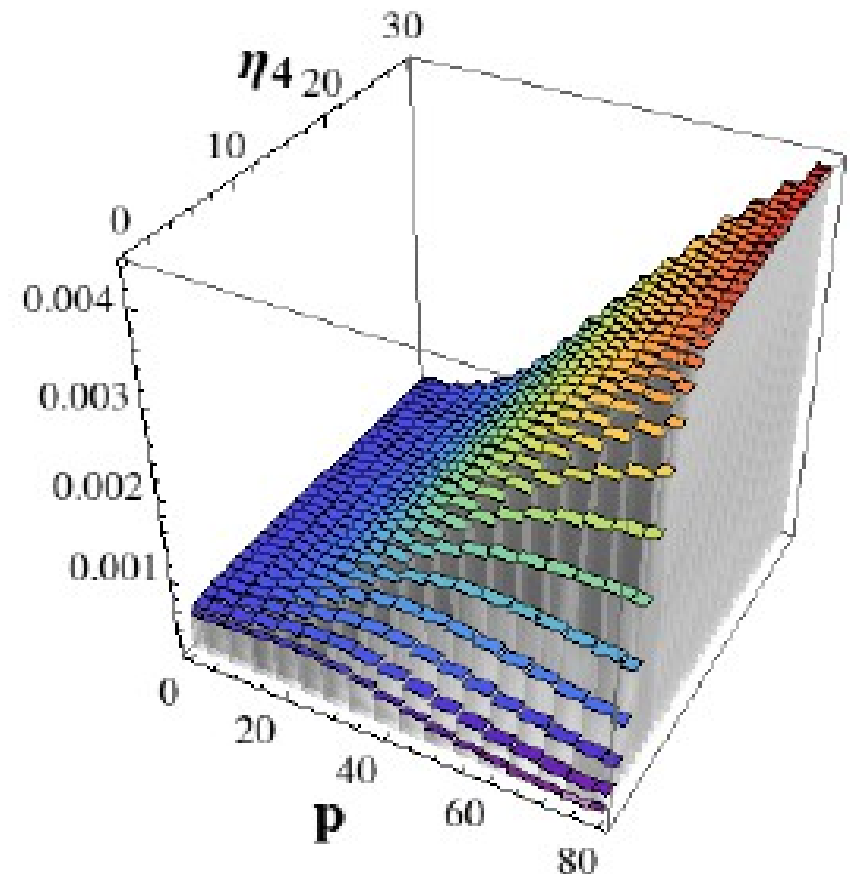
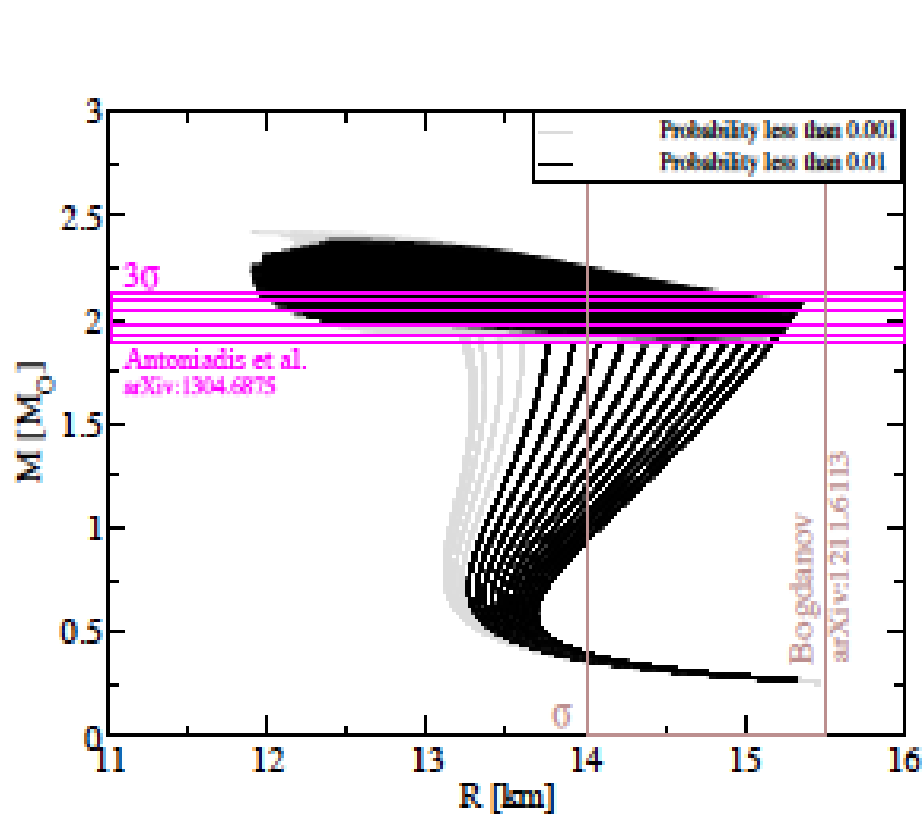
D. Blaschke, H. Grigorian, D. E. Alvarez-Castillo and A. Ayriyan, J. Phys. Conf. Ser. **496**, 012002 (2014).

A. Ayriyan, D. E. Alvarez-Castillo, D. Blaschke, H. Grigorian and M. Sokolowski, Phys. Part. Nucl. **46**, 854 (2015).

3.2. New Bayesian analysis scheme

case A

- a maximum mass constraint from PSR J0348+0432 [10],
- a radius constraint from the nearest millisecond pulsar and PSR J0437-4715 [12],



Phase transition? Measure different radii at 2Mo !

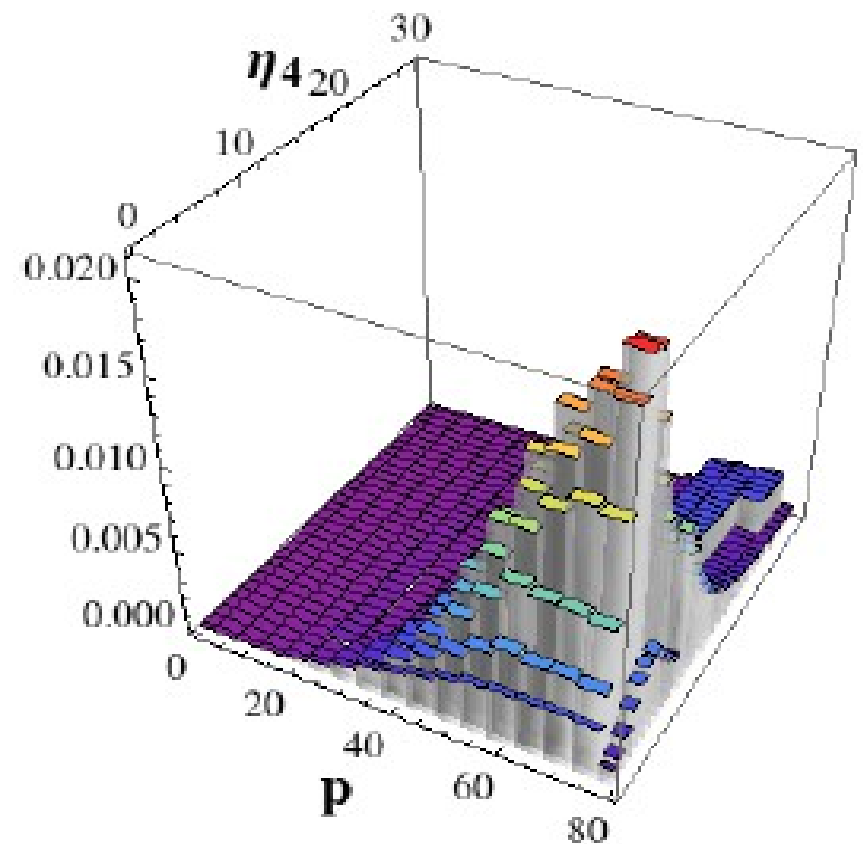
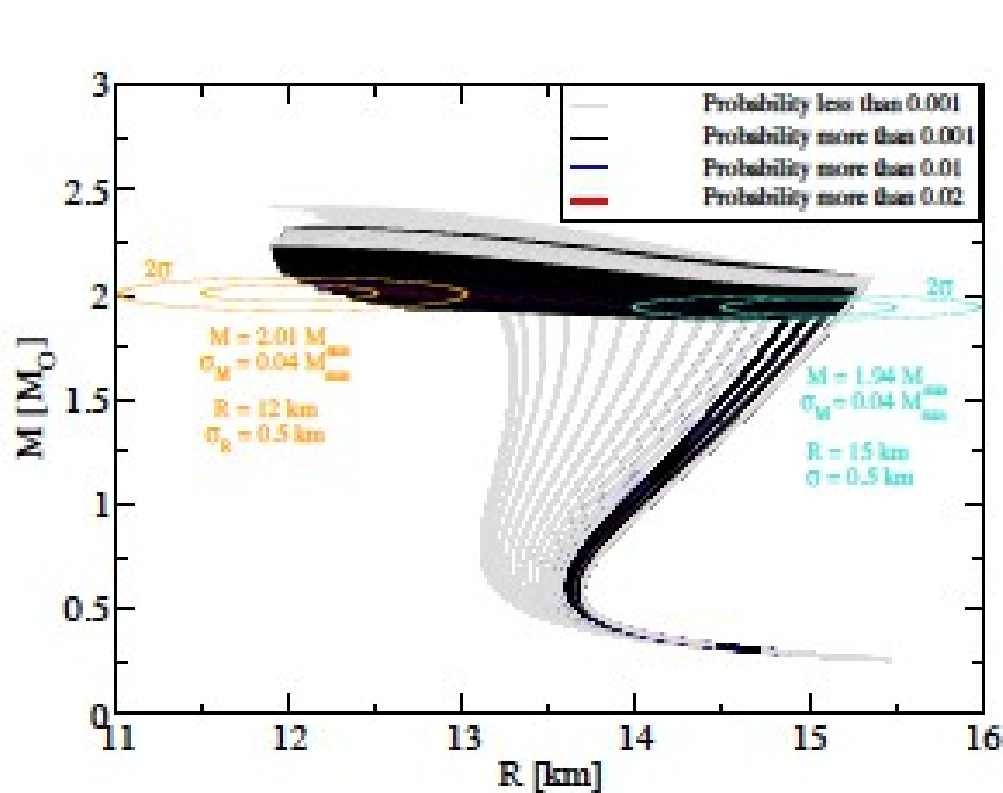
“Now let us travel into future. It is year **2017**, some new, reliable NS radius measurement methods are discovered and were used to find the size of two most massive pulsars, which still are PSR J0348+0432 and PSR J1614-2230. **The community was shocked** when received the results of observations: one radius is 13 ± 0.5 km, while the other is 11 ± 0.5 km!”

– *Michał Sokołowski*, Master Thesis, 2014

3.2. New Bayesian analysis scheme

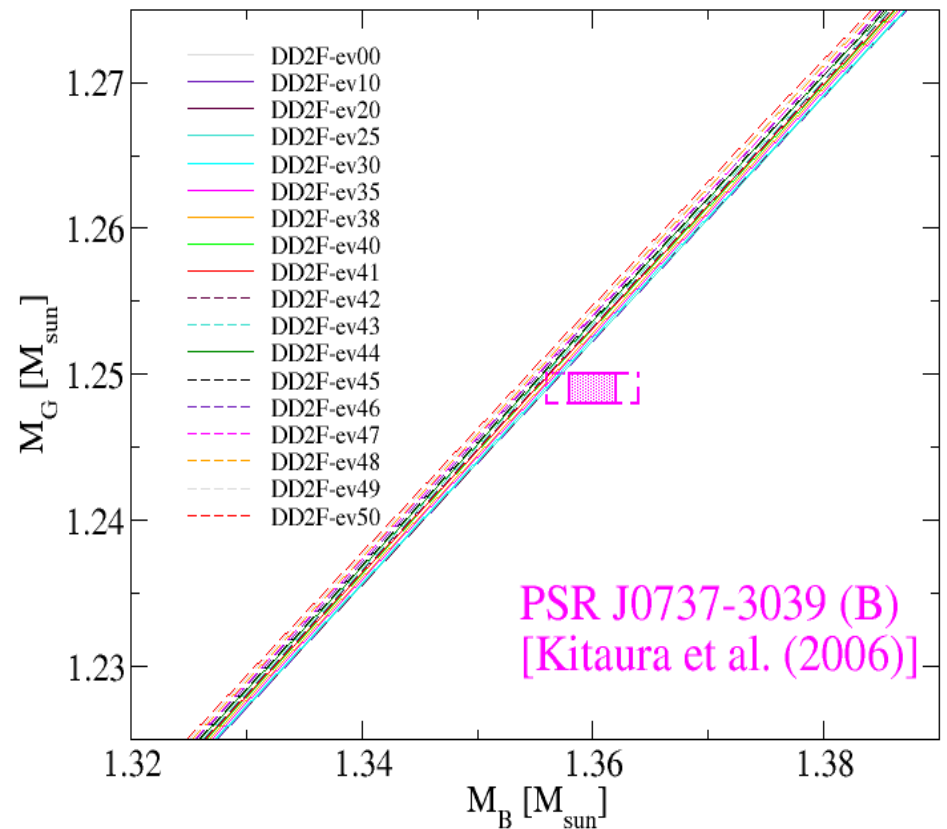
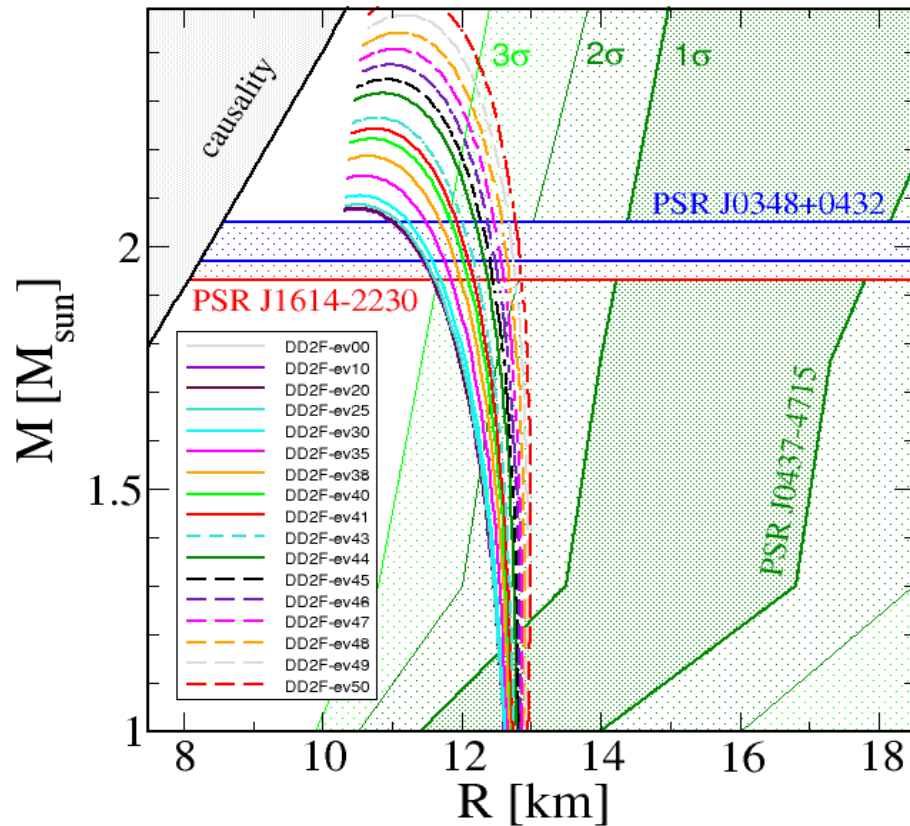
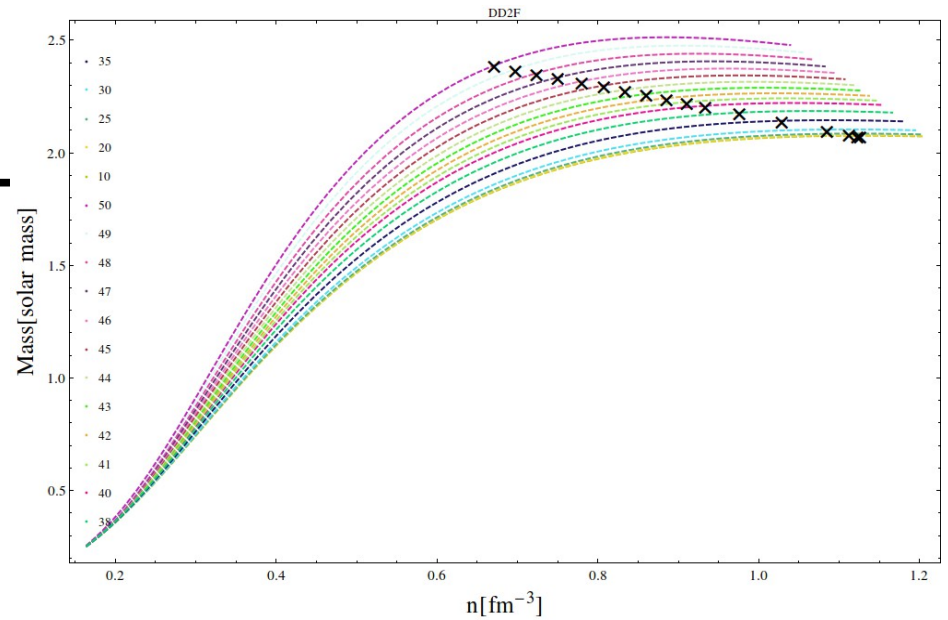
case B

- a radius measurement of $R = 12 \pm 0.5$ km for PSR J0348+0432 with its known mass,
- a radius measurement of $R = 15 \pm 0.5$ km for PSR J1614-2230 with its known mass,



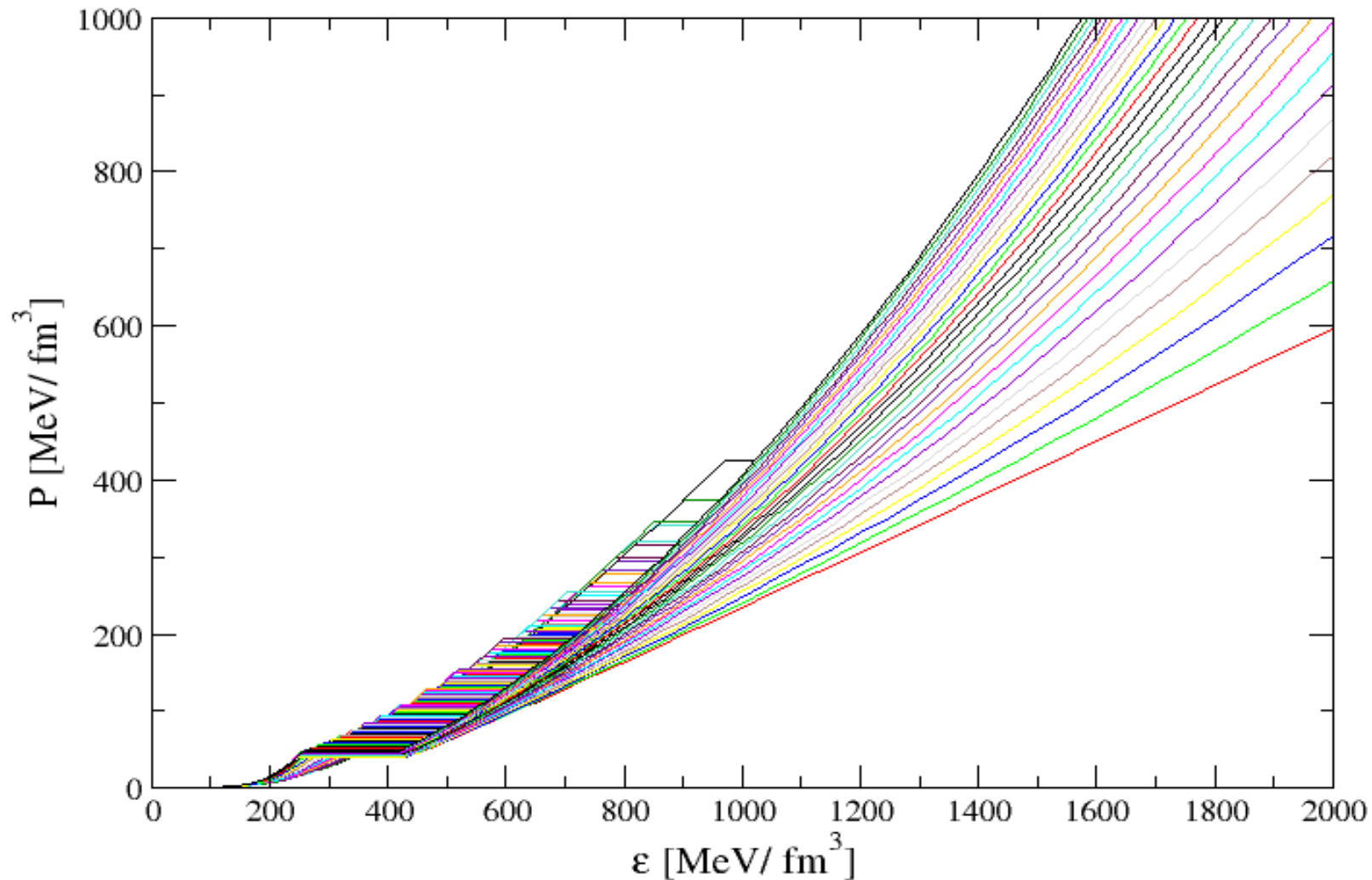
3.3. Outlook

- hadronic EoS too stiff:
 - tension with Danielewicz' flow constraint
 - violates Podsiadlowski's $M-M_B$ relation
- DD2 --> DD2F_ev – Stefan Typel

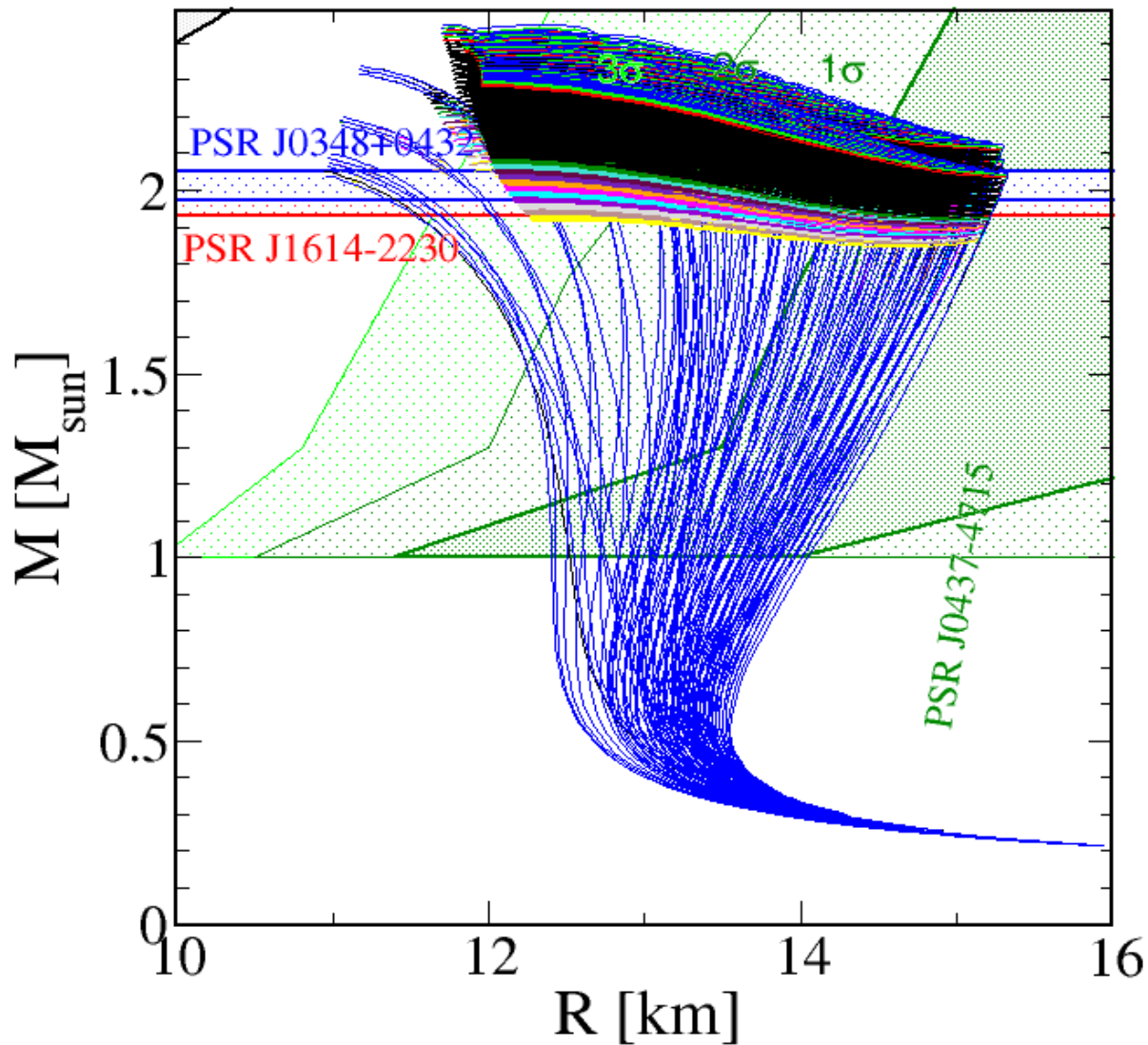


3.3. Outlook: Extended Bayesian analysis scheme

EoS extension: $(DD2 + DD2F) \times (E_s^m + E_s + E_s^p)$
 $= DD2m + DD2 + DD2p + DD2Fm + DD2F + DD2Fp$



3.3. Outlook: Extended Bayesian analysis scheme



Hadronic EoS classes
(varying v_{ex}):

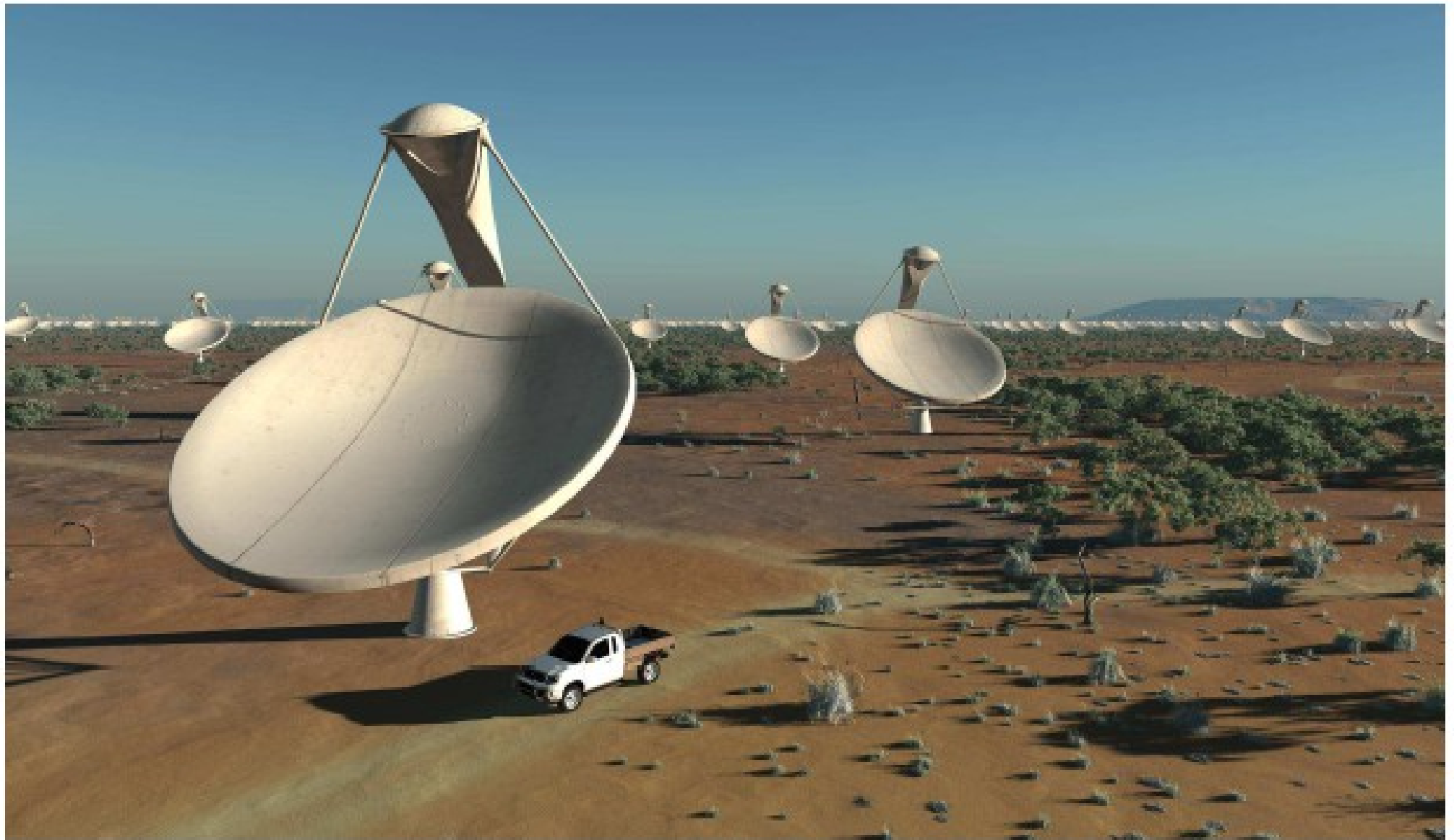
- DD2m
- + DD2
- + DD2p
- + DD2Fm
- + DD2F
- + DD2Fp

Quark matter EoS
(varying η_4):

hNJL

D. Alvarez-Castillo et al.,
Eur. Phys. J. A52, 69 (2016)

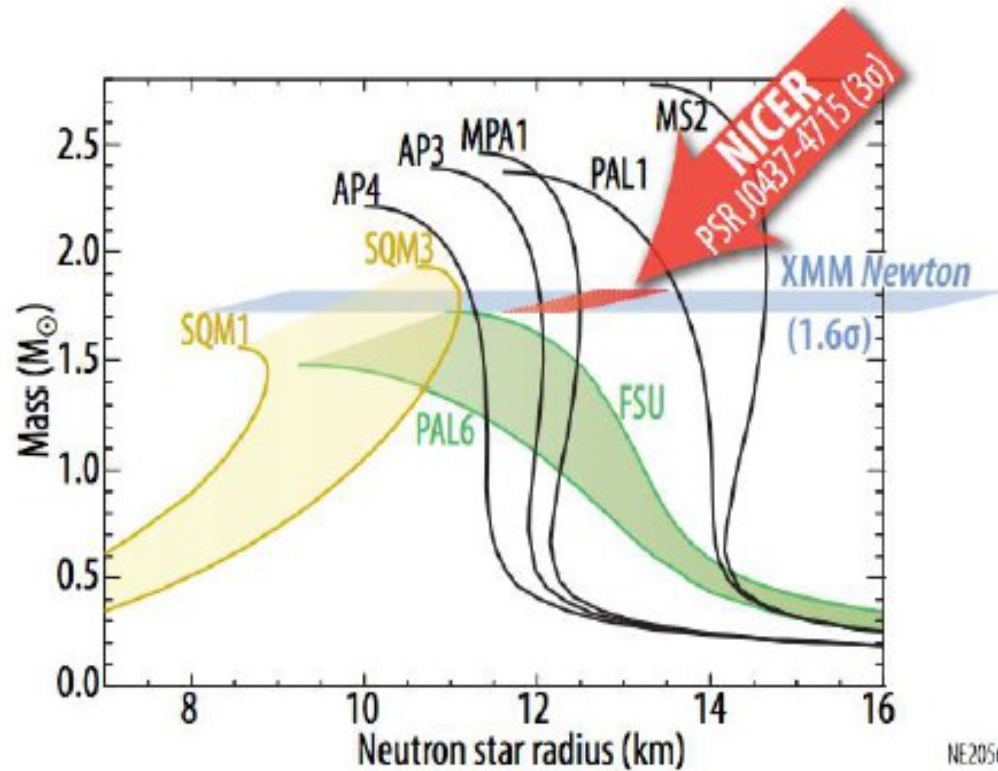
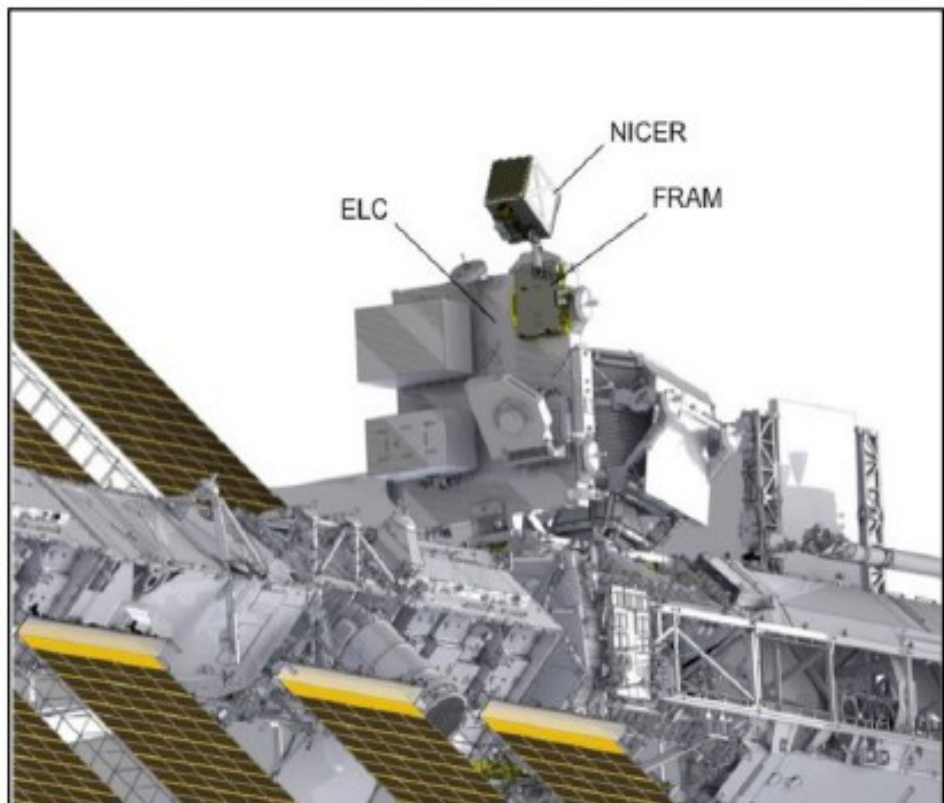
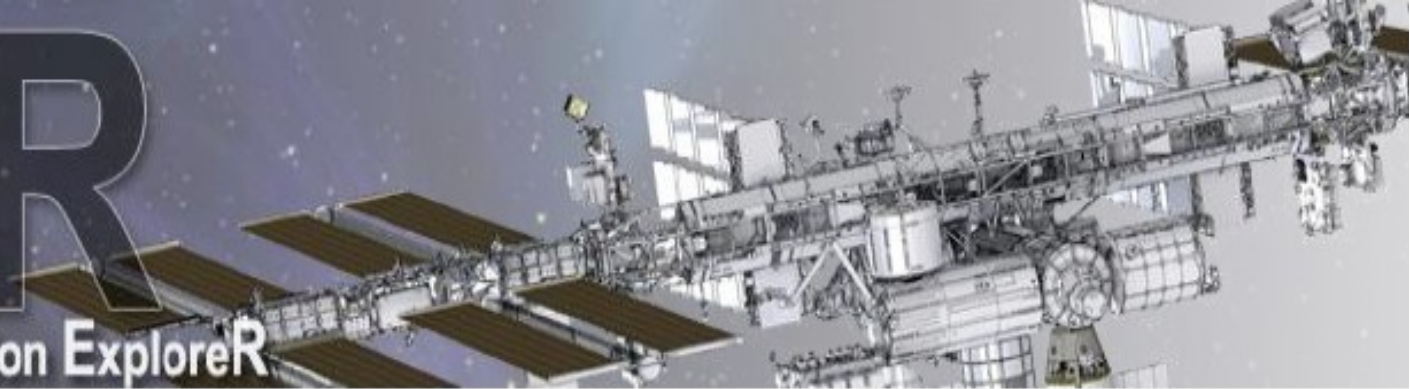
Perspectives for new Instruments?



THE FUTURE: SKA - SQUARE KILOMETER ARRAY

NICER

Neutron star Interior Composition Explorer



NE2056

NICER 2017

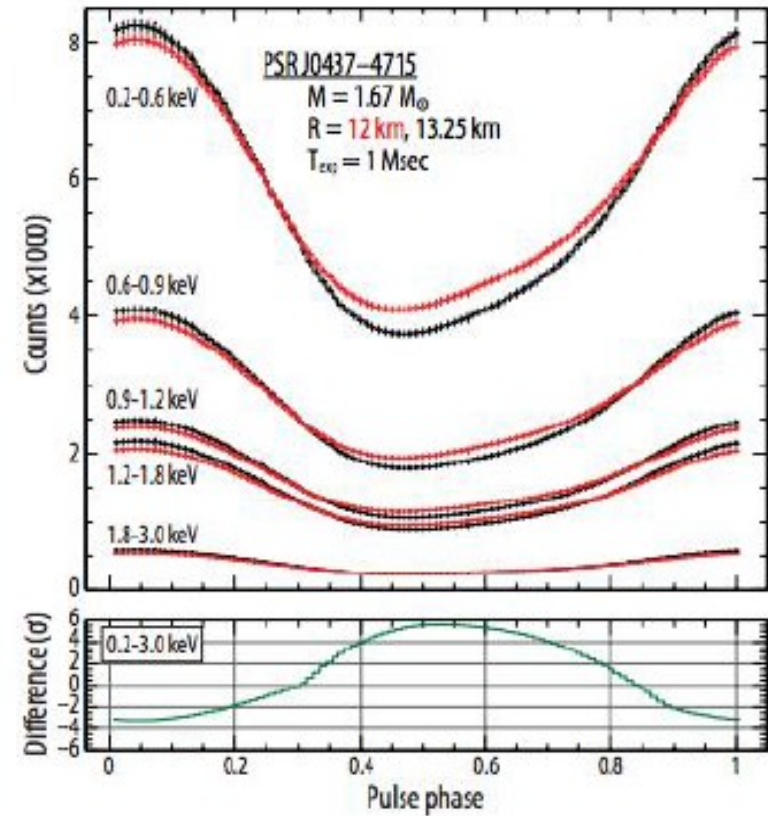
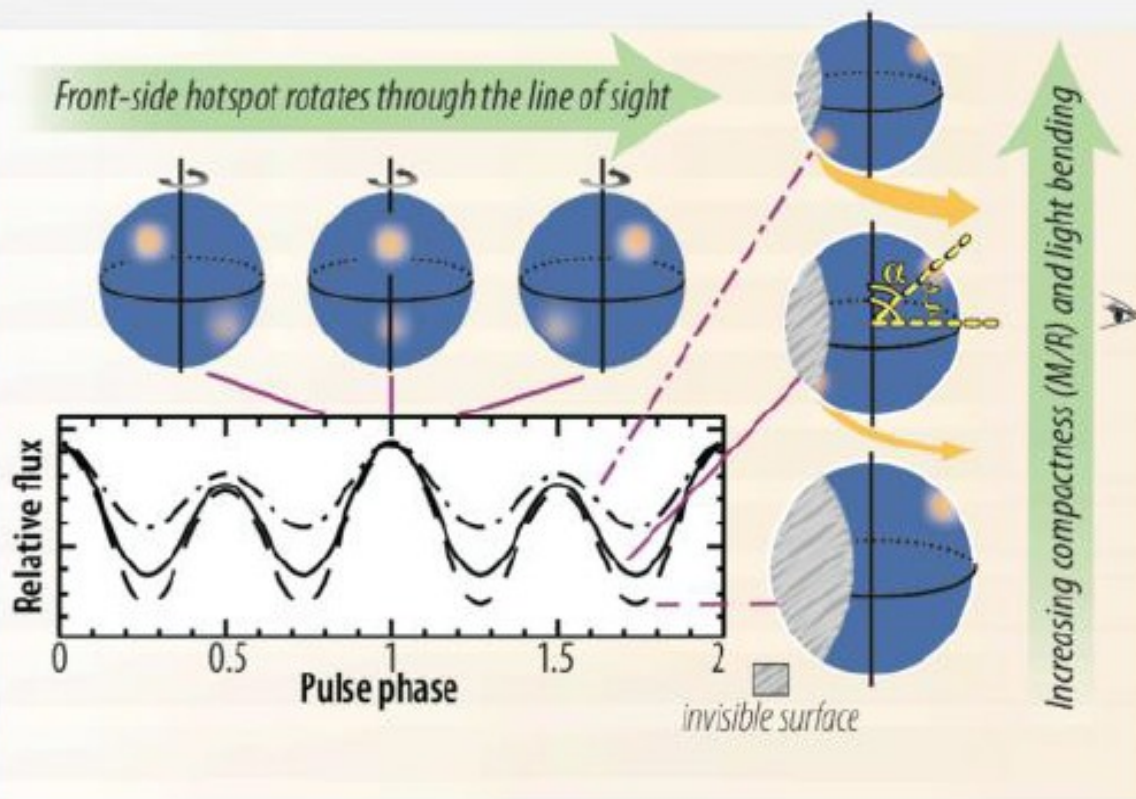
Gendreau, K. C., Arzoumanian, Z., & Okajima, T. 2012, Proc. SPIE, 8443, 844313

NICER

Neutron star Interior Composition Explorer



Thermal Lightcurve Model



Hot Spots

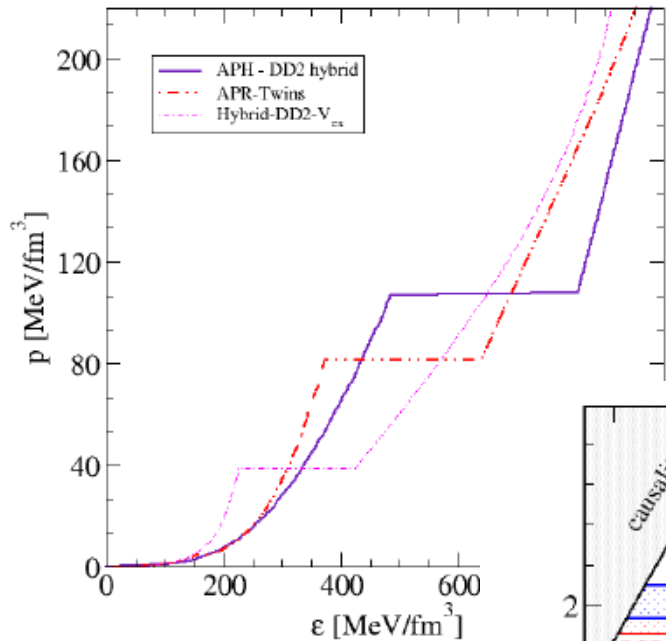
4. Compact Star Matter in Heavy-Ion Collisions?

NICA White Paper – selected topics ...

Many cross-relations with astrophysics of compact stars! High-mass twin stars prove CEP !

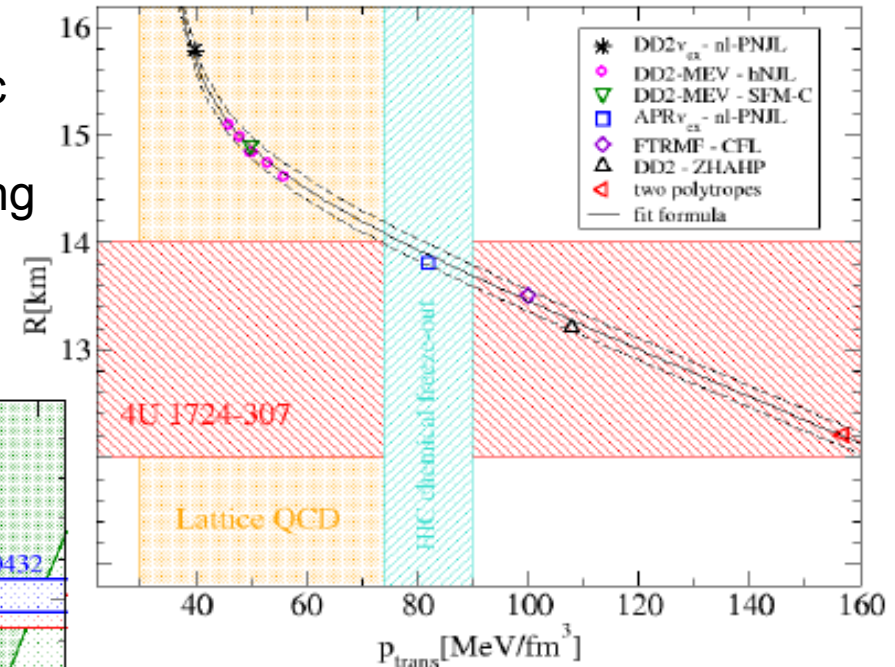
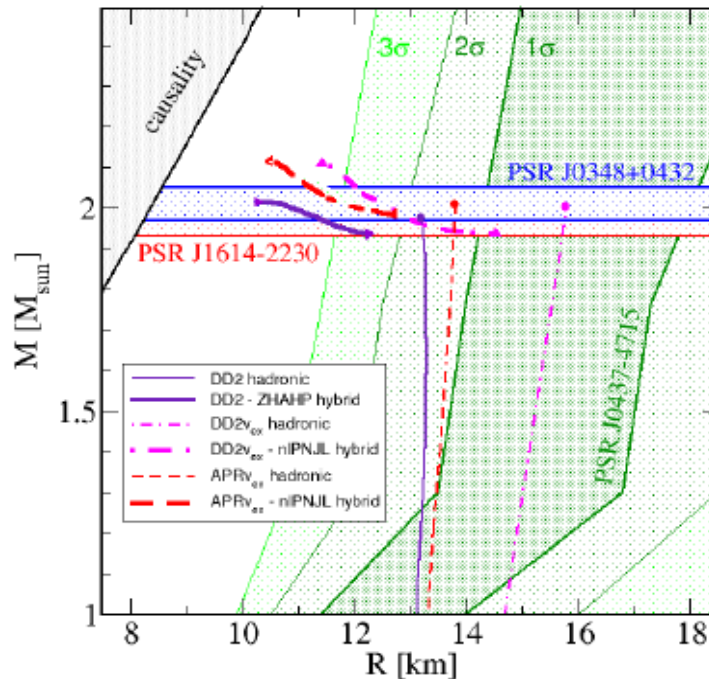
#22 Neutron star mass limit at $2M_{\odot}$ supports the existence of a CEP

D. Alvarez-Castillo^{1,a}, S. Benic^{2,b}, D. Blaschke^{1,3,4}, Sophia Han^{5,6}, and S. Typel⁷



Endpoint of hadronic
Neutron star config.
At $2M_{\text{sun}}$, then strong
Phase transition

Strong phase trans.
High-mass twin stars



Universal transition pressure ?

Petran & Rafelski, PRC 88, 021901

$$P_{\text{trans}} = 82 \pm 8 \text{ MeV/fm}^3$$

4. Compact Star Matter in Heavy-Ion Collisions?

... to be continued in the upcoming lectures !